

Morphology to the rescue: molecular data and the signal of morphological characters in combined phylogenetic analyses—a case study from mysmenid spiders (Araneae, Mysmenidae), with comments on the evolution of web architecture

Lara Lopardo^{a,*}†, Gonzalo Giribet^b and Gustavo Hormiga^a

^aDepartment of Biological Sciences, The George Washington University, 2023 G Street NW, Washington, DC 20052, USA; ^bMuseum of Comparative Zoology, Department of Organismic and Evolutionary Biology, Harvard University, 26 Oxford Street, Cambridge, MA 02138, USA

Accepted 10 June 2010

Abstract

The limits and the interfamilial relationships of the minute orb-weaving symphytognathoid spiders have remained contentious and poorly understood. The circumscription and diagnosis of the symphytognathoid family Mysmenidae have always been elusive, and its monophyly has never been thoroughly tested. We combine sequence data from six genes with a morphological dataset in a total-evidence phylogenetic analysis (*ca.* 6100 characters, 109 taxa: 74 mysmenids), and explore the phylogenetic signal of the combined dataset, individual genes, and gene combinations with different parsimony methods and model-based approaches. Several support values and parameter-sensitivity schemes are explored to assess stability of clades. Mysmenidae monophyly is supported by *ca.* 20 morphological and *ca.* 420 molecular synapomorphies. Mysmenidae is monophyletic under all combined analyses that include morphology. Almost no gene or gene combination supports Mysmenidae monophyly. Symphytognathoids are delimited to include: (Theridiosomatidae (Mysmenidae (Synaphridae (Anapidae + Symphytognathidae))))). Micropholcommatids are a lineage nested within the anapid clade and thus are synonymized with Anapidae (Micropholcommatinae *New Rank*). We provide morphological diagnoses for all symphytognathoid families and discuss the behavioural evolutionary implications of our hypotheses of relationships. The planar orb web evolved independently twice from three-dimensional webs. The orb web was modified into sheet or cobwebs three times independently. The spherical mysmenine web has a single origin. Kleptoparasitism evolved once in mysmenids. We comment on the discrepancies and lack of resolving power of the molecular datasets relative to the morphological signal, and discuss the relevance of morphology in inferring the total-evidence phylogenetic pattern of relationships.

© The Willi Hennig Society 2010.

The superfamily Araneoidea comprises all the lineages of ecribellate orb-weaving spiders, although the ancestral orb web has been modified into a myriad of different web architectures (including cob and sheet webs), and many araneoids do not build typical orbs (such as those in the large families Theridiidae or Linyphiidae). Symphytognathoids are a clade of minute

araneoid spiders that build highly modified orb webs. This clade was originally delimited to include the families Anapidae, Mysmenidae, Symphytognathidae, and Theridiosomatidae (Fig. 1, as delimited by Griswold et al., 1998). The exact composition, interfamilial relationships of “symphytognathoids”, and their placement within Araneoidea are not firmly established and are currently under debate (Figs 2–4) (Schütt, 2003; Lopardo and Hormiga, 2008; Rix et al., 2008; Rix and Harvey, 2010).

Mysmenidae is a small family of minute araneoid spiders that includes 24 genera and 123 described species (Platnick, 2010; but see Rix et al., 2008; Rix and

*Corresponding author:

E-mail addresses: laralopardo@gmail.com; lara@uni-greifswald.de

†Present address: Zoologisches Institut und Museum, Allgemeine und Systematische Zoologie, E-M-A-University, Anklamer Strasse 20, D-17489 Greifswald, Germany.

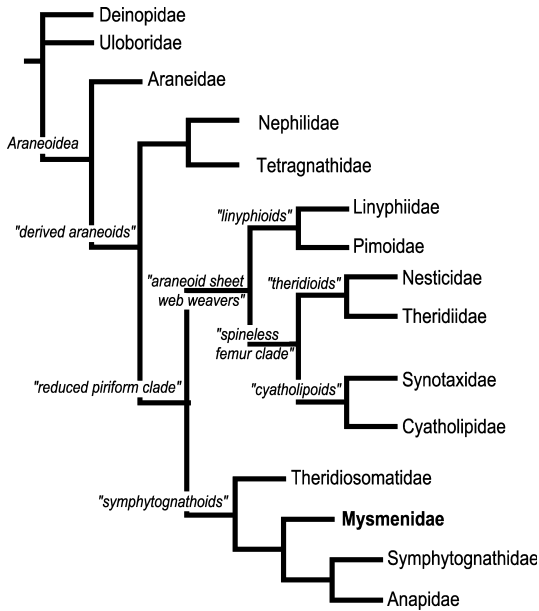


Fig. 1. Summary of the original phylogenetic hypothesis for Orbicularia, showing the position of Araneoidea, “symphytognathoids”, and Mysmenidae (from Griswold et al., 1998). Only the family names are shown, not the actual representatives used in the original analysis.

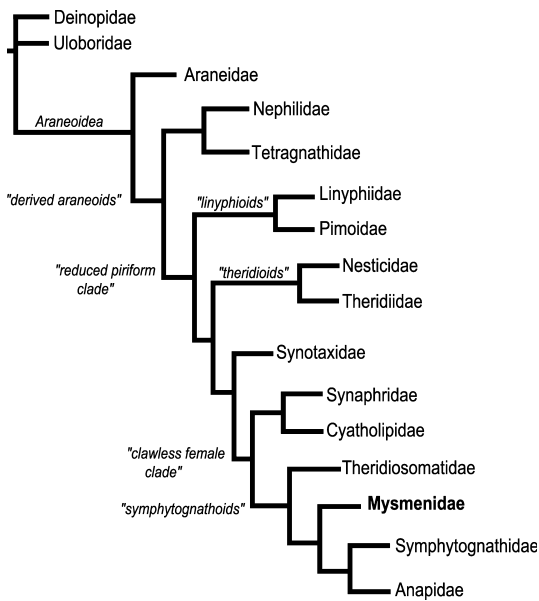


Fig. 2. Summary of the current phylogenetic hypothesis for Orbicularia, showing the position of Araneoidea, “symphytognathoids”, Synaphridae, and Mysmenidae (from Lopardo and Hormiga, 2008; as modified from Griswold et al., 1998). Only the family names are shown, not the actual representatives used in the original analysis.

Harvey, 2010 for a suggested transfer of the monotypic genus *Taphiassa* to Micropholcommatidae) (see Table 1 hereafter for authorship of taxa). Although the family Mysmenidae is distributed worldwide, it is one of the

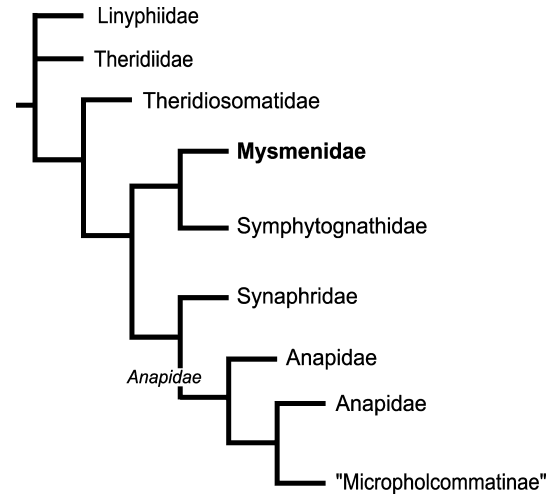


Fig. 3. Summary of the original phylogenetic hypothesis for “symphytognathoids”, showing the position of Mysmenidae (from Schütt, 2003). Only the family names are shown, not the actual representatives used in the original analysis.

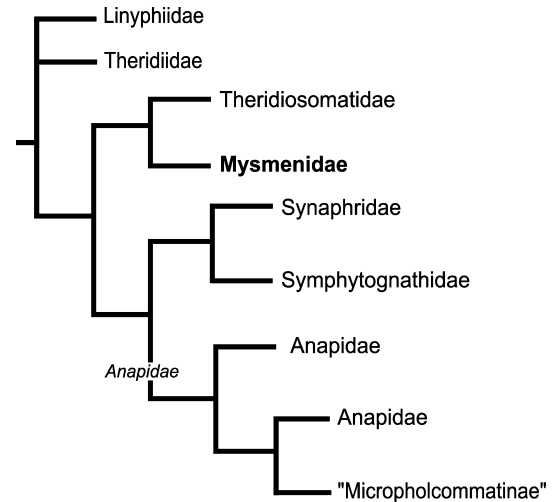


Fig. 4. Summary of the current phylogenetic hypothesis for “symphytognathoids”, showing the position of Mysmenidae (from Lopardo and Hormiga, 2008; as modified from Schütt, 2003). Only the family names are shown, not the actual representatives used in the original analysis.

least-studied family-level groups among orb-weaving spiders, and its diversity is grossly undersampled due to their small size (0.7–3 mm) and cryptic life style. Mysmenids live mainly in leaf litter and other cryptic humid environments. Eleven species in four genera have been reported as kleptoparasites on the webs of other spiders (Platnick and Shadab, 1978b; Griswold, 1985; Baert and Murphy, 1987; Coyle and Meigs, 1989; Eberhard et al., 1993). Members of the kleptoparasitic genera *Isela*, *Kilifina*, and *Mysmenopsis* are not known to build webs of their own, and some have even lost the

Table 1
Author names and list of taxa referred to in text, matrix, and figures

Taxon	Author and year	Family placement	Observations
Anapidae	Simon, 1895		
Mysmenidae	Petrunkevitch, 1928		
Symphytognathidae	Hickman, 1931		
Synaphridae	Wunderlich, 1986		
Theridiosomatidae	Simon, 1881		
<i>Acrobleps</i>	Hickman, 1979	Anapidae	
<i>Acrobleps hygrophilus</i>	Hickman, 1979	Anapidae	
<i>Anapis</i>	Simon, 1895	Anapidae	
<i>Anapisona</i>	Gertsch, 1941	Anapidae	
<i>Anapisona kethleyi</i>	Platnick and Shadab, 1979	Anapidae	
<i>Chasmocephalon</i>	O. Pickard-Cambridge, 1889	Anapidae	
<i>Comaroma</i>	Bertkau, 1889	Anapidae	
<i>Comaroma simoni</i>	Bertkau, 1889	Anapidae	
<i>Conculus</i>	Komatsu, 1940	Anapidae	
<i>Crassanapis</i>	Platnick and Forster, 1989	Anapidae	
<i>Crassanapis chilensis</i>	Platnick and Forster, 1989	Anapidae	
<i>Elanapis</i>	Platnick and Forster, 1989	Anapidae	
<i>Elanapis aisen</i>	Forster and Platnick, 1989	Anapidae	
<i>Micropholcomma</i>	Crosby and Bishop, 1927	Anapidae	This study
Micropholcommatidae/nae	Hickman, 1944	Anapidae	Subfamily, this study
<i>Minanapis</i>	Platnick and Forster, 1989	Anapidae	
<i>Minanapis casablanca</i>	Platnick and Forster, 1989	Anapidae	
<i>Minanapis palena</i>	Platnick and Forster, 1989	Anapidae	
<i>Parapua</i>	Forster, 1959	Anapidae	This study, see Rix and Harvey (2010) for synonymy with <i>Taphiassa</i>
<i>Parapua punctata</i>	Forster, 1959	Anapidae	This study
<i>Sheranapis</i>	Platnick and Forster, 1989	Anapidae	
<i>Sofanapis antillanca</i>	Platnick and Forster, 1989	Anapidae	
<i>Taphiassa</i>	Simon, 1880	Anapidae	This study (but see Rix et al., 2008; Rix and Harvey, 2010)
<i>Taphiassa impressa</i>	Simon, 1880	Anapidae	This study (but see Rix et al., 2008; Rix and Harvey, 2010)
<i>Tasmanapis</i>	Platnick and Forster, 1989	Anapidae	
<i>Tasmanapis strahan</i>	Platnick and Forster, 1989	Anapidae	
<i>Teutoniella</i>	Brignoli, 1981	Anapidae	This study (but see Rix et al., 2008; Rix and Harvey, 2010)
<i>Teutoniella cekalovici</i>	Platnick and Forster, 1986	Anapidae	This study (but see Rix et al., 2008; Rix and Harvey, 2010)
<i>Textricella</i>	Hickman, 1945	Anapidae	
<i>Linyphia</i>	Latreille, 1804	Linyphiidae	
<i>Linyphia triangularis</i>	(Clerck, 1757)	Linyphiidae	
<i>Anjouanella</i>	Baert, 1986	Mysmenidae	
<i>Anjouanella comorensis</i>	Baert, 1986	Mysmenidae	
<i>Brasilionata</i>	Wunderlich, 1995	Mysmenidae	
<i>Brasilionata arborensis</i>	Wunderlich, 1995	Mysmenidae	
<i>Calodipoena</i>	Gertsch and Davis, 1936	Mysmenidae	
<i>Calodipoena incredula</i>	Gertsch and Davis, 1936	Mysmenidae	
<i>Calodipoena mooatae</i>	Baert, 1988	Mysmenidae	
<i>Calomyspoena santacruzii</i>	Baert and Maelfait, 1983	Mysmenidae	
<i>Chanea</i>	Miller, Griswold, and Yin, 2009	Mysmenidae	Miller et al. (2009)
<i>Gaoligonga</i>	Miller, Griswold, and Yin, 2009	Mysmenidae	Miller et al. (2009)
<i>Isela</i>	Griswold, 1985	Mysmenidae	
<i>Isela okuncana</i>	Griswold, 1985	Mysmenidae	
<i>Itapua tembei</i>	Baert, 1984	Mysmenidae	
<i>Kekenboschiella</i>	Baert, 1982	Mysmenidae	
<i>Kekenboschiella awari</i>	Baert, 1984	Mysmenidae	
<i>Kekenboschiella marijkeae</i>	Baert, 1982	Mysmenidae	
<i>Kilifina</i>	Baert and Murphy, 1987	Mysmenidae	
<i>Kilifina inquilina</i>	Baert and Murphy, 1987	Mysmenidae	
<i>Maymena</i>	Gertsch, 1960	Mysmenidae	
<i>Maymena ambita</i>	(Barrows, 1940)	Mysmenidae	

Table 1
(Continued)

Taxon	Author and year	Family placement	Observations
<i>Maymena mayana</i>	(Chamberlin and Ivie, 1938)	Mysmenidae	
<i>Maymena rica</i>	Platnick, 1993	Mysmenidae	
<i>Microdipoena</i>	Banks, 1895	Mysmenidae	
<i>Microdipoena elsae</i>	Saaristo, 1978	Mysmenidae	
<i>Microdipoena guttata</i>	Banks, 1895	Mysmenidae	
<i>Microdipoena nyungwe</i>	Baert, 1989	Mysmenidae	
<i>Mosu</i>	Miller, Griswold and Yin, 2009	Mysmenidae	Miller et al. (2009)
<i>Mysmena</i>	Simon, 1894	Mysmenidae	
<i>Mysmena leucoplagiata</i>	(Simon, 1879)	Mysmenidae	
<i>Mysmena tasmaniae</i>	Hickman, 1979	Mysmenidae	
<i>Mysmenella</i>	Brignoli, 1980	Mysmenidae	
<i>Mysmenella illectrix</i>	(Simon, 1895)	Mysmenidae	
<i>Mysmenella jobi</i>	(Kraus, 1967)	Mysmenidae	
<i>Mysmenella samoensis</i>	(Marples, 1955)	Mysmenidae	
“Mysmeninae”	Petrunkovitch, 1928	Mysmenidae	
<i>Mysmeniola</i>	Thaler, 1995	Mysmenidae	
<i>Mysmeniola spinifera</i>	Thaler, 1995	Mysmenidae	
“Mysmenopsinae”		Mysmenidae	Formal subfamilial assignment elsewhere (Lopardo and Hormiga, unpublished)
<i>Mysmenopsis</i>	Simon, 1897	Mysmenidae	
<i>Mysmenopsis cidrelicola</i>	(Simon, 1895)	Mysmenidae	
<i>Mysmenopsis cienaga</i>	Müller, 1987	Mysmenidae	
<i>Mysmenopsis dipluramigo</i>	Platnick and Shadab, 1978	Mysmenidae	
<i>Mysmenopsis furtiva</i>	Coyle and Meigs, 1989	Mysmenidae	
<i>Mysmenopsis gamboa</i>	Platnick and Shadab, 1978	Mysmenidae	
<i>Mysmenopsis ischnamigo</i>	Platnick and Shadab, 1978	Mysmenidae	
<i>Mysmenopsis kochalkai</i>	Platnick and Shadab, 1978	Mysmenidae	
<i>Mysmenopsis monticola</i>	Coyle and Meigs, 1989	Mysmenidae	
<i>Mysmenopsis palpalis</i>	(Kraus, 1955)	Mysmenidae	
<i>Mysmenopsis penai</i>	Platnick and Shadab, 1978	Mysmenidae	
<i>Mysmenopsis tengellacompa</i>	Platnick, 1993	Mysmenidae	
<i>Simaoa</i>	Miller, Griswold and Yin, 2009	Mysmenidae	Miller et al. (2009)
<i>Tamasesia</i>	Marples, 1955	Mysmenidae	
<i>Tamasesia acuminata</i>	Marples, 1955	Mysmenidae	
<i>Tamasesia rotunda</i>	Marples, 1955	Mysmenidae	
<i>Trogloneta</i>	Simon, 1922	Mysmenidae	
<i>Trogloneta cantareira</i>	Brescovit and Lopardo, 2008	Mysmenidae	
<i>Trogloneta granulum</i>	Simon, 1922	Mysmenidae	
<i>Anapistula</i>	Gertsch, 1941	Symphytognathidae	
<i>Crassignatha</i>	Wunderlich, 1995	Symphytognathidae	Miller et al. (2009); also Lopardo and Hormiga (unpublished)
<i>Curimagua bayano</i>	Forster and Platnick, 1977	Symphytognathidae	
<i>Iardinis</i>	Simon, 1899	Symphytognathidae	Formal transfer elsewhere (Lopardo and Hormiga, unpublished)
<i>Iardinis mussardi</i>	Brignoli, 1980	Symphytognathidae	Formal transfer elsewhere (Lopardo and Hormiga, unpublished)
<i>Patu</i>	Marples, 1951	Symphytognathidae	
<i>Symphytognatha</i>	Hickman, 1931	Symphytognathidae	
<i>Symphytognatha globosa</i>	Hickman, 1931	Symphytognathidae	
<i>Symphytognatha imbulunga</i>	Griswold, 1987	Symphytognathidae	
<i>Symphytognatha picta</i>	Harvey, 1992	Symphytognathidae	
<i>Cepheia</i>	Simon, 1894	Synaphridae	
<i>Cepheia longiseta</i>	(Simon, 1881)	Synaphridae	
<i>Synaphris</i>	Simon, 1894	Synaphridae	
<i>Synaphris lehtineni</i>	Marusik Gnelitsa and Kovblyuk, 2005	Synaphridae	
<i>Synaphris saphrynis</i>	Lopardo Hormiga and Melic, 2007	Synaphridae	
<i>Leucauge venusta</i>	(Walckenaer, 1842)	Tetragnathidae	
<i>Tetragnatha</i>	Latreille, 1804	Tetragnathidae	
<i>Tetragnatha versicolor</i>	Walckenaer, 1842	Tetragnathidae	
<i>Asagena americana</i>	(Emerton, 1882)	Theridiidae	Previously in <i>Steatoda</i> , see Wunderlich (2008)

Table 1
(Continued)

Taxon	Author and year	Family placement	Observations
<i>Steatoda</i>	Sundevall, 1833	Theridiidae	
<i>Theridion</i>	Walckenaer, 1805	Theridiidae	
<i>Epeirotypus</i>	O. Pickard-Cambridge, 1894	Theridiosomatidae	
<i>Epeirotypus brevipes</i>	O. Pickard-Cambridge, 1894	Theridiosomatidae	
<i>Epeirotypus chavarria</i>	Coddington, 1986	Theridiosomatidae	
<i>Epilineutes</i>	Coddington, 1986	Theridiosomatidae	
<i>Naatlo</i>	Coddington, 1986	Theridiosomatidae	
<i>Ogulnius</i>	O. Pickard-Cambridge, 1882	Theridiosomatidae	
<i>Theridiosoma</i>	O. Pickard-Cambridge, 1879	Theridiosomatidae	
<i>Theridiosoma gemmosum</i>	(L. Koch, 1877)	Theridiosomatidae	
<i>Wendilgarda</i>	Keyserling, 1886	Theridiosomatidae	

Taxa names are sorted by family. Familial placement refers to taxonomic changes from this study (noted under “Observations”), otherwise taken from Platnick (2010).

ability to produce the viscid, sticky silk characteristic of orb-weaving spiders (Griswold et al., 1998). Within Mysmenidae, web architecture has been documented only for a few species of *Maymena*, *Mysmena*, and *Microdipoena* (e.g. Forster, 1959; Hickman, 1979; Eberhard, 1982; Coddington, 1986b; Eberhard, 1987; Lopardo and Coddington, 2005; also pers. obs.), and recently for the Chinese genera *Simaoa* and *Gaoligonga* (Miller et al., 2009). Two main types of web are built by different mysmenids: a three-dimensional orb web with a proliferation of out-of-plane radii that result in a unique spherically shaped web (Fig. 5a–c); or a mainly planar orb web with the hub distorted upwards by one to several out-of-plane radial lines that attach to substrate above the web (Fig. 5d,e).

Although mysmenids are morphologically diverse, they have in common a number of diagnostic attributes that distinguish them from other orbicularian families, including the combination of the following features: at least one prolateral claspingspines on the metatarsus or tibia I (or both) in males (Figs 6a,b,f,k,n,o and 7c); a ventral, subapical, sclerotized spot on the femur of at least leg I on most females and some males (Figs 6d,e,h,m and 7b); an apically twisted cymbium (Figs 8a,b and 9a,b) (Platnick and Shadab, 1978b; Brignoli, 1980; Wunderlich, 1995b; Griswold et al., 1998; Schütt, 2003); and a highly elevated carapace in males of some species (Figs 6a,b,i and 10a) (Lopardo and Coddington, 2005). Even though several modern descriptions of mysmenid species are very detailed in terms of genitalic morphology, most species in this family have been poorly described, diagnosed by the general appearance of the genitalia, by eye measurements and interocular distances, or by the somatic coloration patterns. No monographic work exists for Mysmenidae, and most generic diagnoses are almost nondifferential and vague. In addition, the monophyly of the family has not been robustly established until quite recently. An extensive and detailed study on the comparative morphology of mysmenids and their close

relatives was recently completed by the senior author, which tested the monophyly of Mysmenidae using an extensive morphological dataset and a broad taxonomic sample of mysmenids and other symphytognathoids (Lopardo, 2009; see below).

The first three higher-level cladistic analyses including mysmenids are all relatively recent, are based on morphological and behavioural characters, and include only a small number of mysmenid representatives (see also Eberhard, 1987 for a suggested interfamilial pattern of relationships within symphytognathoids based on web-building architectures and stereotyped associated building behaviours). The analysis of orbicularian family relationships by Griswold et al. (1998) included one representative of *Mysmena* and *Maymena*, and placed Mysmenidae as sister to a clade comprising Anapidae and Symphytognathidae *s.s.* (Fig. 1). An earlier analysis of orbicularian families by Coddington (1990), including only the mysmenid *Mysmenella samoensis*, recovered the same pattern of relationships among symphytognathoid families. The study of symphytognathoid relationships by Schütt (2003) included two mysmenids (*Trogloneta*, *Microdipoena*) and *Cepheia* (now classified in Synaphridae) for a total of 12 symphytognathoid terminals. The results of this latter phylogenetic analysis suggested that Mysmenidae was monophyletic (after the exclusion of *Cepheia*), Anapidae was delimited to include Micropholcommatidae, and Mysmenidae (i.e. as *Trogloneta* plus *Microdipoena*) was sister to Symphytognathidae *s.s.* (Fig. 3). Schütt (2003) raised Synaphrinae to family rank and circumscribed the family to include the Old World mysmenid genera *Cepheia*, *Crassignatha*, *Iardinis*, and *Synaphris*. In her analysis, Schütt (2003) included one synaphrid representative (*Cepheia*), thus testing the monophyly of Synaphridae was outside the scope of her matrix. Around the same time, Marusik and Lehtinen (2003) independently raised Synaphrinae to family rank based on morphological data. Some recent studies have proposed synapomorphies for Synaphridae (Marusik and Lehtinen, 2003; Schütt, 2003; Marusik et al., 2005;

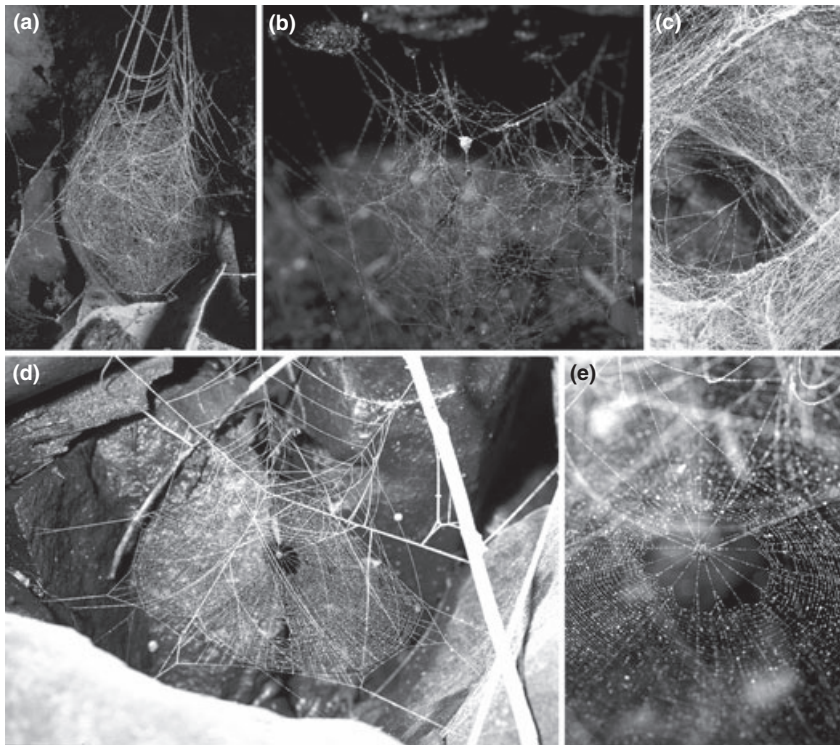


Fig. 5. Webs of Mysmenidae. (a) *Mysmena tasmaniae*; (b) MYSM-005-ARG (*Mysmena*), from Misiones, Argentina, female with eggsac; (c) Mysmenidae from Chiapas, Mexico, detail to centre of web, external threads removed to expose the hub; (d) *Maymena* sp. from Misiones, Argentina; (e) same, detail to centre of web.

Lopardo and Hormiga, 2007; Lopardo et al., 2007; Miller, 2007), although those works tested neither the phylogenetic position of this family nor its monophyly.

Recently, Griswold et al. (1998) and Schütt's (2003) morphologically based hypotheses have been challenged by new phylogenetic analyses for Araneoidea (Figs 2 and 4; Lopardo and Hormiga, 2008). In the reanalysis of Griswold et al. (1998; as modified by Lopardo and Hormiga, 2008), Mysmenidae was sister to a clade comprising Anapidae and Symphytognathidae as originally proposed (Fig. 2). In the reanalysis of Schütt (2003; as modified by Lopardo and Hormiga, 2008), Mysmenidae was placed sister to Theridiosomatidae (Fig. 4). The latter study also provided a placement of Synsphyridae within Araneoidea: either sister to Symphytognathidae (Fig. 4) or sister to Cyatholipidae, as previously suggested by Lopardo et al. (2007) (Fig. 2). The clade including synsphyrids and cyatholipids was sister to symphytognathoids, and this more inclusive lineage was labeled by Lopardo and Hormiga (2008) as the “clawless female clade”. The monophyly of the “clawless female clade” is supported by the absence of the female palpal claw and, at least potentially, by the retention in adult males of at least one of the silk gland spigots of the PLS triad (Lopardo and Hormiga, 2008, p. 19).

Three molecular phylogenetic analyses have included mysmenid representatives, but only as part of the

outgroups. The analyses of theridiid and linyphiid spiders of Arnedo et al. (2004, 2009) included one unidentified *Mysmena* species from Guyana. A more recent molecular analysis of micropholcommatids included a total of three undescribed mysmenids from Australia: one species of *Trogloneta* and two species of the poorly known genus *Taphiassa* (Rix et al., 2008). Interestingly, the undescribed species of *Taphiassa* formed a monophyletic group within the micropholcommatids, which was defined as the informal micropholcommatid subfamily “taphiassine”, suggesting its exclusion from Mysmenidae (see also Rix and Harvey, 2010). Until now, the placement of Mysmenidae within symphytognathoids has been tested exclusively with morphological data, and few synapomorphies have been proposed for the family. The results of a phylogenetic analysis of Mysmenidae and other symphytognathoids based on comparative morphology will be published elsewhere (L.L. and G.H., unpublished; refer to Lopardo, 2009; see above), where we will formally redelimit Mysmenidae and propose several synapomorphies for the family and the remaining symphytognathoid families. The results of the latter study suggest that Mysmenidae is sister to Theridiosomatidae, and this lineage sister to a clade comprising Anapidae (including Micropholcommatidae), Symphytognathidae, and Synsphyridae (see Fig. 11). No extensive phylogenetic



Fig. 6. Composite images of Mysmenidae species. (a–c) “*Microdipoena*”: (a) *Microdipoena nyungwe*, male, lateral view; (b) “*Microdipoena*” (= *Anjouanella*) *comorensis*, male holotype, lateral view; (c) *Microdipoena elsa*, female allotype, lateral view. (d–f) “*Mysmena*”: (d) *Mysmena tasmaniae*, female, lateral view; (e) *Mysmena*-MYSM-017-AUST (*Mysmena* from Queensland, Australia), female, lateral view; (f) MYSM-007-MEX (*Mysmena* from Chiapas, Mexico), male, ventral view. (g–h) *Maymena*: (g) *Maymena ambita*, male, lateral view; (h) *Maymena mayana*, female, frontal view. (i) *Mysmeniola spinifera*, male holotype, lateral view. (j–k) *Mysmenopsis dipluramigo*: (j) female, lateral view; (k) male, lateral view. (l) *Trogloneta granulum*, female, ventral view. (m–n) *Isela okuncana*: (m) female, lateral view; (n) male, ventral view. (o) *Brasilionata arborensis*, male holotype, dorsal view, abdomen detached. Scale bars: a–g, i–o: 0.5 mm; h: 1 mm.

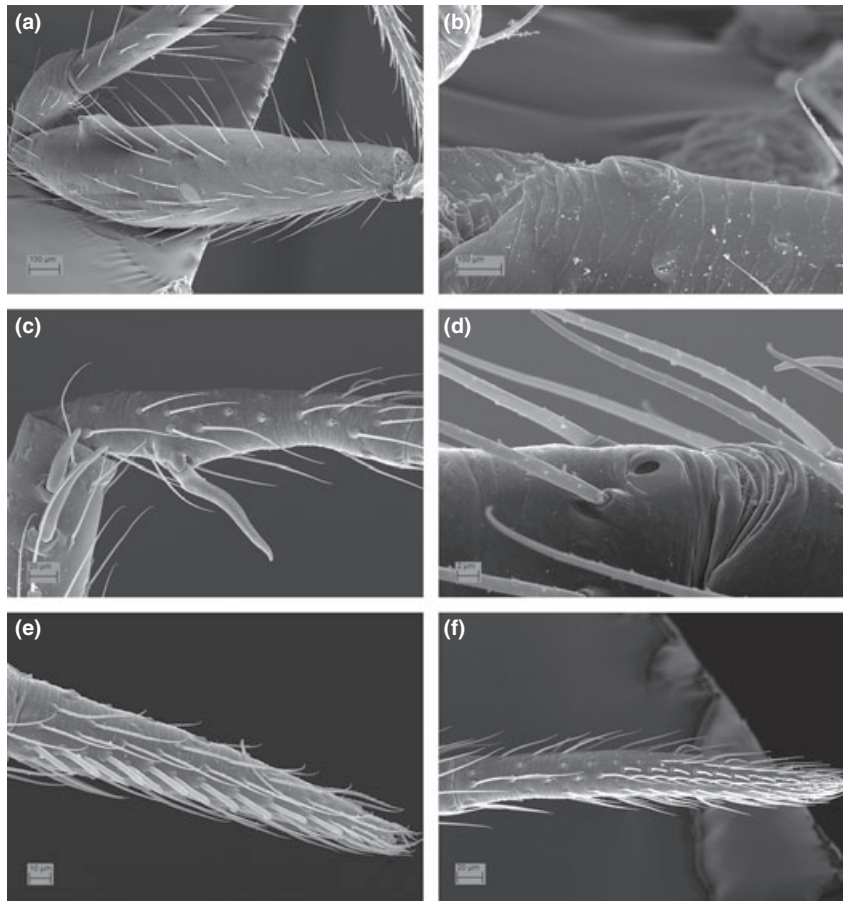


Fig. 7. Legs of Mysmenidae. (a) *Mysmenopsis dipuramigo*, female left femur I, prolateral view. (b) “*Mysmena*” (= *Calodipoena*) *incredula*, female right leg I, femoral spot, retrolateral view. (c) *Microdipoena nyungwe*, male left leg I, tibia–metatarsal junction, prolateral view. (d) *Mysmena*-MYSM-015-MAD (*Mysmena* from Antananarivo, Madagascar), male left leg I, tarsal organ, retrolateral view. (e) *Trogloneta cantareira*, male left tarsus I, prolateral view. (f) *Microdipoena nyungwe*, male left tarsus I, prolateral view.

analysis has ever been done for Mysmenidae at the molecular level.

Goals

The main goals of our study are: to carry out a genus-level “total evidence” phylogenetic analysis of Mysmenidae, using morphological, behavioural, and molecular data; to test the monophyly of Mysmenidae and its genera; and to infer the placement of this family within the symphytognathoids. The phylogenetic hypotheses resulting from our study will provide diagnoses for the family, its constituent genera, and other symphytognathoid families. These results will be used to establish a phylogenetic classification for Mysmenidae, and the resulting hypotheses will provide a comparative framework for the study of character evolution, which is essential for studying the evolution of web architecture and kleptoparasitism. As an additional goal, our study also aims to explore and compare the phylogenetic signal of the combined dataset and the different

molecular partitions using a parsimony approach (refer also to Supporting information).

Materials and methods

Specimens

Sequenced specimens. Specimens for molecular work were preferred if preserved in 96–100% ethanol. If 75% ethanol was used, they were no older than 5 years at the time of DNA extraction. Published sequences were taken from Rix et al. (2008, six species) and Álvarez-Padilla et al. (2009, five species). A total of 81 species are represented by molecular characters (including 81 specimens sequenced in this study). Details of sequenced taxa and voucher information are listed in Table 2, Table S1, and Appendix S2. Appendix 1 provides the abbreviations used in the figures and text.

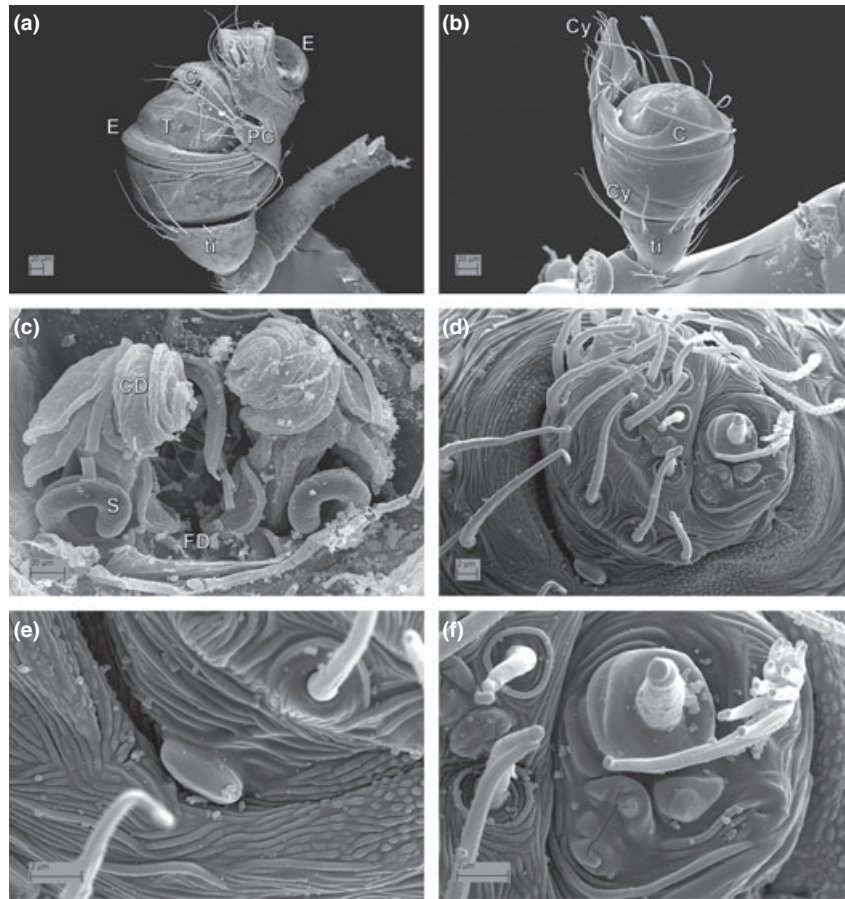


Fig. 8. Mysmenidae genitalia and spinnerets. (a) “*Microdipoena*” (= *Mysmenella*) *samoensis*, male syntype, left palp, retrolateral-ventral view. (b) MYSM-020-MAD (Mysmeninae from Toamasina, Madagascar), male left palp, prolateral-ventral view. (c) *Mysmena*-MYSM-017-AUST (*Mysmena* from Queensland, Australia), female digested abdomen, detail to vulva, tracheae removed. (d–f) *Microdipoena nyungwe*, male: (d) right anterior lateral spinneret; (e) same, detail to intersegmental lobe; (f) same, detail to major ampullate field.

Ingroup. The ingroup for the molecular partition includes sequences from 49 mysmenid species (see Table 1 for authorship of taxa): *Microdipoena guttata*, *Microdipoena nyungwe*, *Maymena mayana*, *Maymena ambita*, *Mysmena tasmaniae*, *Trogloneta granulum*, and 43 undescribed mysmenid species. All ingroup species are represented by at least two genes (Table 2; Table S1). The combined dataset includes 42 mysmenid species scored for morphology (see Lopardo, 2009) and 49 species from the molecular dataset (see Appendix S2). Seventeen species were scored for both morphology and molecules. The total number of mysmenid species in the combined ingroup is 74, including 30 described and 44 undescribed species representing 17 described genera (see Table S1).

Outgroup. Outgroup representatives are based on the phylogenetic hypotheses of Griswold et al. (1998), Schütt (2003), and Lopardo and Hormiga (2008) (see also Lopardo, 2009). The outgroup sample focused on

symphytognathoids, in particular Symphytognathidae and Anapidae, and was based on, and limited by, specimen availability. The outgroup includes sequences from 32 species representing seven araneoid families (see Appendix S2): Anapidae (*Acrobleps hygrophilus*, *Anapisona kethleyi*, *Crassanapis chilensis*, *Elanapis aisen*, *Minanapis casablanca*, *Minanapis palena*, *Tasmanapis strahan*, and two undescribed species of *Acrobleps* and *Conculus*), Symphytognathidae (*Symphytognatha picta* and eight undescribed species), Micropholcommatidae (*Parapua punctata*, *Teutoniella cekalovici*, and two undescribed species of *Taphiassa*), Theridiosomatidae (*Epeirotypus brevipes*, *Epeirotypus chavarria*, *Theridiosoma gemmosum*, and two undescribed species), Linyphiidae (*Linyphia triangularis*), Theridiidae (*Asagena americana*), and Tetragnathidae (*Leucauge venusta*, *Tetragnatha versicolor*, and *Tetragnatha* sp.). All but one species are represented by at least two gene fragments (Table S1). The combined dataset includes 23 outgroup species from the morphological dataset

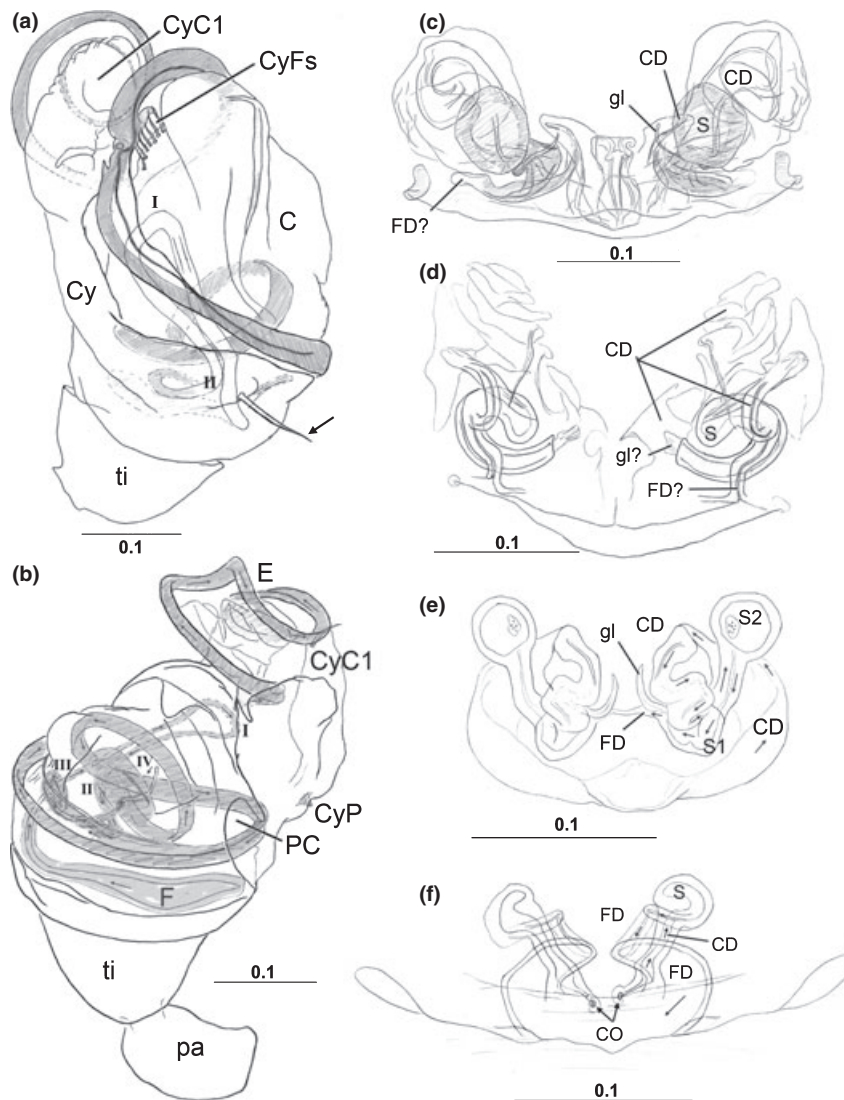


Fig. 9. Mysmenidae genitalia, cleared. (a–b) male left palp; (c–f) female genitalia. (a) *Microdipoena elsae*, prolateral view, arrow to spine of basal prolateral cymbial expansion. (b) “*Microdipoena*” (= *Mysmenella*) *samoensis*, syntype, retrolateral view. (c) *Microdipoena nyungwe*, ventral view. (d) *Mysmena*-MYSM-017-AUST (*Mysmena* from Queensland, Australia), ventral view. (e) *Trogloneta granulum*, ventral view. (f) *Maymena rica*, dorsal view.

from Lopardo (2009), and 32 species from the molecular dataset. Twenty species were scored for both morphology and molecules. The total number of species in the combined outgroup is 35, including 20 described and 15 undescribed species representing 8 families (Table S1). All analyses are rooted using a representative of the family Tetragnathidae.

Methods of study

Morphological and behavioural data. The morphological dataset (refer to Lopardo, 2009) includes a total of 357 characters (including seven continuous characters),

scored for 65 taxa (Table S2; Appendix S1; see also Lopardo, 2009; chapter 2, appendix 2). Morphological continuous characters were treated as ordered and analysed as such (Goloboff et al., 2006). Continuous characters seem to carry useful phylogenetic information (e.g. Thiele, 1993; Rae, 1998; Wiens, 2001; Humphries, 2002; Goloboff et al., 2006; González-José et al., 2008), and this treatment avoids the problems with discretization (e.g. loss of information; assignment of different discrete states to taxa that do not differ significantly and/or *vice versa*; difficulties of state delimitation when there are overlapping distributions of measurements) (e.g. Farris, 1990; Wiens, 2001; Humphries, 2002; Clouse et al., 2009; de Bivort et al.,

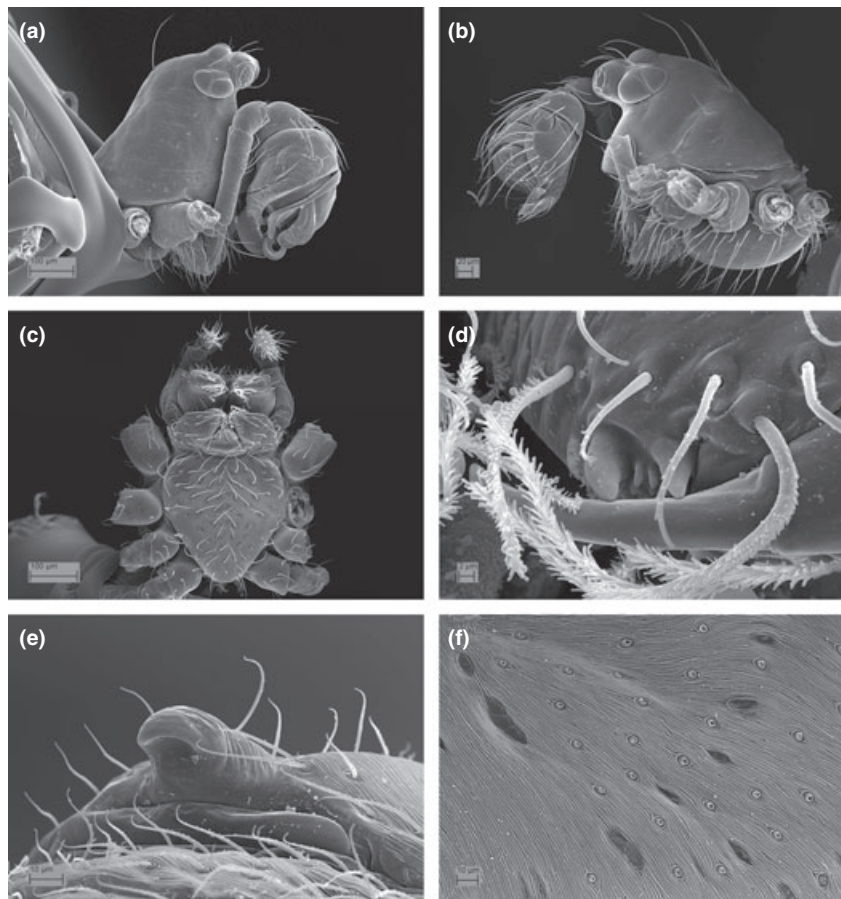


Fig. 10. Mysmenidae, general morphology. (a) *Microdipoena nyungwe*, male prosoma, lateral view. (b) *Mysmena*-MYSM-015-MAD (*Mysmena* from Antananarivo, Madagascar), male prosoma, lateral view. (c) *Microdipoena nyungwe*, female prosoma, ventral view. (d) MYSM-020-MAD (Mysmeninae from Toamasina, Madagascar), male, cheliceral teeth and fang. (e) *Mysmena*-MYSM-015-MAD (*Mysmena* from Antananarivo, Madagascar), female abdomen, epigynal area and scapus, postero-lateral view. (f) *Microdipoena guttata*, male abdomen, detail to abdominal cuticular pattern.

in press). Two of the seven continuous characters represent meristic counts of large ranges, the remaining five correspond to ratio characters (not direct measurements). Scoring of characters based on ratios is difficult as they may conceal information about which of the two features measured is actually undergoing change (changes in either feature can produce identical ratios and therefore similar ratios may originate in different ways; e.g. Hormiga et al., 2000). Since identical ratios could require different evolutionary explanations, each of the measured features ideally should be evaluated independently. In addition, all five ratio characters in this dataset are related to shape or size (as either abdominal shape or leg segment lengths). If measurements scored in each of the ratio characters are included as separate characters, these characters would be highly correlated and size variation would be scored many times under different names. Consequently, these measurements are included as ratio characters in spite of missing evolutionary information. Given the subjectivity

of the discretization and the lack of state definitions in the original discrete ratio characters, this coding represents an improvement in the objectivity of their definition, and can further elucidate a tendency (if any) toward a change in proportion throughout the phylogenetic history of these features. However, we have not tested for correlation of these characters.

Molecular data: DNA sequencing

DNA extraction. Up to four appendages and/or the cephalothorax of a specimen were used for DNA extraction, the remainder of the specimen was kept as voucher. Morphological vouchers will be deposited in the depository institutions or at the Museum of Comparative Zoology (MCZ, Harvard University), California Academy of Sciences (CAS, San Francisco, CA, USA), or the American Museum of Natural History (AMNH, New York, NY, USA) if collected by us and

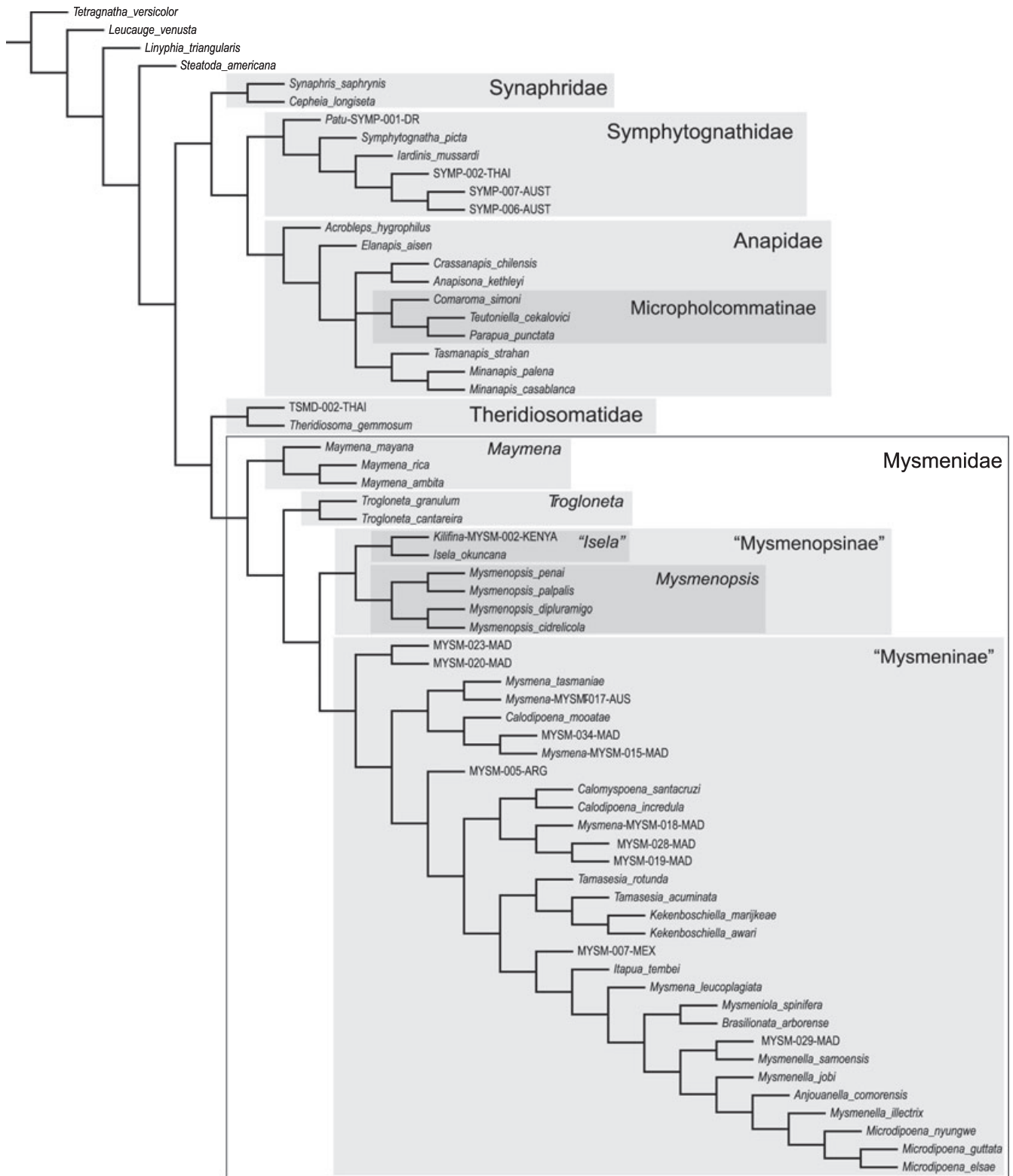


Fig. 11. Strict consensus of the three phylogenetic hypotheses rendered by the morphological dataset analysed under equal weights parsimony. Cladogram taken from Lopardo (2009: chapter 2, figs 154 and 155). Major clades recovered from the complete combined analysis (see Figs 12 and 13) are highlighted in grey boxes. Family codes used for unidentified species: MYSM, Mysmenidae; SYMP, Symphytognathidae; TSMD, Theridiosomatidae.

Table 2
Preparation numbers, source (all or in part), and accession numbers from GenBank for the sequenced taxa

Species	Family	ID preparation	Source	12S	16S	18S	28S	COI	H3
<i>Acropleps hygrophilus</i>	Anapidae	LLS-00088	GWU	GU456730	GU456744	GU456760	GU456820	GU456872	GU456916
<i>Concylus-ANAP-001-THAI</i>	Anapidae	LLS-00047 + 48	USNM	GU456731	GU456745	GU456761	GU456826	GU456873	GU456917
<i>Acropleps-ANAP-002-AUST</i>	Anapidae	LLS-00086	GWU	GU456732		GU456762	GU456821	GU456874	GU456918
<i>Anapisona kethleyi</i>	Anapidae	LLS-00064	GWU			GU456763	GU456822	GU456875	GU456919
<i>Crassanapis chilensis</i>	Anapidae	LLS-00006 + 07	USNM			GU456764	GU456823	GU456876	GU456920
<i>Elinapis aisen</i>	Anapidae	ARAMR000239	AToL		HM030401	GU456768	HM030419	HM030430	HM030437
<i>Minanapis casablanca</i>	Anapidae	LLS-00001 + 02 + 08	USNM			GU456769	GU456827		GU456924
<i>Minanapis palena</i>	Anapidae	LLS-00004 + 05	USNM						
<i>Tasmanapis strahan</i>	Anapidae	ARAMR000685	AToL		HM030406				
<i>Linyphia triangularis</i>	Linyphiidae		FAP	EU003239	AY078664.1	EU003390	HM030426	EU003292	AY078702.1
<i>Parapua punctata</i>	Micropholcommatidae		RIX			EU302946	EU003410		
<i>Teutoniella cekalovici</i>	Micropholcommatidae		RIX			EU302994			
<i>Thapiassa</i> sp Qsld-Rix	Micropholcommatidae		RIX			EU302998			
<i>Thapiassa</i> sp Tasm-Rix	Micropholcommatidae		RIX			EU302935	EU302983		
<i>Maymena ambita</i>	Mysmenidae	LLS-00079 + 80	USNM	GU456733	GU456746	GU456765	GU456824	GU456876	GU456921
<i>Maymena mayana</i>	Mysmenidae	ARAGH000065	AToL		HM030403	HM030411	HM030421		
<i>Microdipoena-AToL-DR</i>	Mysmenidae	ARAGH000003	AToL	HM030397	HM030404	HM030412	HM030422	HM030432	HM030439
<i>Microdipoena guttata</i>	Mysmenidae	LLS-00077 + 78	(GWU) USNM		GU456747	GU456766	GU456825	GU456877	GU456922
<i>Microdipoena nyungwe</i>	Mysmenidae	LLS-00036 + 37	CAS		GU456748	GU456767	GU456826	GU456878	GU456923
<i>MYSM-001-MAD</i>	Mysmenidae	LLS-00014	CAS			GU456770	GU456828	GU456879	GU456925
<i>Maymena-MYSM-003-ARG</i>	Mysmenidae	LLS-00074	MACN			GU456771	GU456829	GU456880	GU456926
<i>Maymena-MYSM-004-MEX</i>	Mysmenidae	LLS-00065	GWU			GU456772	GU456830	GU456881	GU456927
<i>MYSM-005-ARG</i>	Mysmenidae	LLS-00068 + 69	MACN			GU456773	GU456831	GU456882	GU456928
<i>MYSM-006-MAD</i>	Mysmenidae	LLS-00013	CAS		GU456749	GU456774	GU456832	GU456882	GU456929
<i>MYSM-007-MEX</i>	Mysmenidae	LLS-00066	GWU			GU456775	GU456833	GU456883	GU456930
<i>MYSM-008-ARG</i>	Mysmenidae	LLS-00070	MACN			GU456776	GU456834	GU456883	GU456931
<i>MYSM-009-MAD</i>	Mysmenidae	LLS-00017 + 18	CAS			GU456777	GU456835	GU456883	GU456932
<i>MYSM-010-MEX</i>	Mysmenidae	LLS-00067	GWU			GU456778	GU456836	GU456883	GU456933
<i>Mysmena-MYSM-011-ARG</i>	Mysmenidae	LLS-00071	MACN			GU456779	GU456837	GU456883	GU456934
<i>MYSM-012-MAD</i>	Mysmenidae	LLS-00022 + 23	CAS			GU456780	GU456838	GU456884	GU456935
<i>MYSM-013-THAI</i>	Mysmenidae	LLS-00041 + 42 + 46	USNM	GU456734		GU456781	GU456839	GU456885	GU456936
<i>Mysmena-MYSM-014-THAI</i>	Mysmenidae	LLS-00050	USNM			GU456782	GU456840	GU456886	GU456937
<i>Mysmena-MYSM-015-MAD</i>	Mysmenidae	LLS-00020 + 21	CAS			GU456783	GU456841	GU456887	GU456938
<i>Maymena-MYSM-016-ARG</i>	Mysmenidae	LLS-00072	MACN			GU456784	GU456842		
<i>Mysmena-MYSM-017-AUST</i>	Mysmenidae	ARAGH000063	AToL			HM030413	HM030423	HM030433	
<i>Mysmena-MYSM-018-MAD</i>	Mysmenidae	(LLS-00062)	(GWU) CAS						
<i>MYSM-019-MAD</i>	Mysmenidae	LLS-00038 + 39	CAS			GU456785	GU456843	GU456888	GU456939
<i>MYSM-020-MAD</i>	Mysmenidae	LLS-00034	CAS			GU456786	GU456844	GU456888	GU456940
<i>MYSM-021-MAD</i>	Mysmenidae	LLS-00016	CAS			GU456787	GU456845	GU456889	GU456941
<i>MYSM-022-ARG</i>	Mysmenidae	LLS-00019	CAS			GU456788	GU456846	GU456889	GU456942
<i>Trogloneta-MYSM-022-ARG</i>	Mysmenidae	LLS-00073	MACN			GU456789	GU456847		
<i>MYSM-023-MAD</i>	Mysmenidae	LLS-00032 + 33	CAS			GU456790	GU456848	GU456890	GU456943
<i>Trogloneta-MYSM-024-CHILE</i>	Mysmenidae	LLS-00075	MACN			GU456791	GU456848	GU456890	GU456944

Table 2
(Continued)

Species	Family	ID preparation	Source	12S	16S	18S	28S	CO1	H3
<i>Trogloneta</i> -MYSM-025-CHILE	Mysmenidae	LLS-00076	MACN		GU456750	GU456792	GU456849	GU456891	GU456945
MYSM-026-MAD	Mysmenidae	LLS-00015	CAS		GU456751	GU456793	GU456850	GU456892	
MYSM-027-MAD	Mysmenidae	LLS-00024	CAS			GU456794			GU456946
MYSM-028-MAD	Mysmenidae	LLS-00025	CAS			GU456795	GU456851	GU456893	
MYSM-029-MAD	Mysmenidae	LLS-00027	CAS			GU456796	GU456852	GU456894	GU456947
MYSM-030-MAD	Mysmenidae	LLS-00026	CAS			GU456797		GU456895	GU456948
MYSM-031-MAD	Mysmenidae	LLS-00028	CAS	GU456735	GU456752	GU456798	GU456853	GU456896	
MYSM-032-MAD	Mysmenidae	LLS-00029	CAS		GU456753	GU456799	GU456854	GU456897	GU456949
MYSM-033-MAD	Mysmenidae	LLS-00030	CAS		GU456754	GU456800	GU456855	GU456898	GU456950
MYSM-034-MAD	Mysmenidae	LLS-00031	CAS			GU456801	GU456856	GU456899	GU456951
MYSM-035-THAI	Mysmenidae	LLS-00040	USNM			GU456802	GU456857	GU456900	GU456952
MYSM-036-THAI	Mysmenidae	LLS-00044	USNM	GU456736		GU456803	GU456858	GU456901	GU456953
MYSM-037-THAI	Mysmenidae	LLS-00045	USNM	GU456737		GU456804	GU456859	GU456902	GU456954
MYSM-038-ARG	Mysmenidae	LLS-00054	MACN			GU456805	GU456860	GU456903	GU456955
MYSM-039-ARG	Mysmenidae	LLS-00055	MACN			GU456806	GU456861	GU456904	GU456956
MYSM-040-ARG	Mysmenidae	LLS-00056	MACN			GU456807	GU456862	GU456905	GU456957
MYSM-041-ARG	Mysmenidae	LLS-00058	MACN			GU456808	GU456863	GU456906	GU456958
MYSM-042-ARG	Mysmenidae	LLS-00059	MACN			GU456809	GU456864	GU456907	GU456959
<i>Mysmena tasmanica</i>	Mysmenidae	LLS-00089 + ARAGH000062 (LLS-00061)	AToL (GWU)			HM030414	HM030424	HM030434	HM030440
<i>Trogloneta granulum</i>	Mysmenidae	ARAGH000075	AToL		HM030409	HM030418	HM030429		
<i>Trogloneta</i> sp.-Rix-AUST	Mysmenidae		RIX			EU302934	EU302982		
<i>Patu</i> -SYMP-001-DR	Symphytognathidae	LLS-00083	GWU		GU456755	GU456810	GU456865	GU456908	GU456960
SYMP-002-MAD	Symphytognathidae	LLS-00009 + 10	CAS			GU456811	GU456866		GU456961
SYMP-003-MAD	Symphytognathidae	LLS-00011 + 12	CAS		GU456756	GU456812	GU456867	GU456909	GU456962
SYMP-004-THAI	Symphytognathidae	LLS-00049	USNM		GU456757	GU456813		GU456910	GU456963
SYMP-005-AUST	Symphytognathidae	LLS-00085	GWU	GU456738		GU456814	GU456868	GU456911	GU456964
SYMP-006-AUST	Symphytognathidae	LLS-00087	GWU	GU456739		GU456815		GU456912	GU456965
SYMP-007-AUST	Symphytognathidae	LLS-00084	GWU	GU456740		GU456816	GU456869	GU456913	
<i>Symphytognatha</i> -SYMP-008-DR	Symphytognathidae	LLS-00082	GWU	GU456741		GU456817	GU456870		GU456966
<i>Symphytognatha picta</i>	Symphytognathidae	ARAGH000064 (LLS-00063)	RIX + AToL	HM030398	HM030405	HM030415;	HM030425;		
<i>Leucauge venusta</i>	Tetragnathidae		FAP	EU003238	EU003263	EU003350	EU153169;	EU003290	EU003322
<i>Tetragnatha</i> sp	Tetragnathidae	ARAGH000027	AToL	HM030399	HM030407	HM030416	HM030427	HM030435	HM030442
<i>Tetragnatha versicolor</i>	Tetragnathidae	EU003246	FAP	EU003394		EU003394	EU153185;	EU003308	
<i>Steatoda borealis</i>	Theridiidae		FAP	EU003393		EU003393	EU003429	EU003307	
<i>Epeirotypus brevipes</i>	Theridiosomatidae		FAP	EU003347	EU003273	EU003347	EU003428	EU003286	EU003318
<i>Epeirotypus clavarrica</i>	Theridiosomatidae	ARAJC000001	AToL	HM030396	HM030402	HM030410	EU003406	HM030431	HM030438

Table 2
(Continued)

Species	Family	ID preparation	Source	12S	16S	18S	28S	COI	H3
<i>Theridiosoma gemmosum</i>	Theridiosomatidae	ARAJC000010	AToL	HM030400	HM030408	HM030417	HM030428	HM030436	HM030443
TSMID-001-THAI	Theridiosomatidae	LLS-00051	USNM	GU456742	GU456758	GU456818	GU456871	GU456914	GU456967
TSMID-002-THAI	Theridiosomatidae	LLS-00052 + 43	USNM	GU456743	GU456759	GU456819		GU456915	GU456968

Source codes: AToL, Phylogeny of Spiders Project (NSF grant EAR-0228699); CAS, California Academy of Sciences (Charles Griswold); GWU, The George Washington University; FAP, Fernando Alvarez-Padilla (see Alvarez-Padilla et al., 2009); MACN, Museo Argentino de Ciencias Naturales "B. Rivadavia" (Martín J. Ramírez); RIX, data from Rix et al. (2008); USNM, National Museum of Natural History, Smithsonian Institution (Jonathan Coddington).

our collaborators. Genomic DNA was extracted using the Qiagen DNeasy Tissue kit (Qiagen, Valencia, CA, USA) following the manufacturer's protocol, and the appendages were incubated in lysis buffer overnight.

Genes and partitions. We targeted fragments of six genes. Three mitochondrial: the large-subunit ribosomal RNA (16S rRNA, hereafter 16S), the small-subunit ribosomal RNA (12S rRNA, hereafter 12S), and the protein-coding cytochrome *c* oxidase subunit I (COI); and three nuclear: the protein-coding histone H3 (H3), the large-subunit ribosomal RNA (28S rRNA, hereafter 28S), and the nearly complete small-subunit ribosomal RNA (18S rRNA, hereafter 18S). These fragments have been shown to be phylogenetically informative on many studies on arachnid systematics and have been reported to evolve at different rates, potentially providing phylogenetic resolution at different taxonomic levels (e.g. Arnedo et al., 2001; Hormiga et al., 2003; Prendini et al., 2003 and references therein; Giribet et al., 2010). For short gene fragments (up to 600 bp) single amplicons were obtained. For longer fragments, combinations of overlapping amplicons were used and the resulting sequences assembled later. For this taxon sample (considering sequences generated here and those gathered from external sources), the success of the amplification and sequencing processes for different pairs of primers was distinctly different, exhibiting two dissimilar ranges of performance. The performance (and availability) of some pairs of primers was superior in terms of positive sequences vs all sequenced taxa (higher than 63%, that is, 52 or more positive taxa), while other primers performed poorly, with a success equal to or lower than 33% (see Table S1). No success between 33 and 63% was obtained for any pair of primers. However, all fragments were included in the combined dataset.

The 12S fragment (350 bp), was amplified with primers *12sai* (*SR-N-14588*) and *12sbi* (*SR-J-14233*) designed by Kocher et al. (1989) and Simon et al. (1994). This primer pair performed poorly for the selected taxon sample (25%). The 16S fragment (459 bp) was amplified with primers *16Sa* (*LR-J-13417*, reverse complement) designed by Simon et al. (1994) and *16Sb* (*LR-J-12887*) designed by T. Kocher, as reported by Simon et al. (1994). The 16S primer pair also performed poorly for the selected taxon sample (33%). The 18S fragment (*ca.* 1750 bp) was amplified with six overlapping pairs of primers designed by Whiting et al. (1997) and Giribet et al. (1996, 1999). The three overlapping amplicons covering the first portion of this gene performed poorly (10–23%; primer pairs *1F-4R*, *4F-5R*, and *5F-7R*, *ca.* 950 bp in total). The remaining primer pairs covering the last part of the gene (pairs *18Sa2.0-7R*, *18Sa2.0-9R* and *7F-9R*, *ca.* 800 bp in total) performed with 63–80% success. The

28S fragment (D3 region, ca. 2200 bp) was amplified with primers *28Sa* and *28Sb* designed by Whiting et al. (1997), and five overlapping pairs of primers published by Schwendinger and Giribet (2005) and Edgecombe and Giribet (2006). New primers designed here are: *28Sgh2F* (5'-GTACCGTGAGGGAAAGTTGCAAA-GAAC-3'); *28SrD3aGH* (5'-GTTCTTTGCAACTTTC-CCTCACGGTAC-3'); *28Sgh1F* (5'-ATGTGAACAG-CAGTTGAACATGGGT-3'); and *28Sgh1R* (5'-AC-CCATGTTCAACTGCTGTTTCACAT-3'). The fragment resulting from primer pair *28Sa*–*28Sb* (located at positions ca. 880–1220) amplified with great success (79%). Relative positions of primers are with respect to the sequence of *Limulus polyphemus* 28S rRNA from Winchell et al. (2002; AF212167). Flanking combinations of primers around the successful amplicon performed poorly (pairs *28SD1F*–*28SrD3aGH* and *28Sgh2F*–*28SrD4b*, ca. 880 bp, 33% in average; pairs *28Sa*–*28Srd5b*, *28Srd4.8a*–*28Sgh1R*, and *28Sgh1F*–*28Srd7b1*, ca. 1000 bp, 21% in average). The CO1 fragment (658 bp) was amplified with primers *LCO1490* and *HCO2198* designed by Folmer et al. (1994). For our taxon sample, the pair of primers amplified successfully (68%). Finally, the H3 fragment (328 bp) was amplified with primers *H3aF* and *H3aR* designed by Colgan et al. (1998), which performed with high success (79%).

DNA amplification, visualization and purification. Polymerase chain reactions (PCR) were carried out in the Giribet Laboratory (Harvard University) or The George Washington University (GWU) Department of Biological Sciences sequencing facility. Procedures from both laboratories are listed below. In case protocols differ, differences are separated by a slash, the first one applied at Harvard, the second at GWU. Standard PCR (50 μ L) contained 35 μ L autoclaved ddH₂O; 5 μ L 10 \times PCR buffer and 5 μ L 25 mM MgCl₂ solution (Applied Biosystems, Branchburg, NJ, USA)/5 μ L 10 \times *Ex Taq* buffer 20 mM MgCl₂ (Takara Bio USA, Madison, WI, USA); 0.5 μ L 100 μ M each primer (Operon Biotechnologies, Huntsville, AL, USA); 1 μ L 10 mM dNTPs (Invitrogen, Carlsbad, CA, USA)/4 μ L 10 mM dNTPs (Takara Bio USA); 0.25 μ L AmpliTaq DNA polymerase (5 units/ μ L) (Applied Biosystems)/*Ex Taq* DNA Polymerase (5 units/ μ L) (Takara Bio USA); and 2–5 μ L DNA template. PCRs were carried out in a GeneAmp PCR System 9700 thermal cycler (Applied Biosystems)/PTC-200 Peltier Thermal Cycler (MJ Research, Watertown, MA, USA). For the ribosomal genes: initial denaturation step (3 min, 94 °C), 35 cycles of denaturation (30 s, 94 °C), annealing (30 s, 45–47 °C), and extension (30 s/1 min, 72 °C), final extension step (6 min, 72 °C). For the protein-coding genes: initial denaturation step (1 min, 94 °C), 35 cycles of denaturation (30 s, 94 °C), annealing (30 s, 42–44 °C), and extension (1 min, 72 °C), final extension step (6 min,

72 °C). For fragments difficult to amplify, concentrations of MgCl₂ (5–20 μ L) and/or annealing temperatures were modified to attain optimum amplification conditions. Negative amplifications were repeated up to five times under different conditions. PCR results were visualized by means of agarose gel electrophoresis (1.8/1%) in TBE buffer. Successful PCR products were cleaned using the Qiagen QIAquick PCR Purification kit following the manufacturer's protocol.

Sequencing reactions. PCR-purified products from GWU were sent for sequence reactions and determinations to SeqWright DNA Technology Services (SeqWright, Inc, Houston, TX, USA). Samples generated at Harvard were sequenced in house as follows. Sequencing reactions (10 μ L) contained 4 μ L autoclaved ddH₂O, 2 μ L purified PCR template, 3.2 μ L corresponding primer (1 μ M), 0.5 μ L ABI Big Dye Terminator v3.0, and 0.25 μ L ABI BigDye 5 \times sequencing buffer (Applied Biosystems). Sequencing reactions: initial denaturation step (3 min, 94 °C), 30 cycles of denaturation (10 s, 94 °C), annealing (5 s, 50 °C), and extension (4 min, 60 °C), final extension step (6 min, 72 °C). Reaction products were cleaned on Sephadex G-50 Fine columns, centrifuged (5 min, 850 g), and dried in speedvac (1–2 h). Pellets were resuspended in 15 μ L Hi-Di formamide, denaturalized (1 min, 95 °C), and transferred to ice. Sequence determination was performed on an automated sequencer ABI Prism 3730xl Genetic Analyser.

Sequence edition. Chromatogram evaluation, editing, and assemblage were performed using Sequencher 4.7 (Gene Codes Corporation 1991–2007, Ann Arbor, MI, USA). To check for internal contamination, pairwise distances among sequenced specimens were compared using the software Bioedit v. 7.0.9.0 (Hall, 1999). In addition, all edited sequences were BLASTed (Altschul et al., 1997, as implemented by the National Center for Biotechnology Information (NCBI) website <http://ncbi.nlm.nih.gov>) against the GenBank nucleotide database. When sequences from two specimens of the same species were produced, they were tested for monophyly prior to combining sequences (required for fusing molecular and morphological datasets). For each gene, a quick heuristic phylogenetic analysis was performed under dynamic homology with the program POY 4.0.2870 (Varón et al., 2008–2009) for 1 h under equal weights (command search()). All 20 duplicate species were monophyletic. Ribosomal genes were manually divided into homologous regions (segments) based on primer position and availability of sequences (see Table 3; Table S1): 12S (seven segments), 16S (13 segments), 18S (39 segments: first 13 correspond to unsuccessful primers), 28S (45 segments, successful portion: 15–29). Delimitation of homologous regions

Table 3
Summary of analyses performed under parsimony and equal weights using the (a) dynamic homology approach as implemented in POY, (b) static homology approach as implemented in TNT

POY	Partition name	Root	Composition	Number of taxa	Number of MPT	MPT length	Hits						
(a)	Combined	Combined A (preferred hypothesis)	<i>Tetragnotha</i> sp.	Morphology + complete molecular	109	1	16 894.62	7					
		Combined B	<i>Tetragnotha</i> sp.	Morphology + successful primers	109	1	8903.43	2					
		Combined B (minus 4)	<i>Tetragnotha</i> sp.	Morphology + successful primers (excl. <i>Epeirotypus</i> and MYSM=[024-025]-CHILE)	105	5	8397.5	46					
		Combined C	<i>T. versicolor</i>	Morphology + complete molecular, reduced dataset	37	1	10 115.91	89					
	Molecular	Combined D	<i>T. versicolor</i>	Morphology + successful primers, reduced dataset	37	1	5172.65	661					
		12S	<i>Tetragnotha</i> sp.	Segments 0–6	22	1	1047	119					
		16S	<i>Tetragnotha</i> sp.	Segments 0–12	28	34	1257	511					
		18S	<i>Tetragnotha</i> sp.	Segments 0–38	78	1	2808	30					
		18S (partial)	<i>Tetragnotha</i> sp.	18S successful primers: segments 13–18 + 19–38	77	1	1907	18					
		28S	<i>T. versicolor</i>	Segments 0–44	73	1	5892	25					
		28S (partial)	<i>T. versicolor</i>	28S successful primers: segments 15–29	69	1	1233	72					
		COI	<i>T. versicolor</i>		56	12	2612	572					
		H3	<i>T. versicolor</i>		63	227	1187	596					
		Molecular A	<i>Tetragnotha</i> sp.	Complete molecular: all genes	81	1	14 901	48					
		Molecular B	<i>Tetragnotha</i> sp.	Successful primers: 18S (partial) + 28S (partial) + COI + H3	81	1	7226	56					
		Molecular C	<i>T. versicolor</i>	Complete molecular, reduced dataset	37	2	8913	16					
		Molecular D	<i>T. versicolor</i>	Successful primers, reduced dataset	37	1	3972	207					
Mitochondrial Protein	<i>Tetragnotha</i> sp.	12S + 16S + COI	61	7	4988	n/a							
Nuclear	<i>Tetragnotha</i> sp.	COI + H3	71	101	3901	n/a							
	<i>Tetragnotha</i> sp.	Complete nuclear fragments: 18S + 28S + H3	81	1	9893	60							
(b)	Combined A	<i>T. sp.</i>	Morphology + complete molecular	6394	1120	19 430.369	185	3088	48.3%	38.5%	13.2%	66.9%	
	Combined B	<i>T. sp.</i>	Morphology + successful primers	2500	20	9152.099	2	1318	52.7%	35.2%	12.1%	46.5%	
	Combined C	<i>T. versicolor</i>	Morphology + complete molecular, reduced dataset	6394	1	11 476.159	0.528	491	2555	40.0%	45.2%	14.8%	52.8%
	Combined D	<i>T. versicolor</i>	Morphology + successful primers, reduced dataset	2500	1	5310.969	0.442	1000	1078	43.1%	42.7%	14.2%	32.2%

Table 3
(Continued)

TNT	Partition name	Root (<i>Tetragnatha</i>)	Composition	Number of taxa	Number of characters	Number of MPT	MPT length	CI	RI	Hits	Informative characters (%)	Invariant characters (%)	Autapomorphic characters (%)	Missing data (%)
Molecular	12S	<i>T. sp.</i>	Segments 0–6	22	350	2	1204	0.429	0.417	992	72.0%	17.4%	10.6%	5.0%
	16S	<i>T. sp.</i>	Segments 0–12	28	465	13	1375	0.399	0.448	1000	57.2%	32.0%	10.8%	3.1%
	18S	<i>T. sp.</i>	Segments 0–38	78	1821	1995	3039	0.496	0.523	307	36.1%	49.4%	14.4%	52.5%
	18S (partial)	<i>T. sp.</i>	18S successful primers: segments 13–18 + 19–38	77	818	3681	2013	0.418	0.547	432	46.0%	40.8%	13.2%	18.0%
28S	<i>T. versicolor</i>	Segments 0–44	73	2415	28	7872	0.425	0.5	567	47.7%	38.6%	13.7%	59.8%	
28S (partial)	<i>T. versicolor</i>	28S successful primers: segments 15–29	69	339	279	1396	0.322	0.541	983	54.0%	37.2%	8.8%	6.5%	
COI	<i>T. versicolor</i>		56	658	19	2612	0.267	0.406	540	317	48.2%	39.8%	12.0%	8.2%
H3	<i>T. versicolor</i>		63	328	35	1187	0.238	0.549	841	131	39.9%	47.9%	12.2%	1.9%
Molecular A	<i>T. sp.</i>		81	6037	136	17 840	0.387	0.457	136	2777	46.0%	40.8%	13.3%	56.6%
Molecular B	<i>T. sp.</i>		81	2143	474	7564	0.3	0.464	124	1007	47.0%	41.0%	12.0%	26.5%
Molecular C	<i>T. versicolor</i>		37	6037	4	10 283	0.541	0.381	719	2285	37.9%	47.4%	14.8%	55.1%
Molecular D	<i>T. versicolor</i>		37	2143	27	4125	0.447	0.371	995	808	37.7%	48.4%	13.9%	35.2%
Mitochondrial Protein	<i>T. sp.</i>		61	1473	278	5269	0.335	0.406	633	835	56.7%	32.0%	11.3%	40.2%
Nuclear	<i>T. sp.</i>		71	986	1358	3901	0.251	0.441	449	448	45.4%	42.5%	12.1%	22.7%
	<i>T. sp.</i>		81	4564	344	12 404	0.414	0.49	217	1942	42.6%	43.6%	13.9%	57.1%
Nuclear (partial)	<i>T. sp.</i>		81	1485	206	4809	0.327	0.514	84	690	46.5%	41.6%	12.0%	22.0%
Ribosomal	<i>T. sp.</i>		81	5051	1504	13 749	0.431	0.476	417	2329	46.1%	40.4%	13.5%	61.3%
Ribosomal (partial)	<i>T. sp.</i>		80	1157	2899	3482	0.37	0.529	310	559	48.3%	39.8%	11.9%	20.6%

MPT, most parsimonious tree/s; CI, consistency index; RI, retention index.

Composition, root, and resulting statistics as well as informative character proportions are reported for each partition. Informative characters and their percentages exclude autapomorphic characters. Invariant characters refer to characters scored for only one state. See text for explanation of partition names.

was verified by the static alignment generated independently (see below). All sequences from this study are deposited in GenBank (Table 2).

Phylogenetic analyses

Evaluation of cladistic hypotheses: search for most parsimonious trees

Partitions. Seven character partitions were defined in this study: morphology, 12S, 16S, 18S, 28S, CO1, and H3. We analysed each gene partition alone and in different combinations to discern their phylogenetic signal, also including those gene fragments with high and low primer success (see Table 3 for a complete list of partition combinations explored, partition names and compositions, and analysis statistics). The complete molecular partition includes all sequence data merged into a single data matrix (“molecular A”, 81 taxa, 6037 bp), and the total-evidence dataset comprises the morphological and entire molecular partition (“combined A”, 109 taxa and 6394 characters; see Table 3). The “reduced” datasets comprise the 37 taxa scored for both molecules and morphology (e.g. “combined C”, 37 taxa, 6394 characters; see Table 3). Cladistic analyses were carried out using two different approaches. A dynamic (one-step) approach using direct optimization (Wheeler, 1996) as implemented in POY 4.0–4.1 (Varón et al., 2008–2009) and a static (two-step) approach, where the sequences of different lengths were first aligned, then submitted to the program TNT (Goloboff et al., 2003b, 2008) (see below for details).

Dynamic homology approach. Phylogenetic analyses of unaligned molecular and combined partitions, as described above, were executed using direct optimization in the program POY 4.0: build 2870 (individual genes, “mitochondrial” and “protein” partitions); build 2881 (other molecular partitions); and build 2911 (all matrices combining the morphological data) (Varón et al., 2008–2009). Dynamic homology is preferred over the static approach, as it consistently evaluates multiple alignments and phylogenetic hypotheses under the same optimality criterion and parameter set, it dynamically explores multiple equally possible alignments as opposed to just one (Wheeler, 1996; Giribet, 2001; Wheeler et al., 2006), and it outperforms the static approach in topological accuracy and tree length (Lehtonen, 2008; Wheeler and Giribet, 2009). Protein-coding genes and morphology were treated as prealigned. Tree cost-estimation routines were set to standard direct optimization algorithm (Wheeler, 1996, 2002) (command `set(exhaustive_do)`), which is more intense than the default setting (Varón et al., 2008–2009). Heuristic

searches implemented a default search strategy (command `search()`) that includes tree building, tree bisection–reconnection (TBR) branch swapping, perturbation using ratchet (Nixon, 1999), and tree fusing (Goloboff, 1999, 2002). Searches were performed under equal weights (transformation cost set with command `transform(tcm:(1,1))`). Equal weighting analyses were preferred over differential costs to maximize consistency in assumptions for both kinds of data (no differential character transformation could be applied to the morphological partition, and no implied weighting could be applied to dynamic analyses of molecular data). Maximum total execution time for searches depended on the dataset analysed: 2 h (12S, 16S); 3 h (18S, 28S, CO1, H3); 4 h (protein); 6 h (ribosomal and nuclear partitions); 24 h (complete molecular and all combined partitions). Optimal cladograms obtained by the analysis of the combined total-evidence dataset (combined A) under equal weights and dynamic homology were chosen as working hypothesis for mysmenid and symphytognathoid phylogenetic relationships.

Static homology approach. Static alignments were inferred with the online program MAFFT (MAFFT Multiple alignment program for amino acid or nucleotide sequences, version 6, available at <http://align.bmr.kyushu-u.ac.jp/mafft/online/server/>) (Katoh et al., 2002, 2005; Katoh and Toh, 2008). The selected algorithm for pairwise alignment was the E-INS-i strategy, which is one of the most exhaustive algorithms implemented and has the least number of assumptions (MAFFT online documentation). Alignment indel opening penalty was set to default value of 1.53. MAFFT is one of the few available alignment programs that have been shown to produce relatively accurate and fast alignments (see Golubchik et al., 2007). To account for historical information contained in insertion and deletion events, gaps were treated as fifth state during phylogenetic analyses and thus considered independent events. This treatment maximizes independence of characters and logical consistency of phylogenetic analyses, at the expense of up-weighting otherwise potentially single events (Giribet and Wheeler, 1999). Extension gaps were down-weighted during alignment (Bayesian strategy, see below), and later considered as independent events during analysis (dynamic homology approach). While many different combinations of gap treatments and weightings are possible, the compromise between the two different gap treatments while aligning and analysing was adopted here as a strategy to make the static parsimony analyses more comparable with both the dynamic homology and the model-based approaches. Even though an “almost infinite” combination of factors may well affect the outcome of an analysis, and consequently the impossibility of fully comparing all analytical approaches, results from the different search strategies

are reported here and compared according to their taxon/clade composition. Heuristic searches were performed with parsimony under equal weights using the program TNT v. 1.1 (Goloboff et al., 2003b, 2008). Searches consisted of 1000 replicates of random addition sequences (RAS), followed by 500 iterations of TBR and parsimony ratchet as implemented in TNT (alternating search and perturbation phases, with periodic rounds of original weights) (Goloboff et al., 2003b; program documentation), retaining 10 trees per replication (commands `ratchet : iter 500 equal; mult = ratchet repl 1000 tbr hold 10;`). Internal branches were considered unsupported and collapsed during searches if they were supported ambiguously (that is, when some optimization lacks support, rule 1 of TNT, that is, when the minimum length is zero; see discussion in Coddington and Scharff, 1994).

Sensitivity analyses

To explore stability of the results to variation in analytical parameters, for example, the effect of data perturbation on phylogenetic results (“sensitivity analysis” *sensu* Wheeler, 1995; see also Giribet, 2003), the complete and reduced combined datasets (combined A and combined C) were analysed under parsimony using differential character-weighting schemes. These searches were performed solely to explore the stability of relationships proposed in the resulting phylogenetic hypotheses, although sensitivity of groups to changes in analytical parameters might also provide an insight to the support of groups (Giribet, 2003). Stable clades remain under a wide range of parameters, while unstable groups are supported only under one or a few particular sets of parameters. Under the dynamic approach, the weighting scheme explored applied different substitutions vs indel transformation costs (as in Wheeler, 1995; Prendini et al., 2003; see also Spagna and Álvarez-Padilla, 2008). Under the static approach, the weighting scheme explored applied implied weights (Goloboff, 1993) (see below).

Transformation cost matrices (POY). Eleven sets of parameters were defined, following Prendini et al. (2003, see their table 7, p. 197). Transversion costs were equal to or more costly than transitions by a factor of two or four, and an extreme transversion-only scheme (transition cost was zero). Relative costs of indels varied from equal to transversions, to two or four times as costly. Such indel costs are below the upper limit suggested by Spagna and Álvarez-Padilla (2008). Given the treatment of continuous characters in the complete combined dataset (analysed as such, see above), and that transformation costs are not logically or directly applicable to morphological states, costs for both discrete and continuous morphological characters remained as in the original equal weights analysis. Heuristic searches (same

commands as the dynamic approach) were performed for an execution time of 24 h for each transformation cost. Stability of clades is plotted as “Navajo rugs” at the base of clades in the strict consensus of the equal weights dynamic hypotheses (Fig. 12; Appendix S4: Fig. 1).

Implied weights (TNT). Sensitivity of the results in the static homology approach was assessed performing heuristic searches (same commands as the static approach) using different integer values of the constant of concavity (k). The selection of 11 k values was taken from the morphological analysis ($k = 1, 2, 3, 6, 8, 10, 12, 20, 35, 50, 99$). Stability of clades is displayed as “Navajo rugs” in the strict consensus of the equal weights static hypotheses (Figs 14; Appendix S4: Fig. 22).

Support values: clade support

The following support measures were calculated for the parsimony analyses: under the static approach, absolute Bremer support (BS, Bremer, 1988, 1994); relative Bremer support (relative fit difference, RFD; Goloboff and Farris, 2001); partitioned Bremer support (PBS; Baker and DeSalle, 1997; Baker et al., 1998); and symmetric resampling frequencies (SFq; Goloboff et al., 2003a); under the dynamic approach, Bremer support and Jackknifing frequencies (Jfq; Farris et al., 1996; Farris, 1997; Goloboff et al., 2003a).

Absolute and relative Bremer support measures. Under the static approach, BS was calculated heuristically in TNT searching for suboptimal trees using the optimal trees as starting point. TBR branch swapping was performed filling the tree-buffer, sequentially increasing the number of steps of suboptimal trees by one (1–2 steps), by five (5–50 steps) and by 10 (60–100 steps), retaining increasing numbers of trees by 3000 (from 2000 to 50 000) (series of commands `sub 1 hold 2000; bb=tbr fillonly; sub 2 hold 5000; bb=tbr fillonly; etc.`). Lowest values of BS are reported. RFD calculates relative amounts of evidence contradictory, and favorable, to a clade. RFD was calculated as BS, using only suboptimal trees in a number of steps no greater than the Bremer support of the group (i.e. only suboptimal trees within absolute support; command: `bsupport] ;`). Under dynamic homology, suboptimal trees were retained during the heuristic searches for best trees with the argument `visited` on the `search` command in POY. Since this procedure takes an immense execution time cost in POY 4.0, 4 h of visited trees were stored. For BS calculations (in POY 4.1), the command `report (“BSoptimal-trees.ps”, graphsupports:bremer: “visited.trees”)` was used to generate a postscript file with BS values for the optimal trees.

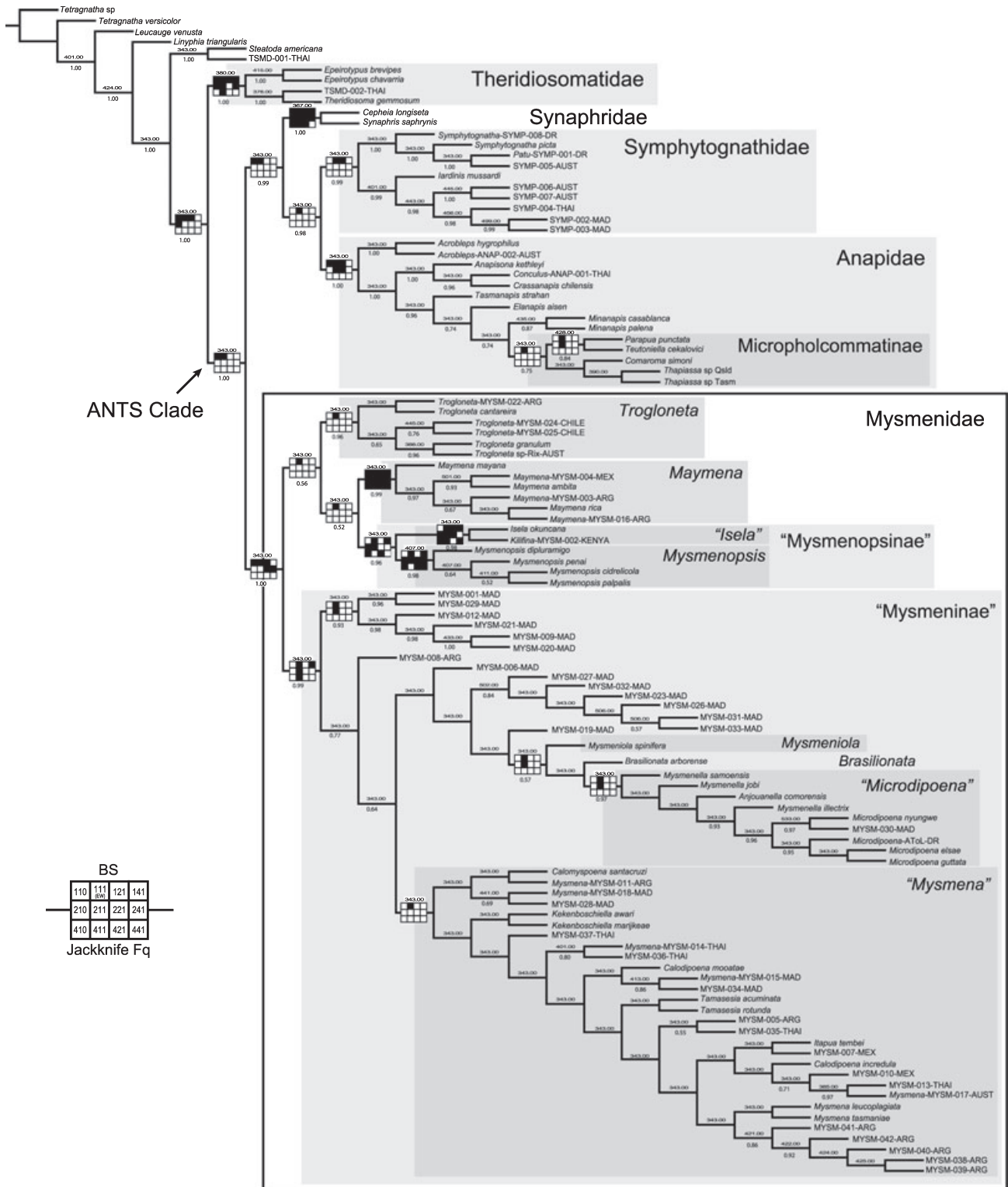


Fig. 12. The most parsimonious tree that resulted from the analysis of the complete combined (morphological, behavioural, and molecular) dataset (combined A) using the dynamic homology approach under parsimony and equal weights as implemented in POY. See tree statistics in Table 3a. Numbers above each node indicate absolute Bremer support values (BS). Numbers below each node indicate Jackknife frequencies (Fq). Filled spaces on Navajo rugs indicate recovered groups by the sensitivity scheme performed under different parameter costs (see reference rug beside tree; see text for explanation). Major clades representing taxonomic decisions discussed in the text are highlighted in grey boxes. Family codes used for unidentified species: ANAP, Anapidae; MYSM, Mysmenidae; SYMP, Symphytognathidae; TSM-D, Theridiosomatidae.

Partitioned Bremer support. The assessment of the contribution of each partition to the total Bremer support was performed only under the static approach. Since the most parsimonious hypotheses from the static approach are similar to those produced from the dynamic approach (see Results), resulting PBS values are regarded here as representatives for both datasets. PBS values were calculated for the combined and complete molecular datasets in TNT, using a script written by Carlos Peña (“pbsup.run”, available at <http://www.zmuc.dk/public/phylogeny/TNT/scripts>). The script was modified to include searches consisting of 100 replicates of RAS, followed by 100 iterations of TBR and Parsimony Ratchet as implemented in TNT, retaining five trees per replication (commands: `ratchet: iter 100 equal; mult = ratchet repl 100 tbr hold 5;`). Since PBS and BS search strategies differ, the sum of the calculated PBS values for a node is not expected to match its absolute BS value, although such values appear correlated in most nodes.

Jackknifing frequencies. Heuristic searches were computed in POY 4.0 (probability of character deletion: 0.36) performing 2000 pseudoreplicates of 10 RAS, followed by 10 TBR iterations, holding one tree (commands `calculate_support (jackknife: (remove:0.36, resample:2000), build(), swap(tbr, trees:1))`). To perform character resampling at the level of individual nucleotides (not sequence segments), the dynamic datasets were transformed into static characters (command `transform`

`(static_approx)`) prior to computing pseudoreplicates. This strategy, although not directly comparable with a dynamic homology approach, is used to increase the number of characters for jackknifing (see also POY documentation).

Symmetric resampling frequencies. Absolute SFq were calculated in TNT by computing 4000 pseudoreplicates (probability of character elimination: 0.33) performing heuristic searches consisting of 10 RAS, followed by 10 iterations of TBR, holding one tree (commands `mult: noratchet repl 10 tbr hold 1; resample sym repl 4000 freq from 0[mult];`). SFq are reported in the strict consensus of the static analysis of the combined dataset (Fig. 14), the complete molecular dataset (Fig. 16), and the reduced dataset (combined C, Appendix S4: Fig. 22). Absolute symmetric frequencies have been shown to be less biased than traditional bootstrap or jackknifing estimations (Goloboff et al., 2003a). In addition to symmetric resampling, group frequencies under traditional bootstrap (Felsenstein, 1985) and jackknife (Farris et al., 1996; Farris, 1997; Goloboff et al., 2003a) resampling schemes were also calculated (same search strategies, commands `boot` or `jak` instead of `sym` for bootstrap or jackknife resampling, respectively). Since all values were highly correlated, we report only the symmetric resampling values.

For the support values calculated in the static analyses and all resampling frequencies reported below, we refer to low support for values 0.01–2.99 (BS), 0–39 (RFD), and 50–74% (frequencies); intermediate support

Table 4

Summary of selected models with Modeltest under the Akaike information criterion (AIC), actual model and model settings for each partition as implemented in MrBayes

Partition number	Gene fragment	AIC	Model run in MrBayes	MrBayes model settings
1	12S	GTR + I + G	GTR + I + G	<code>lset applyto = (1,2,6,8,9,10) nucmodel = 4by4 nst = 6 rates = invgamma; unlink shape = (all) pinvar = (all) statefreq = (all) revmat = (all); prset applyto = (all) ratepr = variable</code>
2	16S	GTR + I + G	GTR + I + G	As partition 1
3	18S (segments 0–12)	SYM + I + G	SYM + I + G	<code>lset applyto = (3,5,7) nucmodel = 4by4 nst = 6 rates = invgamma; prset applyto = (3,5,7) statefreqpr = fixed(equal)</code>
4	18S (segments 13–18)	K80 + G	K80 + G	<code>lset applyto = (4) nucmodel = 4by4 nst = 2 rates = gamma; prset applyto = (4) statefreqpr = fixed(equal)</code>
5	18S (segments 19–38)	SYM + I + G	SYM + I + G	As partition 3
6	28S (segments 0–14)	TVM + I + G	GTR + I + G	As partition 1
7	28S (segments 15–29)	TrNef + I + G	SYM + I + G	As partition 3
8	28S (segments 30–44)	GTR + I + G	GTR + I + G	As partition 1
9	COI	TVM + I + G	GTR + I + G	As partition 1
10	H3	TVM + I + G	GTR + I + G	As partition 1
11	Morphology (discrete characters)		Standard discrete model	<code>lset applyto = (11,12) rates = gamma; prset applyto = (11,12) statefreqpr = fixed(equal)</code>
12	Gap		Standard discrete model	As partition 11

for values 3–9.99 (BS), 40–79 (RFD), and 75–84% (frequencies); and high support for values 10 or higher (BS), 80–100 (RFD), and 85–100% (frequencies). The range of values calculated for the Bremer support under the dynamic approach is unusually high (lowest BS values around 14, 150 or 350 steps) and differs for each dataset (compare BS values in Figs 12 and 15, and Appendix S4: Figs 1, 3 and 5). One of the possible explanations for such lowest values might be that the search strategies or the sample of suboptimal trees are not exhaustive enough. As a preliminary approach to address this issue (and since both static and dynamic approaches produced similar trees—see Results), the suboptimal trees generated by the BS calculation under the static approach were used to calculate BS values for the most parsimonious trees resulting under the dynamic approach. Dynamic BS calculation based on static suboptimal trees produced uninterpretable values (not shown), and this issue requires further investigation, which is beyond the scope of this study. In any case, the range of BS values calculated in the dynamic analyses was taken to represent the minimum and maximum values for each dataset. For the dynamic BS values reported below, we refer to low support for values 343–359 (total evidence combined A dataset), 14–27 (combined C dataset), and 153–184 (complete molecular A dataset); intermediate support for values 360–489 (combined A), 28–39 (combined C), and 185–229 (molecular A); and high support for values higher than 490 (combined A), 40 (combined C), and 230 (molecular A).

Bayesian phylogenetic inference. Bayesian analyses of the total evidence (combined A excluding continuous morphological characters), morphological, and complete molecular (molecular A) datasets were performed in MrBayes v. 3.1.2 (Huelsenbeck and Ronquist, 2001; Ronquist and Huelsenbeck, 2003). The analysis with the most aggressive searches (the total-evidence analysis, see below) was run on the computer cluster PYRAMID at GWU. For each gene fragment, best-fit models of sequence evolution were selected using Modeltest v. 3.7 (Posada and Crandall, 1998) under the Akaike information criterion (AIC; see Posada and Buckley, 2004). Best-fit models for each partition and commands for MrBayes are reported in Table 4. Since the number of models (and parameters) explored by Modeltest is larger and more complex than the models implemented in MrBayes, selected models were simplified to fit computational capability (see Table 4 for selected AIC models and those implemented in MrBayes). The morphological (only discrete characters) and gap partitions (see below) were parameterized under the “standard discrete (morphology) model” of Lewis (2001) with fixed state frequencies (see Table 4). Two independent runs of 50 000 000 generations for the combined analysis (18 000 000 for

the molecular; 10 000 000 for the morphological partitions) using four chains (eight chains in the combined dataset) and saving one tree every thousand generations were performed (e.g. commands `mcmc ngen=18000000 printfreq=1000 samplefreq=1000 nchains=4 temp=0.15 savebrlens=yes`). Standard deviation of posterior probabilities lower than 0.01% ensured convergence of the results in the morphological partition. Analyses of the complete molecular and the combined (total evidence) datasets, however, failed to reach convergence after 18 000 000 and 50 000 000 generations, respectively, and low difference of temperature (0.15) between cold and heated chains (standard deviation in both analyses *ca.* 0.17%). Failure to reach convergence in independent parallel analyses of large datasets has been reported recently, and seems to be not uncommon (e.g. Moore et al., 2007; Soltis et al., 2007; Hackett et al., 2008). The negative log likelihood values were plotted against generations to detect the number of initial generations until the values stabilized (*ca.* 80 000 for the morphological, *ca.* 600 000 for the molecular partition). The combined partition reached a plateau after 16 800 000 generations. Trees from initial generations before stabilization were discarded (command `burnin`). Effective sample sizes (ESS) higher or much higher than 200 in all analyses indicate that a relatively large number of independent samples were drawn from the posterior distribution, minimizing correlation among the samples. Posterior probabilities were calculated and reported as a majority-rule consensus of the saved trees. Gaps were converted into binary characters following the method of Simmons and Ochoterena (2000) as implemented in GapCoder (Young and Healy, 2002). Gaps provided 446 additional informative characters and were included in the total evidence and molecular datasets.

Results

This section reports the results of all cladistic analyses performed in this study. Names of mysmenid taxa in quotation marks refer to informal taxon names based on the preferred hypothesis of relationships (Fig. 12; see below). Formal taxonomic and nomenclatorial actions will be done elsewhere. Original taxonomic names from previous works or formally addressed here are depicted without quotation marks.

Dynamic homology approach: all successfully amplified data

Combined analyses: complete dataset (combined A). Analysis of the total-evidence dataset (109 taxa, *ca.* 6400 bp) produced a single most parsimonious tree

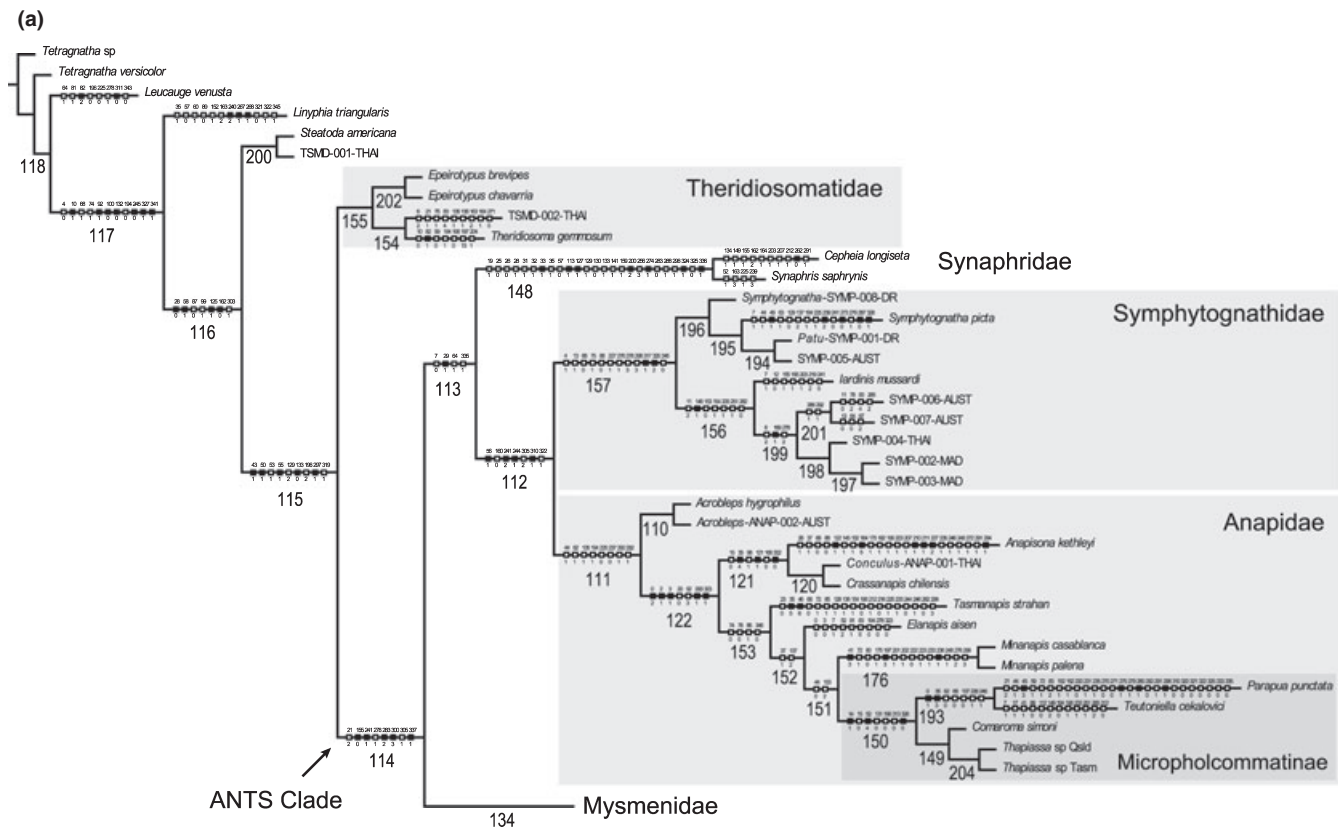


Fig. 13. The most parsimonious tree that resulted from the analysis of the combined (morphological, behavioural, and molecular) dataset (combined A) using the dynamic homology approach under parsimony and equal weights as implemented in POY. See tree statistics in Table 3a. Unambiguous morphological character optimizations are shown for every branch in the tree. Node numbers are shown below each node. Empty and filled boxes represent homoplasious and non-homoplasious transformations, respectively. Major clades representing taxonomic decisions discussed in the text are highlighted in grey boxes. Family codes used for unidentified species: ANAP, Anapidae; MYSM, Mysmenidae; SYM, Symphytognathidae; TSMD, Theridiosomatidae.

(MPT) of 16 894.62 steps (Figs 12 and 13). This cladogram is chosen as the working hypothesis for this study and, unless otherwise stated, all other analyses are compared with it. Autapomorphic or unambiguous synapomorphic morphological changes are reported in Appendix S3.

Mysmenidae (Node 134). The results of this analysis support the monophyly of Mysmenidae as redefined here (i.e. excluding the genus *Iardinis*), in agreement with analysis of the morphological partition (compare with Fig. 11; see also Lopardo, 2009). Morphology and absence of molecular data for *Iardinis* place it within Symphytognathidae with relatively high support (see below). Support for Mysmenidae is contradicting (BS 343, Jfq 100%), and the family is recovered in five parameter sets. Internal relationships of Mysmenidae are fully resolved. Most of the traditional nonmonotypic mysmenid genera, as represented in this dataset, are monophyletic (except *Calodipoena* and *Mysmenella*). There are two main mysmenid lineages: Node 161 sister to Node 133 (“Mysmeninae”).

Node 161. This node includes a basal *Trogloneta*, sister to *Maymena* and “Mysmenopsinae” (*Mysmenopsis* plus “*Isela*”, both kleptoparasitic), and has low support (BS 343, Jfq 56%), recovered only under equal weights. In addition, the clade is recovered in just three molecular partitions related to the 28S gene fragment. *Maymena*, *Mysmenopsis*, and “*Isela*” are well supported in terms of Jfq and stability. *Trogloneta* is recovered only under equal weights; different weighting schemes place this genus paraphyletic with respect to “Mysmeninae” (not shown).

“*Mysmeninae*” (Node 133). This clade comprises the remaining mysmenid representatives. Support is contradicting (BS 343, Jfq 99%), recovered by four different parameter sets. Moreover, the clade is recovered by several individual gene fragments, partial fragment combinations, and the complete molecular and combined datasets (and morphology; Table 5). However, relationships within this lineage are unstable and are affected by variations in data partitions and taxon composition (Table 5). A paraphyletic assemblage of

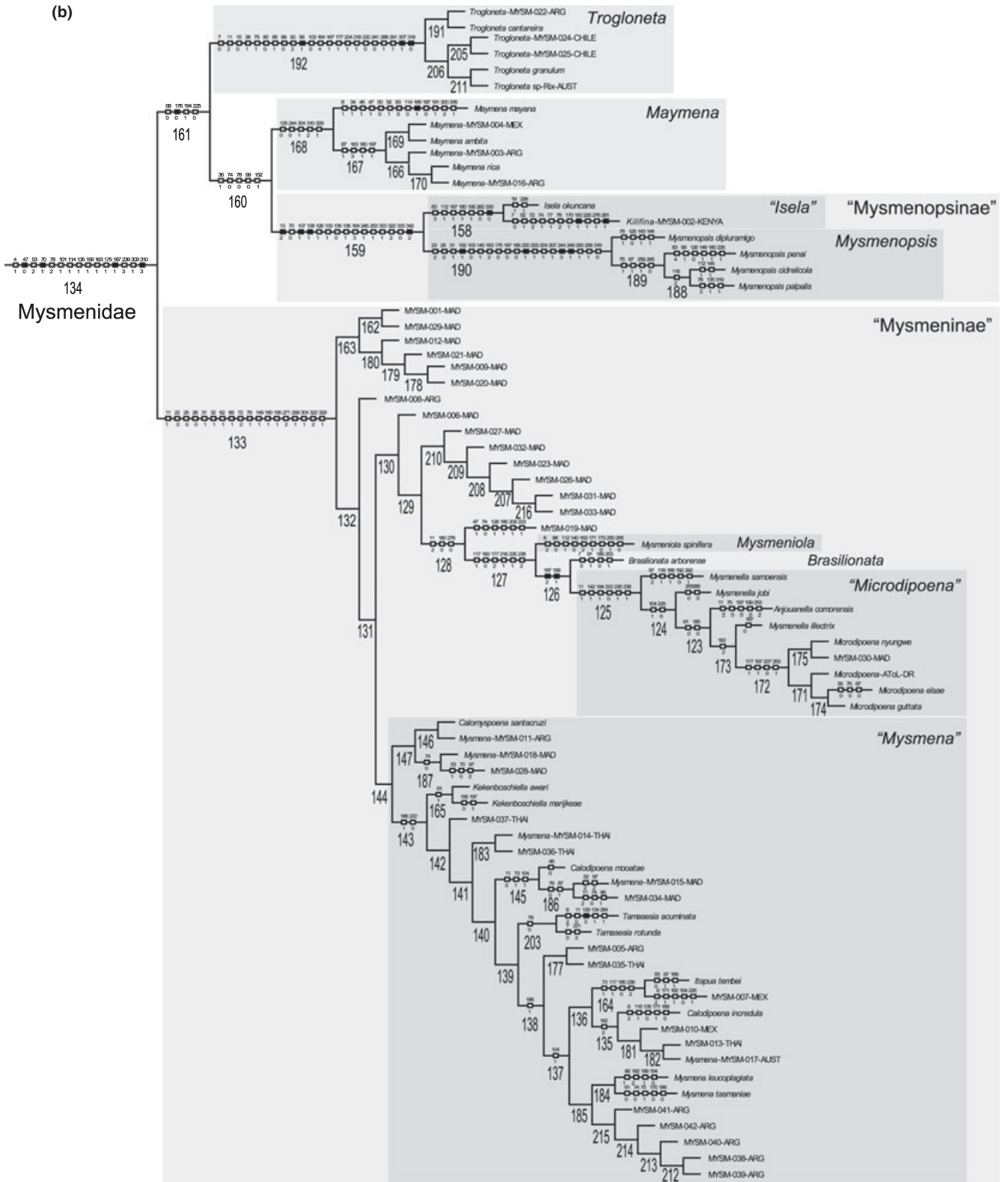


Fig. 13. Continued.

Table 5
Clade sensitivity to different data partitions under the dynamic homology criterion (POY)

Node number	Clade name/ composition	Dataset/partition																								
		Combin B	Combin C	Combin D	Morphology	Morphology reduced	12S	16S	18S	18S (partial)	28S	28S (partial)	COI	H3	Molecular A	Molecular B	Molecular C	Molecular D	Mitochondrial	Protein	Nuclear	Nuclear (partial)	Ribosomal	Ribosomal (partial)		
115	"Symphytothooids" [excl. TSMID-001-THAI]																									
155	"Theridiosomatidae" [excl. TSMID-001-THAI]																									
114	ANTS clade																									
113	Synaphiridae + Symphytothooids + Anapidae																									
148	Synaphiridae																									
112	Symphytothooids + Anapidae																									
157	Symphytothooids																									
111	Anapidae																									
150	Conaroma + Taphiassa + micropholcommatines																									
193	Micropholcommatines																									
134	Mysmenidae																									
161	Troglogneta + Maymena + "Isela" + Mysmenopsis																									
192	Troglogneta																									
160	Maymena + "Isela" + Mysmenopsis																									
168	Maymena																									
159	"Mysmenopsinae"																									
158	"Isela"																									
190	Mysmenopsis																									
133	"Mysmeninae"																									
165	Kekentboschiella																									

"n/a", clade not represented or not enough information available for clade monophyly.

Nodes are compared to the preferred phylogenetic hypothesis (complete combined dataset analysed under the dynamic homology criterion in POY). Dark grey squares indicate recovered clades. See "Materials and Methods" and Table 3 for description and composition of each partition.

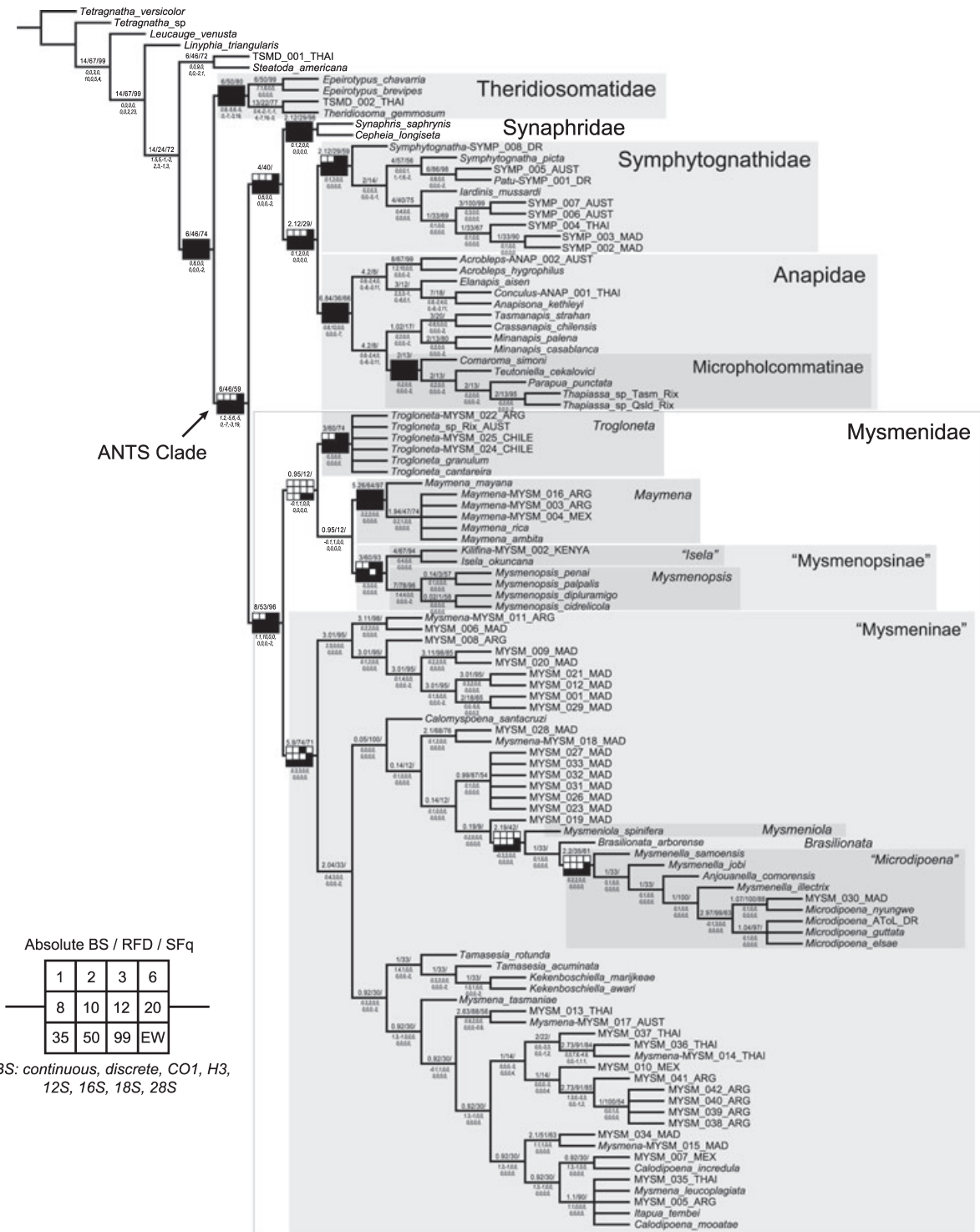


Fig. 14. Strict consensus of the 1120 most parsimonious trees that resulted from the analysis of the combined (morphological, behavioural, and molecular) dataset (combined A) using the static homology approach under parsimony and equal weights as implemented in TNT. See tree statistics in Table 3b. Numbers above each node indicate absolute Bremer support values (BS), relative BS (RFD), and symmetric resampling frequencies (SFq). Numbers below each node indicate partitioned BS (PBS) values for two morphological (“continuous” and “discrete”) and six molecular partitions. Filled spaces on Navajo rugs indicate groups recovered by the sensitivity scheme performed under different implied weighting concavities (see reference rug beside tree; see text for explanation). Major clades recovered from the complete combined analysis (see Figs 12 and 13) are highlighted in grey boxes. Family codes used for unidentified species: ANAP, Anapidae; MYSM, Mysmenidae; SYMP, Symphytognathidae; TSMD, Theridiosomatidae.

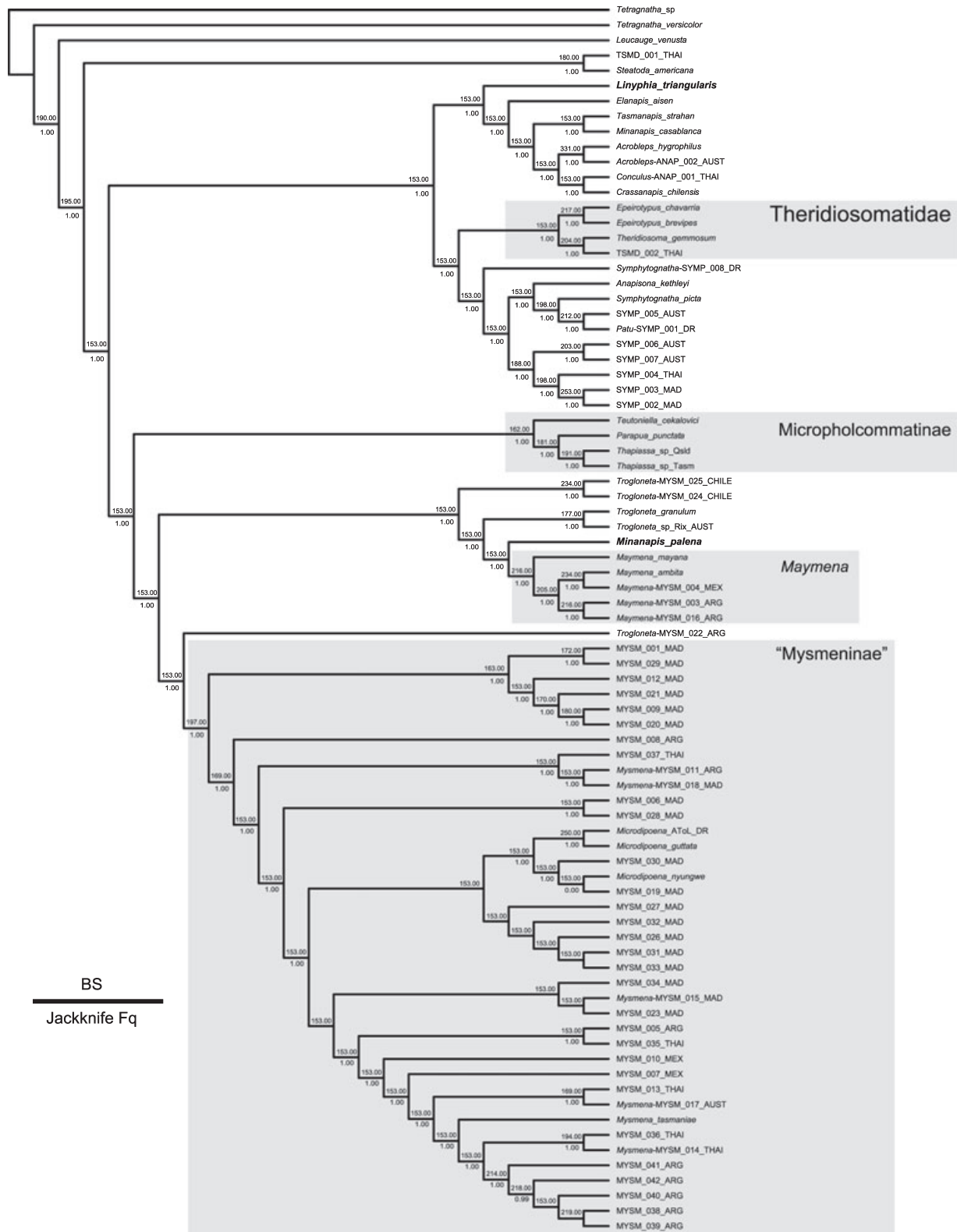


Fig. 15. The most parsimonious tree that resulted from the analysis of the complete molecular partition (molecular A) using the dynamic homology approach under equal weights parsimony as implemented in POY. See tree statistics in Table 3a. Numbers above each node indicate absolute Bremer support values (BS). Numbers below each node indicate jackknife frequencies (Fq). Taxa in controversial placements are in bold (see text for discussion). Major clades recovered from the complete combined analysis (see Figs 12 and 13) are highlighted in grey boxes.

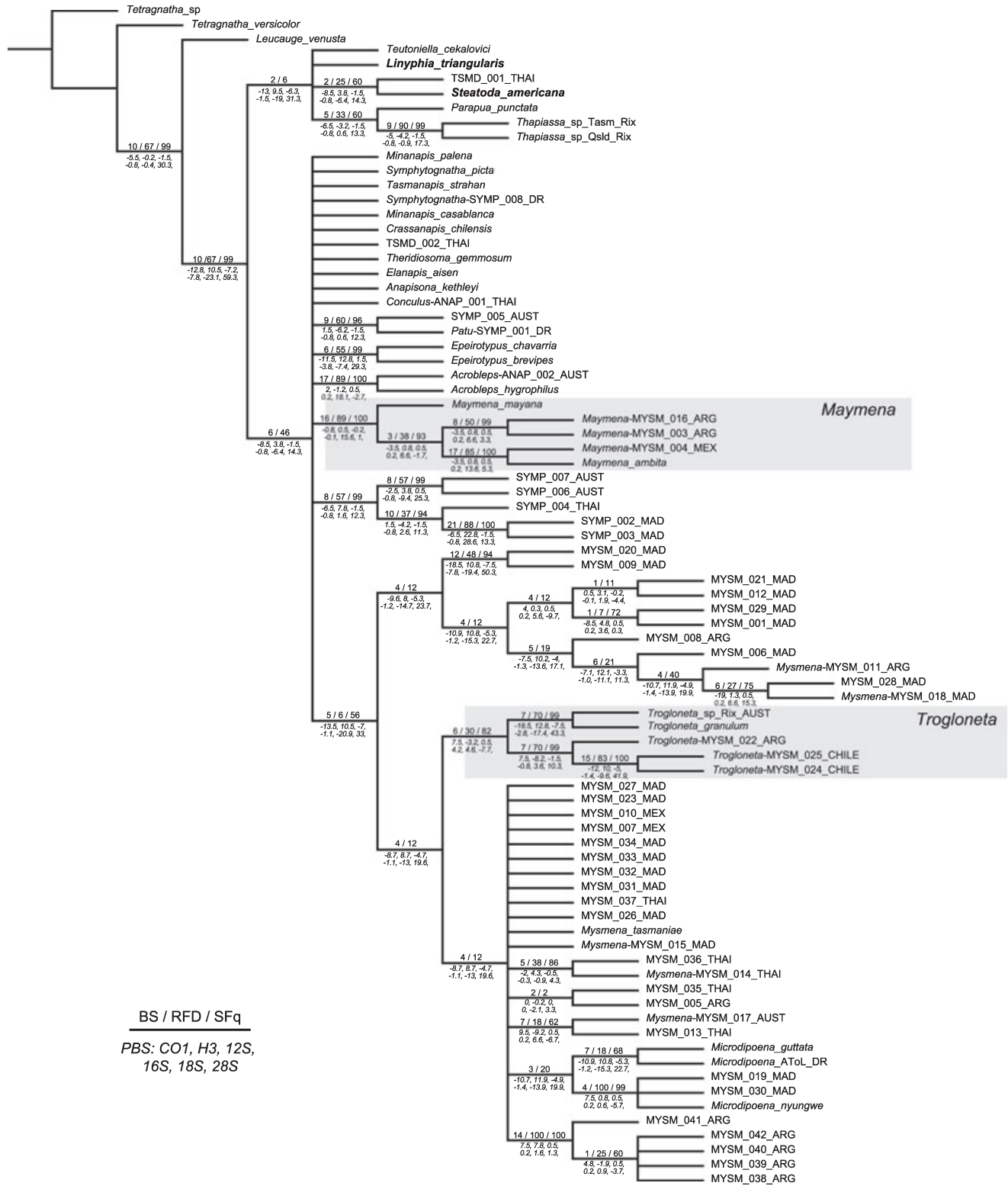


Fig. 16. Strict consensus of the 136 most parsimonious trees that resulted from the analysis of the complete molecular partition (molecular A) using the static homology approach under equal weights parsimony as implemented in TNT. See tree statistics in Table 3b. Numbers above each node indicate absolute Bremer support values (BS), relative BS (RFD), and symmetric resampling frequencies (SFq). Numbers below each node indicate partitioned BS (PBS) values for six molecular partitions. Taxa in controversial placements are in bold (see text for discussion). Major clades recovered from the complete combined analysis (see Figs 12 and 13) are highlighted in grey boxes.

seven undescribed species is placed at the base of two relatively large clades, both comprising all (but not exclusively) described species. None of these clades is supported by any unambiguous morphological synapomorphies. Node 130 includes *Mysmenella* (polyphyletic), *Microdipoena* (monophyletic), and the monotypic genera *Anjouanella*, *Brasilionata*, and *Mysmeniola*. Node 144 comprises *Calodipoena* (polyphyletic), *Mysmena*, *Kekenboschiella*, and *Tamasesia* (monophyletic).

“*Symphytognathoids*” (Node 115). Results of this analysis support relationships of “symphytognathoids” as proposed by Griswold et al. (1998, in part), and modified by Schütt (2003), and Lopardo and Hormiga (2008). Theridiosomatidae is polyphyletic, and when all five representatives of this family were included, none of the analyses of different data partitions recovered them as monophyletic. The undescribed theridiosomatid from Thailand, TSMD-001-THAI (scored only for sequence data), is sister to *Steatoda*, and across the different analyses this species was also related to *Linyphia*, Symphytognathidae, some anapids, micropholcommatids, or *Epeirotypus*, among other hypotheses (Figs 12, 14 and 15; see also Appendix S4: Figs 3, 5 and 8–21). The remaining theridiosomatids form a monophyletic group (Fig. 12; Table 5), and are referred to as Theridiosomatidae (Node 155, that is, excluding TSMD-001-THAI). Support for symphytognathoids is contradicting (BS 343, Jfq 100%), recovered under four parameter sets; its monophyly is not obtained in any molecular partition analysed, as non-symphytognathoid outgroup species are consistently placed within this group, although in no consistent pattern and with variable support values (Table 5; Figs 12 and 15; Appendix S4: Figs 1–21).

Theridiosomatidae is sister to a clade containing all other symphytognathoid families, the Anterior Tracheal System clade (ANTS, Node 114; Fig. 12; see below). Symphytognathoids and the ANTS clade are monophyletic only in those combined partitions that include the morphological data or under morphology alone. The ANTS clade comprises two main lineages (BS and stability for this clade are low): Mysmenidae and a second lineage (Node 113) comprising Synaphridae sister to Anapidae + Symphytognathidae. This latter lineage has contradicting support (BS 343, Jfq 99%) and is one of the most unstable interfamilial clades within symphytognathoids, recovered by two parameter sets. Synaphridae monophyly (Node 148) finds support on the morphological dataset (no sequence data available); the family is relatively well supported and stable. Anapidae plus Symphytognathidae (Node 112) is also found only when the morphological dataset is combined with the molecular partition (and with the morphological dataset alone), except for the 12S partition. This relationship (BS 343, Jfq 98%) is recovered only by the equal weights scheme.

Symphytognathidae (Node 157; BS 343, Jfq 99%) is monophyletic under two parameter sets, and includes *Iardinis mussardi* (misplaced in Mysmenidae by Petrunkevitch (1928); see above). Anapidae (Node 111) is monophyletic and includes a distal clade grouping the micropholcommatid taxa (Node 150) with *Comaroma simoni* (currently in Anapidae). Molecular evidence places *Taphiassa* representatives closely related to other micropholcommatids (as recently proposed by Rix et al., 2008; although excluding the genus *Teutoniella*), and morphology does so with *Comaroma*. Support and stability for the redefined Anapidae are contradicting (BS 343, Jfq 100%, five parameter sets). Although Micropholcommatidae could be monophyletic if *Comaroma* is interpreted as micropholcommatid, treating the latter lineage at the family rank renders Anapidae paraphyletic. The familial placement of the controversial Australian genus *Acrobleps* as anapid is here confirmed, corroborating the hypothesis of Lopardo and Hormiga (2008). *Acrobleps* is basal according to the combined data, and *A. hygrophilus* is sister to an undescribed Australian species. *Minanapis* is monophyletic.

Comparison between total-evidence and morphological hypotheses. At the interfamilial level, the results of the combined dynamic analysis differ from the analysis of the morphological partition in the placement of Theridiosomatidae (compare Figs 11 and 12). Morphological data place Theridiosomatidae sister to Mysmenidae (Fig. 11). The total-evidence analysis, however, places Theridiosomatidae basally as sister to the ANTS clade. The pattern of relationships among Anapidae, Symphytognathidae, and Synaphridae remains identical between the two hypotheses, differing only within each family (except Synaphridae, represented by two species) (see Lopardo, 2009). Within Mysmenidae, morphology recovers a pectinated generic pattern, with *Maymena* sister to all other mysmenids, then *Trogloneta*, and finally “Mysmenopsinae” sister to “Mysmeninae”. The total-evidence analysis, in contrast, supports two main clades: “Mysmeninae” and a clade comprising all other genera.

Combined analyses: reduced (overlapping) dataset (combined C). The taxon sampling in this dataset (37 taxa scored for molecules and morphology, ca. 6400 bp) includes representatives of most main groups from the complete dataset of 109 taxa. Cladistic analysis results in a single MPT of 10 115.91 steps (see Appendix S4: Figs 1 and 2). Symphytognathoids, Mysmenidae, Theridiosomatidae, and Symphytognathidae are monophyletic. Bremer support for main clades is not particularly high (BS between 14 and 29), except Theridiosomatidae, Symphytognathidae, and “Mysmeninae” (BS 50, 37, and 38, respectively). Jackknife frequencies, however, are the highest (100%) for

almost all clades. Stability is in agreement with BS values. As in the total-evidence analysis, Anapidae (poorly supported and unstable) includes a distal “Micropholcommatinae”. Relationships among families and within Mysmenidae differ from the complete dataset. Anapidae is sister to all other families, which are split into two clades: Mysmenidae (BS 21, Jfq 100%, recovered in six parameter sets), and Theridiosomatidae plus Symphytognathidae (recovered under three parameter sets, BS 14). This pattern of familial relationships has never been proposed (compare with Figs 1–4 and 11). Within Mysmenidae, “Mysmeninae”, *Maymena*, and *Microdipoena* are monophyletic, with high support. *Trogloneta* is basal.

Molecular partitions: individual genes. None of the gene fragments analysed separately supported the monophyly of symphytognathoids, Mysmenidae, or any of the interfamilial relationships recovered by the total-evidence analysis, with exception of the 12S fragment (see strict consensus of each gene in Appendix S4: Figs 8, 10 and 12–15; see also Tables 3a and 5). In all six analyses, non-symphytognathoid outgroup taxa were placed within symphytognathoid clades. Theridiosomatidae is monophyletic in the 28S partition, Anapidae in the 16S partition, and Symphytognathidae in both 28S and 16S. Mysmenidae is never monophyletic, “Mysmeninae” is recovered in two partitions (12S and 18S), and *Maymena* and *Trogloneta* are recovered in three partitions each (*Maymena* in 16S, 18S, and 28S; *Trogloneta* in 16S, CO1, and H3).

Molecular partitions: combinations of individual genes (mitochondrial, protein, nuclear, ribosomal). None of the four combinations of genes supported symphytognathoid monophyly or any interfamilial relationships rendered by the total-evidence analysis (Tables 3a and 5; see the strict consensus of each analysis in Appendix S4: Figs 16–18 and 20). Only the nuclear partition supported Symphytognathidae, “Mysmeninae”, *Maymena*, and Mysmenidae, although the latter family is not monophyletic in the analyses of each individual gene belonging to this partition (18S, 28S, and H3). Just one mysmenid genus is monophyletic in the remaining partitions: *Trogloneta* (mitochondrial and protein partitions) and *Maymena* (ribosomal partition).

Molecular partitions: complete and reduced molecular datasets (molecular A, molecular C). Analysis of the complete molecular dataset produced a single MPT of 14 901 steps (Fig. 15; Tables 3a and 5). Symphytognathoids are nonmonophyletic due to *Linyphia* (Linyphiidae) as sister to most anapids (and TSMD-001-THAI as sister to *Steatoda*, Theridiidae). Ignoring the position of *Linyphia* and TSMD-001-THAI for descriptive purposes, two main clades resulted. One clade comprises most

traditional anapids (i.e. excluding Micropholcommatidae), Theridiosomatidae, and Symphytognathidae. The second clade includes all micropholcommatid and mysmenid representatives (Fig. 15). In the first clade, anapids grouped together, except *Anapisona* and *Minanapis palena* (placed within Symphytognathidae and Mysmenidae, respectively). Theridiosomatidae, Micropholcommatidae, *Maymena*, and “Mysmeninae” are monophyletic.

Analysis of the reduced molecular dataset (molecular C) resulted in two MPTs of 8913 steps (see strict consensus in Appendix S4: Fig. 6; see also Tables 3a and 5). Symphytognathoids are not monophyletic because *Steatoda* (Theridiidae) is placed within a clade including most anapids. In addition, the anapid *Anapisona kethleyi* was placed within Symphytognathidae, and *Minanapis palena* within Mysmenidae. The clade comprising most anapids, however, includes the micropholcommatid representatives. Mysmenidae is not monophyletic, “Mysmeninae” and Theridiosomatidae are monophyletic.

Dynamic homology approach: partial data

The analysis of the molecular dataset comprising fragments obtained from pairs of primers with successful amplification rate (18S partial, 28S partial, CO1, and H3) and the morphological dataset (i.e. combined B, a total of 109 taxa and ca. 2500 bp; Table 3a) produced one MPT of 8903.43 steps (see Appendix S4: Fig. 3). Symphytognathoids are monophyletic. The general topology is in agreement with the morphological partition (compare with Fig. 11). However, four taxa showed conflicting positions (in addition to TSMD-001-THAI): two representatives of the theridiosomatid genus *Epeirotypus* are placed within *Trogloneta* and, conversely, a clade with two undescribed *Trogloneta* species from Chile are basal, sister to all other symphytognathoids. DNA sequences of the four specimens were obtained from three different sources (Table 2), suggesting that contamination is unlikely to be the cause of this conflicting placement. Excluding the four taxa recovers the monophyly of *Trogloneta*, Theridiosomatidae, and Mysmenidae (cladogram not shown, see statistics in Table 3a).

The same dataset reduced to overlapping taxa (combined D, 37 taxa, ca. 2500 bp) rendered one MPT of 5172.65 steps (Appendix S4: Fig. 4). Symphytognathoids are monophyletic, with a pattern of familial relationships resembling the complete total-evidence analysis, except *Maymena*, which is sister to Theridiosomatidae, forming the most basal clade. “Mysmeninae”, Theridiosomatidae, Symphytognathidae, and Anapidae, including a distal Micropholcommatinae, are all monophyletic.

Analyses of the partial ribosomal fragments separately, or combined into ribosomal and nuclear

partitions, or into complete and reduced molecular datasets (Table 3a) failed to support most clades obtained in the total-evidence analysis. Symphytognathoids, and its families “Mysmeninae” and *Trogloneta*, are nonmonophyletic, and relationships among these taxa are not recovered (Table 5; Appendix S4: Figs 5, 7, 9, 11, 19 and 21). In contrast, *Maymena* is consistently monophyletic in all analyses.

Static homology approach: additional analyses

Parsimony analyses. The total-evidence analysis (combined A) yielded 1120 MPTs of 19 430.369 steps (see strict consensus in Fig. 14; Table 3b for statistics). Overall, the pattern of familial and mysmenid relationships is similar to the results of the dynamic homology analysis (Figs 12 and 13), except as noted. Relationships within the Anapidae plus Symphytognathidae clade differ. Micropholcommatinae is placed distally within Anapidae, sister to *Comaroma*. Relationships within *Trogloneta* and *Maymena* are mostly unresolved; only Node 129 within “Mysmeninae” is recovered (node numbers refer to the dynamic hypothesis, see Fig. 13). All families and their relationships are similar under most implied weighting concavity values, suggesting a strong level of stability, at least at the familial and interfamilial levels (Fig. 14). BS values are generally low. PBS values suggest a relatively minimal contribution of the molecular partitions to the combined topology, except the 28S fragment, which seems to contradict several clades; the morphological partition supports most of the nodes. RFD values are greater particularly in main clades of Mysmenidae. Symmetric resampling frequencies are highest in Mysmenidae, *Maymena*, and several clades containing taxa scored only for morphology.

The combined analysis, including partial molecular partitions and morphology (combined B), resulted in 20 MPTs of 9152.099 steps, with a mostly unresolved strict consensus in terms of familial relationships (Appendix S4: Fig. 23; Table 3b). Lack of resolution in the consensus is due to two *Trogloneta* species from Chile grouping with other *Trogloneta* species, or alternatively with Anapidae. The main structure of the cladogram (ignoring the position of the two *Trogloneta*) is largely congruent with the hypothesis of interfamilial relationships from the morphological partition alone (compare with Fig. 11). Relationships within “Mysmeninae” differ.

The analysis of the reduced dataset (combined C) produced a single MPT of 11 476.159 steps (Appendix S4: Fig. 22). As the dynamic analysis, the results support the monophyly of symphytognathoids, Mysmenidae, Theridiosomatidae, and Symphytognathidae. Micropholcommatidae is basal to a clade comprising a

paraphyletic Anapidae with respect to Symphytognathidae. Mysmenidae comprises a basal *Maymena* sister to *Trogloneta* and “Mysmeninae”. The same reduced combined dataset including the successful molecular partitions (combined D) resulted in one MPT of 5310.969 steps (Appendix S4: Fig. 24). The resulting hypothesis agrees with the previous dataset in the monophyly of the main taxa, and the paraphyly of Anapidae. Theridiosomatidae is sister to Mysmenidae, and Micropholcommatidae is placed distally. As with the dynamic homology analysis, the complete molecular dataset (molecular A) did not support the monophyly of symphytognathoids and its families, or their interrelationships (Fig. 16). *Maymena* is monophyletic, but it falls outside a clade formed by the remaining Mysmenidae. PBS values suggest that the nuclear fragments H3 and 28S support (and therefore are most probably influencing) the complete molecular topology, while it is contradicted in different degrees by the remaining genes. RFD values are somehow in agreement with symmetric resampling frequencies. Finally, the analyses of different static gene combinations or individual genes resulted overall in optimal cladograms that were comparable with, and equally or less resolved than, the corresponding dynamic trees (Fig. 16; Appendix S4: Figs 25–41).

Bayesian analyses. The pattern of relationships obtained in the majority-rule consensus tree resulting from the total evidence Bayesian analysis (Fig. 17; 109 taxa, 350 discrete morphological, 6037 molecular characters) differs from the dynamic homology parsimony hypothesis as follows (compare with Fig. 12; percentages in parentheses represent posterior probabilities). Mysmenidae (100%), “Mysmenopsinae” (100%, scored only for morphology), “Mysmeninae” (58%), the “mysmenine” Node 163 (100%, see Fig. 13), Synaphridae (93%, scored only for morphology), Symphytognathidae (100%, excluding *Iardinis mussardi*), and Anapidae (57%) are monophyletic. Theridiosomatidae and “symphytognathoids” are not monophyletic (as *Epeirotypus* grouped with *Steatoda*, 85%). The remaining theridiosomatids (100%) are sister to Mysmenidae (100%). Relationships within “Mysmeninae” are mostly unresolved. Familial relationships excluding *Epeirotypus* (100%) are mostly in agreement with the combined dynamic homology parsimony hypothesis, except for the sister relationship between Mysmenidae and the theridiosomatid representatives scored for morphology.

The pattern of relationships obtained in the majority-rule consensus tree resulting from the complete molecular Bayesian analysis (Appendix S4: Figs 42 and 43; 81 taxa, 6037 characters) differs from the total-evidence dynamic analysis as follows (compare with Fig. 12). Symphytognathoids (and Anapidae) are not monophyletic, as *Steatoda* is placed within Micropholcommatidae

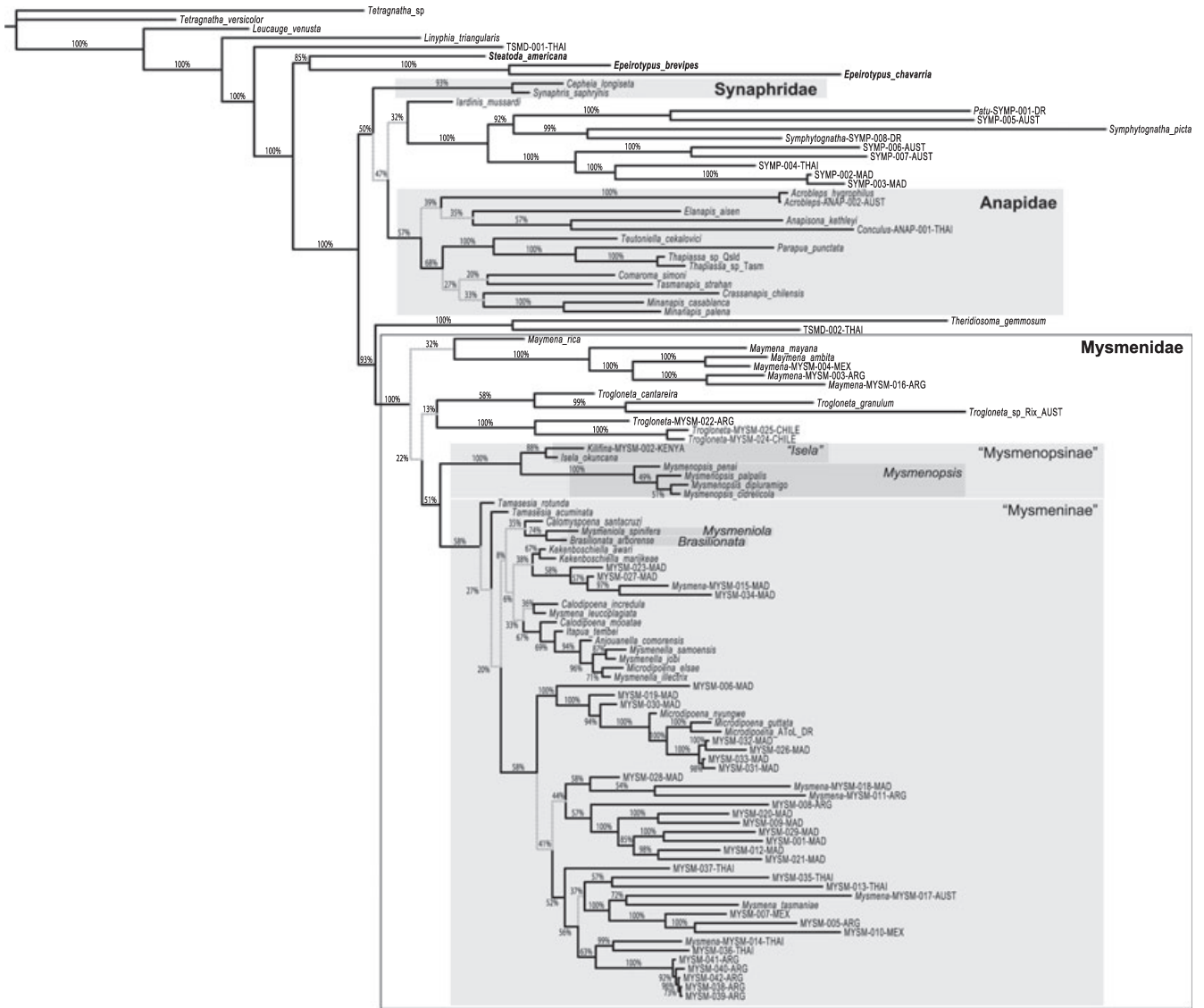


Fig. 17. Bayesian trees that resulted from the Bayesian analysis of the combined (morphological, behavioural, and molecular) dataset (combined A excluding continuous morphological characters). All compatible groups are represented. Numbers above each node indicate posterior probabilities. Nodes with posterior probabilities lower than 50% are depicted by dotted grey lines. See selected models and model settings in Table 4. Taxa in controversial placements are in bold (see text for discussion). Major groups recovered from the complete combined analysis (see Figs 12 and 13) are highlighted in grey boxes. Family codes used for unidentified species: ANAP, Anapidae; MYSM, Mysmenidae; SYMP, Symphytognathidae; TSMD, Theridiosomatidae.

(100%). Mysmenidae (62%), *Trogloneta* (54%), *Maymena* (100%), “Mysmeninae” (62%, relationships mostly unresolved), the “mysmenine” Node 163, and Theridiosomatidae (95%, including *Epeirotypus*) are monophyletic. Familial relationships (100%; i.e. ignoring *Steatoda*) are mostly unresolved.

The Bayesian analysis of the morphological partition (Appendix S4: Figs 44 and 45; 65 taxa, 350 characters) recovered the monophyly of symphytognathoid (99%) and all its families (100% each). Interfamilial relationships (mostly with high posterior probabilities) differ from the morphological parsimony analysis (compare

with Fig. 11) in the basal placement of Synaphridae. Within Mysmenidae, relationships within the clade comprising *Trogloneta*, “Mysmenopsinae”, and “Mysmeninae” (98%), are unresolved. *Maymena* is not monophyletic.

Discussion

The total-evidence analysis using dynamic homology under parsimony and equal weights supports the monophyly of Mysmenidae, although support values

for this family are contradicting, and stability values are intermediate (Fig. 12). Within Mysmenidae, only the monophyly of *Maymena* is highly stable, although with contradicting support, and it is recovered by most data partitions. It is followed, in terms of support, by “*Isela*” and *Mysmenopsis*. However, relationships among *Maymena*, *Trogloneta*, and “Mysmenopsinae” are sensitive to parameter costs and character variation. “Mysmeninae” monophyly is recovered by most combined partitions, but support and sensitivity values are not high and relationships within this clade are very unstable. Our preferred phylogenetic hypothesis for Mysmenidae (Figs 12 and 13) is based in all available data, and it provides the basis for the family classification. The concomitant formal taxonomic changes will be published elsewhere.

Theridiosomatidae and Synsphyridae are the two most robustly supported and stable symphytognathoid families, but their phylogenetic placement varies depending on the parameter costs used in the analyses. Parameter changes within the morphological dataset place Synsphyridae as sister to a clade comprising Anapidae plus Symphytognathidae, or as a basal symphytognathoid family (Lopardo, 2009). In addition, when molecular data are combined with morphology, the placement of Theridiosomatidae becomes unstable. Morphology alone places Theridiosomatidae sister to Mysmenidae (Fig. 11), while a reduced dataset comprising molecules and morphology of only those taxa scored for both data partitions (37 taxa in total) places Theridiosomatidae as sister to Symphytognathidae (Appendix S4: Fig. 1). The total-evidence hypothesis preferred here (Fig. 12) places Theridiosomatidae basally within symphytognathoids, sister to all other families (i.e. sister to the ANTS clade; see discussion below). The parsimony analysis of the complete dataset under a static homology criterion recovers a similar topology, although with decreased resolution (Fig. 14). The PBS values suggest a relatively minimal contribution of the molecular partitions to the combined topology, except the 28S fragment, which seems to contradict several clades; however, the morphological partition supports most of the nodes. In the total-evidence Bayesian analysis, the relationship among symphytognathoid families is in agreement with the parsimony analyses, but, as the morphological partition, it recovered a sister relationship between Mysmenidae and the theridiosomatid representatives scored for morphology (see above and Fig. 17).

Given the sensitivity of the total-evidence dataset to parameter variation and character composition, future hypotheses on the relationships among symphytognathoid families might change. Different genes and combinations of genes provide a mixture of signals that, when analysed separately, fail to recover symphytognathoid monophyly, or even the monophyly of the individual families. The lack of strong signal in the different

molecular partitions used in this study is evident by the placement of non-symphytognathoid outgroup taxa within the symphytognathoids, even the distantly related members of the families Linyphiidae and Tetragnathidae.

Exploration of different molecular partitions, including individual genes, combinations of genes, total molecular data comprising all evidence, and sequences from primers with high amplification success, shows high levels of homoplasy and a mixture of signals in terms of the monophyly of the symphytognathoid families (or patterns of familial relationships). Partitioned Bremer support values for the different genes when all genes are combined into a single molecular dataset suggest contradicting signals, where the nuclear fragments of H3 and 28S seem to support the combined molecular topology (static homology parsimony; Fig. 16), while the remaining fragments contradict (to different degrees) most of its nodes. When the morphological data are incorporated into the analysis, the monophyly of most of the families is supported and a more resolved pattern of relationships among them is also recovered. Under the static homology parsimony approach, the topology of the total-evidence analysis seems to be supported mostly by the morphological partition, while each of the six molecular partitions provides a minimal contribution of information, except for the nuclear 28S fragment, which contradicts most of the nodes (see PBS values in Fig. 14). The morphological dataset is not free of homoplasy either (Lopardo, 2009), and the morphological characters represent *ca.* 11.5 or 27% of the total informative characters when all molecular or the most successful genes, respectively, are combined. Therefore, even though representing a smaller proportion of characters (also when compared with the 28S partition alone), the morphological data supersede the molecular data and play an important role in determining the topology of the preferred hypothesis. Additional data, both taxa and characters from different sources, are needed for a more robust and stable hypothesis of relationships.

Discrepancies in the phylogenetic signal between morphological and molecular partitions, and even within molecular partitions, in arachnid datasets are not new (see below). Furthermore, it seems that incongruent signals among partitions are not uncommon in various animal groups such as squamates (Lee, 2005; Wiens et al., 2008); birds (McCracken et al., 1999); cichlid fishes (Farias et al., 2000; López-Fernández et al., 2005); polychaetes (Bleidorn et al., 2009); salamanders (Wiens et al., 2003); marsupials (Asher et al., 2004); and insects (Wahlberg and Nylin, 2003). When different datasets provide extremely different phylogenetic signals, at least one of them might not reflect the evolutionary history of lineages. Our notion of character evolution and phylogenetic patterns of relationships

might be extremely dissimilar if only one of the partitions were used in the phylogenetic analyses.

Despite trivial or considerable incongruence between molecular and morphological partitions, the molecular data do not supersede the morphological partitions in combined analyses (Álvarez-Padilla et al., 2009). This is especially so in cases where the different gene partitions are incongruent with each other, or they lack phylogenetic signal when all data are combined, as is (in part) the case in our study. Overall, morphology seems to contribute equally in terms of support measures (Wahlberg and Nylin, 2003). To date, phylogenetic analyses of DNA sequence data in spiders have been based on a small fraction of all the potentially available nucleotide data (see below), providing a somewhat limited resolution, typically at a certain taxonomic level. Although the role of morphology in phylogenetic studies has been hotly debated recently (Scotland et al., 2003; Jenner, 2004; Wiens, 2004; Prendini, 2005; Smith and Turner, 2005; Assis, 2009), the ultimate goal of a phylogenetic analysis should be to gather as many independent lines of evidence as possible to resolve the relationships of the study taxa. From that particular point of view, a nucleotide substitution is no different from a transformation in a morphological feature or a change in a stereotyped behaviour.

In spite of the overwhelming amount of DNA sequence data produced to date, and the rapidly improving technological advances to gather large quantities of such data, in spider systematics the choice of genetic markers has been largely limited by primer availability. In addition, signal congruence between morphological and molecular partitions seems hard to predict. Current sequence data may fail to provide robust support for interfamilial, intrafamilial, or even intrageneric relationships (Hedin and Maddison, 2001; Arnedo et al., 2004; Bond and Hedin, 2006; Dimitrov et al., 2008; Vink et al., 2008; Blackledge et al., 2009), or may well be of intermediate congruence (Arnedo et al., 2001; Hormiga et al., 2003; Bruvo-Madžarić et al., 2005; Álvarez-Padilla et al., 2009). In only a few cases, congruence is found to be high among partitions in arachnids (Giribet et al., 1999; Giribet and Boyer, 2002). This is interesting because, in many other groups of arthropods in general, the markers utilized here robustly resolve high-level relationships, perhaps indicating that in spiders, or at least symphytognathoids, these genes may evolve somehow differently with respect to other arthropod groups, a pattern already noticed in the earliest molecular analyses of spider systematics (Hayashi, 1996).

Phylogenomic approaches may offer a possibility for finding new informative genetic markers (Pineau et al., 2005; Li et al., 2007; Dunn et al., 2008; Regier et al., 2008, 2010; Townsend et al., 2008) or a solution to phylogenetic problems by using large amounts of genes

not previously preselected (Dunn et al., 2008; Hejnol et al., 2009), which in turn might help in finding congruent signal among genes, and hopefully with morphology. We nevertheless emphasize that, regardless of the type of data used in phylogenetic analyses, total-evidence (i.e. simultaneous) analyses combining all available data are to be preferred. They represent the best approach to phylogenetic inference in terms of maximizing explanatory power and providing the context for assessing incongruence (Nixon and Carpenter, 1996), in addition to allowing the incorporation of fossils into combined analyses of morphology and molecules (Giribet, 2010). In that line, the present study has produced and combined an extensive molecular and morphological dataset for symphytognathoids, and it represents the best-informed cladistic hypothesis to date for mysmenids and their close relatives.

Familial phylogenetic relationships

The taxonomic decisions taken here are based on the phylogenetic hypothesis resulting from the total-evidence analysis (Figs 12 and 13). The morphological and behavioural synapomorphies optimized for the clades reported in the following sections will be discussed in more detail elsewhere (refer to Lopardo, 2009). Figures within this paper are referred to as “Fig.”; those from other references as “fig.”.

Symphytognathoids

Griswold, Coddington, Hormiga, and Scharff (1998) (Node 115)

In this study, Symphytognathoids include Anapidae (with the micropholcommatids nested within; see comments below), Mysmenidae, Symphytognathidae, Synaphridae, and Theridiosomatidae. The families Synaphridae and Micropholcommatidae are provisionally placed within symphytognathoids, as their familial association with some of the other Araneoidea lineages remains untested. An alternative hypothesis places Synaphridae as sister to Cyatholipidae (Lopardo and Hormiga, 2008). The suprafamilial placement of Micropholcommatidae within Araneoidea (rather than in Palpimanoidea, as proposed by Forster and Platnick, 1984) has been tested recently (Schütt, 2000, 2002; Rix et al., 2008). The hypothesis of interfamilial relationships of symphytognathoids is nearly identical to that proposed by Griswold et al. (1998), but modified as in Schütt (2003), and also recovered by Lopardo and Hormiga (2008), although in the latter study Synaphridae was not a symphytognathoid. Synaphridae shares with Cyatholipidae a broad posterior spiracle, the absence of nubbins from minor ampullate gland spigots,

and one PLS cylindrical gland spigot, but the support for this sister-group relationship is low (Lopardo and Hormiga, 2008). Under the phylogenetic hypothesis proposed here, the sister relationship of Synsphyridae with Anapidae + Symphytognathidae (Node 113) has contradicting support and is unstable (see statistics above), and this sister relationship is diagnosed just by the retention of at least one aggregate gland spigot in adult males (except in *Parapua*) and the uniform dorsal color pattern on the abdomen. Given the absence of cyatholipids in the present dataset and the instability in the placement of Synsphyridae within symphytognathoids, the current placement of Synsphyridae as a symphytognathoid should be taken cautiously. In our working hypothesis, Theridiosomatidae is the sister group of a lineage that groups all other symphytognathoid families (ANTS clade, see below), and Anapidae and Symphytognathidae are sister taxa. However, an alternative placement of Theridiosomatidae as sister to Mysmenidae has been proposed by Lopardo and

Hormiga (2008), based on morphology and behaviour, and this hypothesis is supported by the phylogenetic signal of the morphological partition. The symphytognathoid morphological synapomorphies proposed by Schütt (2003) were all corroborated, as are almost all those proposed by Griswold et al. (1998).

The following combination of unambiguous morphological synapomorphies supports symphytognathoid monophyly: domed sternum in lateral view (Figs 6a,b and 10b; secondarily flat in *Maymena mayana*); carapace fovea absent (Lopardo, 2009; chapter 2, fig. 142E); colulus with three or fewer setae (Lopardo, 2009; chapter 2, figs 67F and 78B; four or more setae in most *Mysmenopsis* species, variable in *Cepheia*, and *Maymena mayana*); sternum posterior margin not pointed (intermediate in most mysmenids, Fig. 10c; truncate in all other symphytognathoids, Lopardo, 2009; chapter 2, figs 70B and 145K; pointed in some *Maymena* species); tarsus I superior claws with a row of one to three short teeth oriented forward (Lopardo, 2009; chapter 2, figs

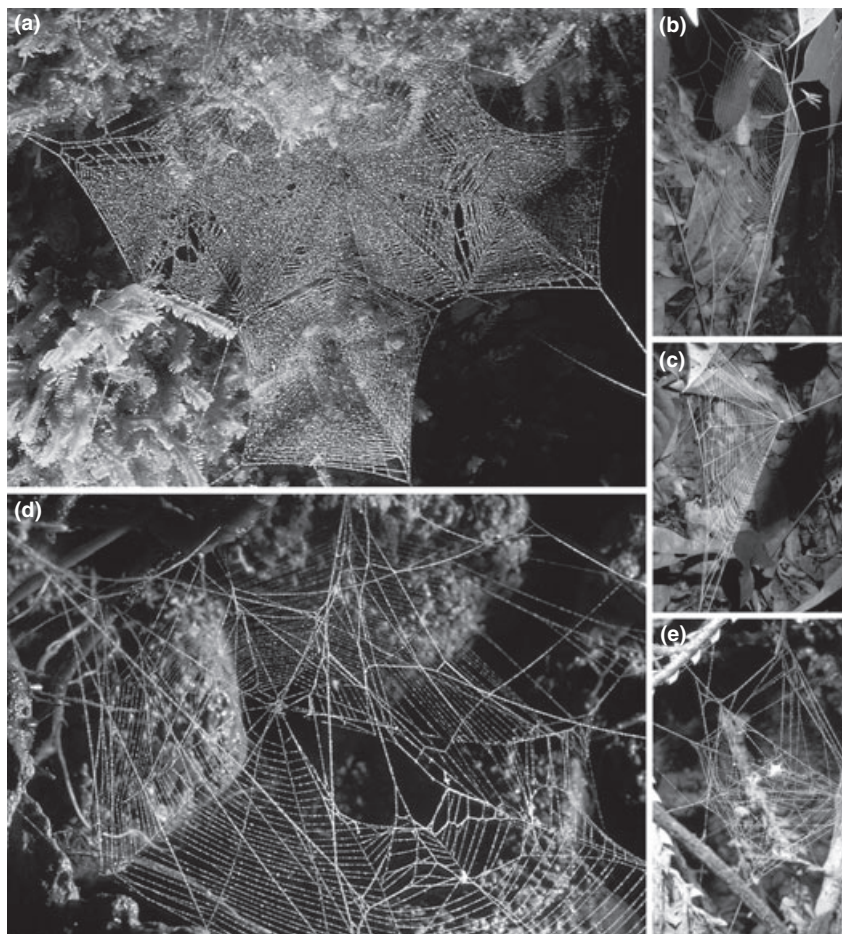


Fig. 18. Symphytognathoids webs. (a) *Tasmanapis strahan* (Anapidae), spider not collected; (b–c) *Epeirotypus* sp. (Theridiosomatidae) from Mexico; (d) *Anapisona kethleyi* (Anapidae), male; (e) potential web and eggsac of a *Symphytognatha* species (Symphytognathidae), from Tasmania, Australia, spider escaped.

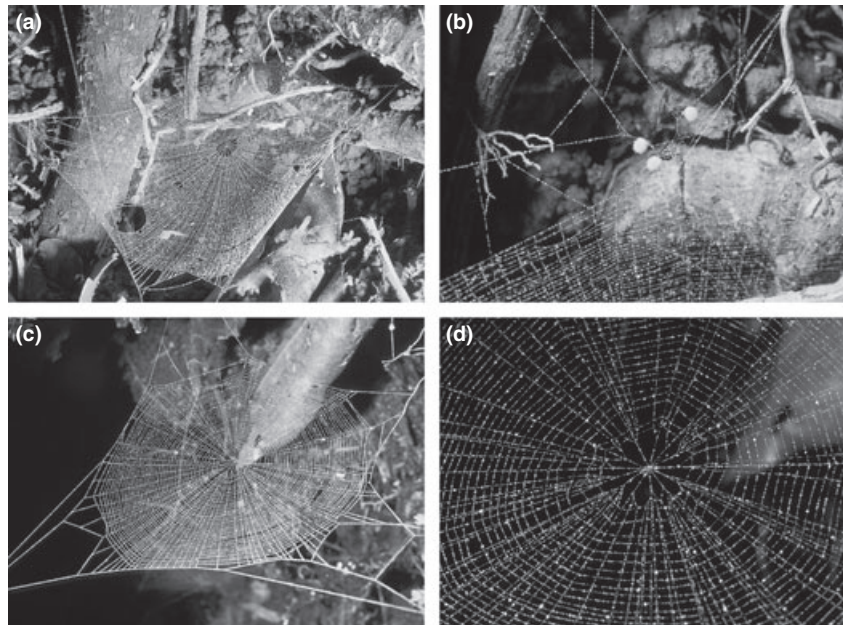


Fig. 19. Webs of Symphytognathidae from Tasmania, Australia. (a) SYMP-006-AUST, female with eggsacs; (b) same, detail to edge of web where eggsacs are attached, note female spider close to one of the eggsacs; (c) SYMP-007-AUST, female; (d) same, detail to hub.

26B and 52D; claws with a distinct row of four or more teeth of decreasing length occur in synaphrids, also arising independently in *Maymena mayana* and “Mysmenopsinae”); proximal tarsal organ (Fig. 7d; median on synaphrids and “Mysmenopsinae”); absence of female palpal claw (Lopardo, 2009; chapter 2, figs 22E and 69B); eggsac doubly attached (e.g. Griswold and Yan, 2003; fig. 5; scarce information available); and long embolus (some clades/taxa have an independently derived short or medium embolus). Furthermore, symphytognathoids exhibit many additional potential synapomorphies, including their minute size (< 2 mm of body length; secondary small size in *Maymena mayana*); the pedicel located centrally on ventral abdomen (Figs 6b,e,i,k,m; anterior and intermediate pedicels in synaphrids; intermediate pedicel in *Comaroma*); long and slender median claw IV (e.g. Griswold et al., 1998; fig. 22B; subequal in synaphrids, *Comaroma*, females *Teutoniella* and *Maymena rica*, and male *Parapua*); and fixed, nonmembranous embolus–tegulum junction (i.e. continuous transition between the two structures, Lopardo, 2009; chapter 2, figs 10E and 71A; few taxa scored; flexible junction derived independently in *Mysmenopsis*, *Cepheia*, *Anapisona*, and *Comaroma*). Additional putative synapomorphies are provided by their web-building behaviour (although data are available for only a few species; e.g. Eberhard, 1987): three-dimensional orb webs (Figs 5a,d and 18c,d; secondarily bidimensional independently in Symphytognathidae, Fig. 19a–d, and a node within Anapidae including *Tasmanapis* and *Elanapis*, Fig. 18a), lengthened radii, post-sticky silk hub

loops, and closed hubs. Symphytognathoid monophyly is also supported by 485 molecular synapomorphies.

The “Anterior Tracheal System” (ANTS) clade (Node 114)

This lineage includes all symphytognathoids except the basal Theridiosomatidae. The composition of the ANTS clade is identical to what Forster (1959) referred to as Symphytognathidae *sensu lato* (see also Schütt, 2003). Since the ANTS clade includes most symphytognathoid families, Forster’s original label of the group may generate confusion or ambiguous terminology, given that it refers to a familial status but is neither a family nor a superfamily. We hence prefer to label this lineage informally as the ANTS clade. Unambiguous synapomorphies for the ANTS clade include a row of plumose curved setae on the retromarginal distal margin of chelicerae (scarce setae or even absent in synaphrids); the anterior tracheal respiratory system (reduced book-lungs evolving independently in some anapids and some mysmenids); aggregate and flagelliform spigots of similar size; two aciniform gland spigots on the posterior median spinnerets (one in Anapidae and Symphytognathidae); males with subterminal conductor; medial paracymbium (in synaphrids and most mysmenids; basal in *Trogloneta*; apical in some anapids and symphytognathoids); and female palpal tibia with one trichobothrium (two in *Maymena mayana*, three in “Mysmenopsinae”). The monophyly of the ANTS clade is also supported by 335 molecular synapomorphies.

Theridiosomatidae Simon, 1881 (Fig. 18b,c; Node 155)

This family is basally placed within symphytognathoids, as sister to a clade composed by all remaining families. In our preferred hypothesis, four of the five theridiosomatid representatives form a clade (hereafter referred to as Theridiosomatidae): *Theridiosoma gemmosum*, *Epeirotypus brevipes*, *E. chavarria*, and TSMD-002-THAI. Although the undescribed theridiosomatid species from Thailand, TSMD-001-THAI (scored only for molecular data), has most of the morphological diagnostic features for the family (see below), and thus from morphological point of view it is a member of Theridiosomatidae, its placement within this family remains uncertain, given that in the combined analysis it is placed as sister to the theridiid representative. As mentioned above, this undescribed species appears as related to various non-theridiosomatid taxa in the analyses of the different partitions (see Figs 12, 14 and 15, see also Appendix S4: Figs 3, 5 and 8–21). Given the conflicting and remarkably different placements for the aforementioned undescribed species, and that the other theridiosomatids are monophyletic in the analyses of several data partitions, we have excluded TSMD-001-THAI from Theridiosomatidae for descriptive purposes. Theridiosomatidae monophyly is supported by the following combination of morphological synapomorphies: sternal pits (observed in all—described and undescribed—theridiosomatid species in this dataset, Lopardo, 2009; chapter 2, figs 123D and 125A); sparse, strongly serrated bristles on ventral tarsus IV; longest trichobothria on tibia III–IV long (Coddington, 1986a; fig. 141); relatively higher proportion of maxillary clavate setae (Lopardo, 2009; chapter 2, fig. 125B); seta on major ampullate (MAP) field with a row of long branches; cymbium and bulb as large as prosoma; paracymbium with process (Lopardo, 2009; chapter 2, fig. 124G); no loops, or less than one ascending loop of the spermatid duct before entering the embolus; and several pairs of switchbacks after SB II (Coddington, 1986a; fig. 146). Potential additional synapomorphies for Theridiosomatidae include: minute distal promarginal cheliceral curved seta; anterior median eyes on protruded area; denticles in cheliceral fang furrow (Coddington, 1986a; fig. 2); shallow furrow between the major ampullate and piriform fields (Coddington, 1986a; fig. 7; Griswold et al., 1998; fig. 24B); rugose cuticle on piriform field (Coddington, 1986a; fig. 7; Griswold et al., 1998; fig. 24B); width of proximal shaft of minor ampullate gland spigot as wide as apical spigot base, shaft as long as wide (Coddington, 1986a; fig. 8); males with cymbial prolateral basal expansion (e.g. Coddington, 1986a; fig. 134); lobed or slightly projected embolic base; and median apophysis (Lopardo, 2009, chapter 2, fig. 124C). Theridiosomatidae is also supported by 569 molecular synapomorphies.

Theridiosomatidae comprises to date 13 genera and 85 species (Platnick, 2010). Coddington (1986a) revised the genera of the family, including a detailed comparative morphological and behavioural study and a genus-level phylogenetic analysis. Previously proposed synapomorphies for the family include (from Coddington, 1986a; Griswold et al., 1998) connate spermathecae, sternal pits, and greatly elongate dorsal trichobothria on the fourth tibiae. The sternal pits, discovered by Wunderlich (1980), appear to be unique for the family (see also Coddington, 1986a), and an elongated tibial trichobothrium, although homoplastic, seems to diagnose the family as well. However, the third synapomorphy, connate spermathecae, is not general for the family (see separate spermathecae on Lopardo, 2009; chapter 2, fig. 124A); it might be a derived feature defining a clade within Theridiosomatidae (see also Miller et al., 2009).

Synaphridae Wunderlich 1986 (Node 148)

The family Synaphridae (represented here by *Cepheia* and *Synaphris*) is sister to the clade comprising Anapidae plus Symphytognathidae. Synaphrid monophyly is supported by the following unambiguous morphological synapomorphies: wide and advanced posterior spiracular opening, located midway between the spinnerets and epigastric groove; absence of booklung cover (Lopardo et al., 2007; fig. 33); posterior lateral tracheae branched and extending into prosoma (Lopardo et al., 2007; figs 34 and 37); posterior median tracheae sharing a common basal trunk with the lateral tracheae, resulting in two bundles arising from the atrium (Lopardo et al., 2007; fig. 37); absence of trichobothrium on metatarsus III (Lopardo, 2009; chapter 2, fig. 109D); absence of tibial dorsal macrosetae (Lopardo et al., 2007; figs 11 and 15); metatarsus–tarsus joint with both segment tips constricted (Lopardo and Hormiga, 2007; fig. 22); tarsal organ located medially; tarsus I superior claws with a distinct row of four or more teeth of decreasing length, oriented forward and usually touching (teeth can be short; Lopardo et al., 2007; figs 23 and 24); median claw IV as long as superior claws; cheliceral keel ending in single promarginal tooth (Lopardo and Hormiga, 2007; figs 13 and 15); retrolateral distal cheliceral setae absent; relatively higher proportion of maxillary clavate setae; labium pointed anteriorly; imbricate clypeus cuticle; distal segment of posterior lateral spinnerets (PLS) long and cylindrical (Lopardo and Hormiga, 2007; fig. 31); smooth intersegmental cuticle on anterior lateral spinnerets (ALS); no distinct separation between MAP and piriform field (Lopardo and Hormiga, 2007; figs 32 and 33); males with one triad spigot; epiandrous fusules dispersed in a row (Lopardo et al., 2007; fig. 32); embolus originating prolateral-ventrally; conductor with small ridges or other cuticular modifications (Lopardo and Hormiga, 2007, figs 38 and 50); and

retrolateral palpal tibial rim. Potential additional synapomorphies for Synaphridae include the posterior median tracheae extending into the prosoma and the absence of a cheliceral distal promarginal curved seta. No suitable tissues of synaphrids were available for sequencing at the time when this study was conducted, consequently we lack nucleotide data for this family.

Synaphrids were first described as a subfamily within Anapidae, currently comprising three genera and 12 species (Platnick, 2010), and have been the focus of an increasing number of studies dealing with its comparative morphology, some of them proposing several potential synapomorphies corroborated here (Wunderlich, 1995a; Marusik and Lehtinen, 2003; Schütt, 2003; Marusik et al., 2005; Lopardo and Hormiga, 2007; Lopardo et al., 2007; Miller, 2007). Lopardo and Hormiga (2008) hypothesized that synaphrids were sister to Cyatholipidae. In the present study, Synaphridae is suggested to be sister to Anapidae plus Symphytognathidae. Since the taxonomic sample in the present study is biased towards symphytognathoids and does not include any cyatholipids, or synaphrid sequences, its symphytognathoid placement is tentative.

Symphytognathidae sensu stricto Hickman 1931
(Figs 18e and 19; Node 157)

Symphytognathidae is monophyletic, and includes *Iardinis mussardi*, which had been misplaced in Mysmenidae (see below). Symphytognathidae is sister to Anapidae, a hypothesis also supported by the morphological partition. Unambiguous morphological synapomorphies supporting the monophyly of Symphytognathidae include: loss of anterior median eyes (AME; Griswold et al., 1998; figs 11D and 21A); abdomen with fingerprint cuticle pattern and covered by distinctly thick and long setae (Lopardo, 2009; chapter 2, fig. 147J; thin and short setae in SYMP-007-AUST); one or two promarginal cheliceral teeth originating from a common base or raised plate (Griswold et al., 1998; fig. 21B); loss of colulus (Lopardo, 2009; chapter 2, figs 117F and 120C); ALS intersegmental cuticle with fingerprint pattern (Griswold et al., 1998; fig. 36B); two-dimensional orb webs (Fig. 19a–d); females with reduced palp (Griswold et al., 1998; fig. 21A); lateral copulatory duct–spermatheca junction (unknown for several symphytognathids); absence of epigynal atrium (Lopardo, 2009; chapter 2, fig. 115G); and spermatheca performing one loop before SB III (Lopardo, 2009, chapter 2, fig. 140C). Ambiguously optimized synapomorphies for this family include absence of the posterior respiratory system; smooth leg cuticle; modified area on prolateral femur I; long trichobothria on tibia III–IV (short in *S. picta*); absence of a cheliceral distal promarginal curved seta; one pair of spermatheca switchbacks (SB III and IV) after SB

II; and narrow copulatory ducts of uniform diameter encircling spermathecae. Symphytognathidae monophyly is also supported by 326 molecular synapomorphies.

Synapomorphies from previous phylogenetic studies are corroborated here (Griswold et al., 1998; Schütt, 2003; see Forster and Platnick, 1977 for the diagnosis of the family). Griswold et al. (1998) also found Symphytognathidae to be sister to Anapidae. The traditional symphytognathid diagnostic feature, the chelicerae fused along the midline (as proposed in the revision of Symphytognathidae by Forster and Platnick, 1977; or from the phylogenetic analyses of Griswold et al., 1998 and Schütt, 2003), is here ambiguously optimized as a family synapomorphy. Fused chelicerae are difficult to discern under light and scanning electron microscopy because a sclerotized suture may still remain between the paturons, even if they are fused. This suture is observable under light microscopy in taxa with completely fused chelicerae and under SEM in those taxa with chelicerae fused at the base (see Lopardo, 2009; chapter 2, figs 112G and 121B). The removal of one chelicera as a test for the fused condition is sometimes impractical in minute taxa where the fusion is subtle (symphytognathids are among the smallest known spiders, see e.g. Baert and Jocqué, 1993; Cardoso and Scharff, 2009). Some mysmenids have a dubious fusion at their base, similar to that of some symphytognathids (scored as “?” in the morphological dataset, Ch. 264). Symphytognathidae currently comprises seven genera and 56 species (Platnick, 2010). Under the proposed recircumscription, one genus (*Iardinis*) and two species will be added to the family.

Anapidae Simon 1895 (Fig. 18a,d; Node 111)

New Synonymy: Micropholcommatidae Hickman, 1944

The family Anapidae is here recircumscribed to include the subfamily Micropholcommatinae *NEW RANK*, which is nested as a distal monophyletic group (Node 193) within Anapidae. Retention of the family rank for micropholcommatines would render Anapidae paraphyletic. This result, to some extent, has already been obtained in previous analyses (Schütt, 2003; Lopardo and Hormiga, 2008). Micropholcommatine genera in our study include *Parapua*, *Teutoniella*, and *Taphiassa*. Neither the micropholcommatine type genus *Micropholcomma* nor *Textricella* was included in our taxon sampling. However, based on the results of our study, published descriptions of other micropholcommatines (e.g. Hickman, 1944, 1945; Forster, 1959; Rix, 2008) show no character evidence that contradicts our hypothesis. The morphological cladistic analysis of Rix and Harvey (2010, fig. 2) recovers a clade that includes *Teutoniella*, *Taphiassa*, and *Micropholcomma*, and three

other micropholcommatines. We give here a revised diagnosis for the newly re-delimited Anapidae. Under our new circumscription, Anapidae monophyly is supported by the following morphological synapomorphies: distal labium concave and fused to sternum (Lopardo, 2009; chapter 2, figs 85E and 89B; straight labium in *Parapua*); pore-bearing prosomal depressions (Platnick and Forster, 1989; figs 5 and 6; absent in *Minanapis*, *Comaroma*, and *Teutoniella*, regained in *Parapua*); tarsal organ opening subequal or larger than setal sockets (Lopardo and Hormiga, 2008; fig. 13B,C); females with internal copulatory openings (external in *Parapua* and *Teutoniella*); spermatic duct with no loops or less than one ascending loop before entering the embolus (Lopardo, 2009; chapter 2, figs 139C,G and 140E; *ca.* 1–1.5 loops in *Tasmanapis*); thick embolus; and loss of paracymbium (present in *Comaroma*). Ambiguously optimized synapomorphies for Anapidae include: minute AME (Lopardo and Hormiga, 2008; fig. 10E,F; ambiguous due to absence of AME in Symphytognathidae; normal eyes in *Parapua*; absent in *Anapisona* and *Teutoniella*); deep abdominal sigilla (polymorphic in *Acrobleps*); absence of supra pedicellate proprioceptors (present in *Teutoniella*); fatiscent leg cuticle (Lopardo and Hormiga, 2008; fig. 13A–D; smooth in *Crassanapis* and *Comaroma*); females with membranous atrium and long fertilization ducts (Lopardo and Hormiga, 2008, fig. 20C; short in *Parapua* and *Teutoniella*). Anapidae is also supported by 627 molecular synapomorphies.

The total-evidence analysis supports an expanded circumscription of Micropholcommatinae, to include Rix et al.'s (2008) “taphiassines” and *Comaroma* (i.e. Node 150; but see Rix et al. (2008) and Rix and Harvey (2010) for the exclusion of *Teutoniella*). No morphological data were available for the “taphiassines” and therefore its placement within Micropholcommatinae is based only on the molecular evidence, although, as noted above, the morphological analysis of Rix and Harvey (2010) places *Taphiassa* in the same clade as *Micropholcomma*. Conversely, no molecular data were available for *Comaroma* and therefore its placement within Micropholcommatinae is based exclusively on morphological data. The monophyly of the recircumscribed Micropholcommatinae is supported by the following synapomorphies: abdominal strong setae with plates at base; absence of abdominal supra-pedicellate nubbins; punctate cuticle on sternum; tarsus IV median claw subequal to superior claws; no tartipore or nubbin accompanying the minor ampullate gland spigots on the posterior median spinnerets (PMS); smooth cuticle on posterior spinnerets spigot bases; and short embolus (medium in *Teutoniella*). Synapomorphies for the clade containing the original micropholcommatid representatives *Parapua punctata* and *Teutoniella cekalovici* (Node 193) include clypeus cuticle punctate; ventral setae on

tarsus IV similar to dorsal setae; females with external copulatory openings and no epigynal atrium; male dorsal abdomen scattered with sclerotized spots; male palpal tibia with retrolateral expansion; and spermatic duct narrowing before entering the embolus. Ambiguously optimized synapomorphies for this node include the punctate cuticle on carapace edge and short fertilization ducts.

Anapidae includes *Acrobleps* as its most basal lineage. The placement of micropholcommatines within Anapidae is not a new hypothesis (see Brignoli, 1970; also supported by Schütt, 2003; Lopardo and Hormiga, 2008; but see Forster and Platnick, 1984; Platnick et al., 1991; Rix et al., 2008; Rix and Harvey, 2010). Our analysis corroborates the placement of micropholcommatines within Anapidae. Many of the characters proposed and discussed here and in previous studies (Platnick and Shadab, 1978a; Platnick and Forster, 1986, 1989; Platnick et al., 1991; Griswold et al., 1998; Schütt, 2000, 2002, 2003; Ramírez et al., 2004), such as the pore-bearing prosomal depressions, the labral spur, or the male ventral and dorsal abdominal scuta, are homoplastic (reviewed in Lopardo and Hormiga, 2008). For example, the labral spur (see discussion in Lopardo and Hormiga, 2008; Lopardo, 2009; Miller et al., 2009) is absent in the most basal anapid lineage (*Acrobleps*) and it has been lost in *Minanapis* and *Comaroma* (although the latter optimization is ambiguous). The family Anapidae (excluding Micropholcommatinae) was re-delimited by Forster and Platnick (1977) and the South American and Australasian species were monographed by Platnick and Forster (1989).

Mysmenidae Simon 1922 (Figs 5–10; Node 134)

The monophyly of Mysmenidae is supported by the following unambiguous morphological synapomorphies: males with a metatarsal clasping spine (Figs 6a,b,f,k,n,o and 7c); cymbium oriented ventrally or prolatero-ventrally in the palp (Figs 8a,b and 10a,b; retrolateral-dorsal or fully prolateral in a few mysmenid taxa) and distinctly modified prolaterally and/or apically into an internal cymbial conductor (Figs 8a,b and 9a,b; absent in *Mysmenopsis*); cymbial fold (see Lopardo, 2009; chapter 2, figs 4G and 18E; absent in *Maymena mayana* and *Mysmenopsis*); a flat, rounded paracymbium (Figs 8a, 9b and 10b; hook-shaped in *Mysmenopsis*); and conductor globose, like a voluminous membrane, lacking a groove for the embolus tip (Figs 8b and 9a). Mysmenid females have a distinct modification on the apical ventral surface of at least femur I, either a sclerotized spot or a projection (Figs 6d,e,h,j,m and 7a,b; absent in some *Mysmenopsis* species and MYSM-005-ARG); an epigynal median plate projecting from the epigastric furrow (Fig. 10e); and either a more-or-less straight trajectory or

convoluted trajectory of the copulatory ducts (Figs 8c and 9c–f). Other synapomorphies for Mysmenidae include: a lobe located on the intersegmental groove of the ALS (Fig. 8d,e); the single seta on major ampullate field with two rows of long “branches” (Fig. 8d,f), or just one row of long “branches” (Lopardo, 2009; chapter 2, figs 11E, 13C and 16B); a distinctly thicker distal promarginal curved seta on chelicerae (Fig. 10d); intermediate sternum posterior margin (i.e. between pointed and truncate, Fig. 10c; see Lopardo, 2009; chapter 2, character 53; pointed in some *Maymena* species); a prolateral row of modified setae on tarsus I (Fig. 7e,f); tarsal organ opening subequal or larger than setal sockets (Fig. 7d); abdomen with fingerprint cuticle pattern (Fig. 10f; imbricate in *Maymena ambita*); and sparse imbricate cuticular pattern on carapace border (Fig. 10b; smooth in *Maymena mayana*). Ambiguously optimized synapomorphies for Mysmenidae include the anterior median eyes on protruded area (Fig. 10a,b) or all eyes on tubercle (Lopardo, 2009, chapter 2, figs 63G,H and 66A); denticles in cheliceral fang furrow (Fig. 10d); shallow furrow between the major ampullate and piriform fields (Fig. 8d); sternum cuticle imbricate-fingerprint (Fig. 10c); and male palpal tibial rim setae longer than the remaining tibial setae and arranged distally in a row or two (Figs 8a,b and 10a,b; equally short and of irregular conformation arising convergently in *Trogloneta* and a few other mysmenids). In addition, the monophyly of Mysmenidae is supported by 422 molecular synapomorphies.

Three decades ago, Brignoli (1980) provided a partial review of Mysmenidae in the only revisionary work performed for the family to date. Recent phylogenetic studies, including a small fraction of mysmenid diversity, have hypothesized synapomorphies of Mysmenidae, all in agreement with those proposed here (Thaler, 1975; Platnick and Shadab, 1978b; Brignoli, 1980; Wunderlich, 1995b; Griswold et al., 1998; Schütt, 2003). Mysmenidae is here circumscribed to include 109 described species in eight genera, namely: *Brasilionata*, *Maymena*, *Mysmeniola*, *Mysmenopsis*, *Trogloneta*, and a redefined “*Iseia*”, “*Microdipoena*”, and “*Mysmena*” (see comments below). Miller et al. (2009) have recently described four new mysmenid genera from China (*Simaoa*, *Gaoligonga*, *Mосу*, and *Chanea*) comprising a total of nine species. Their work was published after the completion of ours, thus these new taxa have not been included in our analyses. Potential placement of Chinese mysmenids within the family will be discussed elsewhere. Formal transfer of genera previously regarded as mysmenids, such as *Crassignatha* (see also Miller et al., 2009), *Iardinis*, *Leviola* Miller 1970, and *Phricotelus* Simon 1895 will be published elsewhere. The monotypic genus *Taphiassa* is placed in the anapid subfamily Micropholcommatinae based exclusively on multi-gene sequence data of two undescribed species, a

hypothesis in agreement with Rix et al. (2008) and Rix and Harvey (2010). We did not examine specimens of *Taphiassa impressa*, but Rix et al. (2008) and Rix and Harvey (2010) did. According to the two latter studies, evidence from morphological examination supports the placement of *T. impressa* within Micropholcommatinae.

Evolution of kleptoparasitism in Mysmenidae

Little is known about the biology and natural history of mysmenids, with a few notable exceptions. The natural history of *Trogloneta granulum* has been studied in detail, as has the web-building behaviour of a few species of *Mysmena*, *Maymena*, and *Microdipoena guttata* (see below; Fage, 1931; Gertsch, 1960; Coddington, 1986b; Eberhard, 1987; Hajer, 2000, 2002; Hajer and Reháková, 2003). In addition, some mysmenids have been reported to be kleptoparasites on the webs of other spider species.

Kleptoparasitism, the thieving of already acquired food by individuals of one species from individuals of the same or another species, occurs in several groups of animals, suggesting that this behaviour has evolved convergently multiple times. It is well documented for many birds (Brockmann and Barnard, 1979; Furness, 1987; King and Rappole, 2001), but has also been described for mammals (especially in hyenas: Kruuk, 1972; Curio, 1976; Wittenberger, 1981; Parker and Ruttan, 1988; Carbone et al., 1997), a few marine invertebrates (e.g. snails, sea stars, whelks and crabs: Rosenthal, 1971; Wobber, 1975; Sloan, 1979, 1984; Zamora and Gómez, 1996; Morissette and Himmelman, 2000; Iyengar, 2002), fishes (Pitcher, 1986; Dominey and Snyder, 1988), squamate reptiles (Cooper and Pérez-Mellado, 2003), and several orders of insects (Wilson, 1975), including dung beetles (Coleoptera; Hammond, 1976 and references therein), flies (Diptera; Sivinski and Stowe, 1980; Sivinski et al., 1999; Reader, 2003), water crickets (Heteroptera; Erlandsson, 1988), ants (Hymenoptera; Lucas, 1986; Zamora, 1990), scorpion flies (Mecoptera; Thornhill, 1979), and thrips (Thysanoptera; Crespi and Abbot, 1999).

Kleptoparasitic behaviour has been reported for members of several spider families (such as Anapidae, Symphytognathidae, Uloboridae, Theridiidae, Pholcidae, and Dictynidae) on the webs of members of other spider families such as Nephilidae, Araneidae, Dipluridae, Psecridae, Theridiidae, Tenggellidae, Austrochilidae, or Eresidae, among others (Exline and Levi, 1962; Roth and Craig, 1970; Platnick and Shadab, 1978b; Vollrath, 1978, 1979a,b, 1984; Whitehouse, 1986; Griswold and Meikle-Griswold, 1987; Elgar, 1988; Eberhard et al., 1993 and references therein; Tso and Severinghaus, 1998; Ramírez and Platnick, 1999; Agnarsson, 2002; Lopardo et al., 2004). Within symphytognathoids, Anapidae and Symphytognathidae have one known

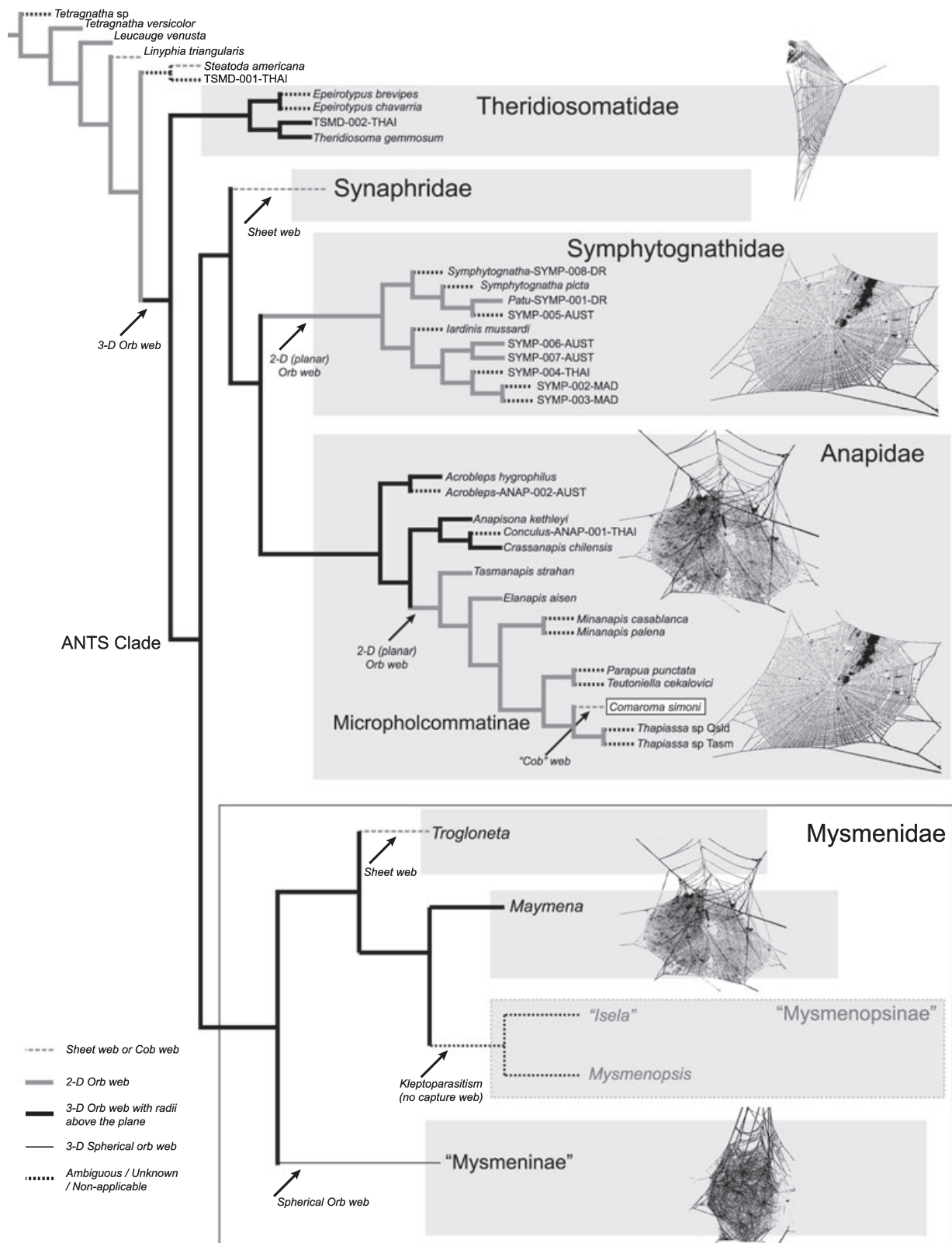


Fig. 20. Simplified cladogram representing the phylogenetic hypothesis rendered by the total-evidence analysis (see Figs 12 and 13). The evolution of the symphytognathoid web architecture is depicted. See text for explanation. Family codes used for unidentified species: ANAP, Anapidae; SYMP, Symphytognathidae; TSMD, Theridiosomatidae.

kleptoparasitic species each, *Sofanapis antillanca* and *Curimagua bayano*, respectively (Forster and Platnick, 1977; Vollrath, 1978; Ramírez and Platnick, 1999). In Mysmenidae, 11 species in three genera have been reported to be kleptoparasites: “*Isela*” (*I. okuncana*, Griswold, 1985; *Isela* (= *Kilifina*) *inquilina*, Baert and Murphy, 1987); *Maymena rica* (Eberhard et al., 1993; but see below); and *Mysmenopsis* (*M. cidrelicola*, *M. dipluramigo*, *M. gamboa*, *M. ischnamigo*, *M. palpalis* (see also Kraus, 1955; Forster, 1959; Gertsch, 1960; taxonomic revision in Platnick and Shadab, 1978b), *M. monticola*, *M. furtiva* (Coyle and Meigs, 1989), and *M. tengellacompa* (Eberhard et al., 1993). These kleptoparasitic interactions occur on the webs of diplurids (Mygalomorphae; Kraus, 1955; Platnick and Shadab, 1978b; Griswold, 1985; Baert and Murphy, 1987) and/or tengellids (Araneomorphae; Eberhard et al., 1993). Given the ability of *Maymena rica* to spin orb webs, its reported kleptoparasitic behaviour is suspected to be accidental (Eberhard et al., 1993).

“*Isela*” and *Mysmenopsis* belong to the same monophyletic group, the subfamily “Mysmenopsinae” (Figs 13 and 20), suggesting a single origin of kleptoparasitism within Mysmenidae. Several synapomorphies characterize this subfamily (and each of the member genera), including features that do not seem to be directly related to the kleptoparasitic lifestyle. The PLS spigot triad is partially lost in both sexes of *Mysmenopsis*, where only the flagelliform silk gland spigot remains. Moreover, the triad is completely lost in the “*Isela*” species studied, thus the adults of these species have lost the ability to spin sticky silk (it is not known whether juvenile or subadult stages retain the triad). It has been suggested that the kleptoparasitic lifestyle may have mediated such loss of spinning activities (Griswold et al., 1998), a hypothesis that is further supported by the data in this study. The spinning organs of other kleptoparasitic symphytognathoids are unknown. Unfortunately, the natural history of most *Mysmenopsis* species is not known. Out of 27 species (the largest mysmenid genus), just eight have been reported as kleptoparasites. One species (*M. cienaga*) has been collected in leaf litter (Müller, 1987), and one (*M. kochalkai*) from large epiphytic bromeliads (Platnick and Shadab, 1978b). Interestingly, no *Mysmenopsis* species has been positively reported as free-living, suggesting that if not all, most species might potentially be kleptoparasitic. Whether other *Mysmenopsis* species are kleptoparasites, and how kleptoparasitism evolved within the genus, remain to be studied.

Web architecture and web-building behaviour in symphytognathoids

Web architecture in symphytognathoids is quite diverse, both across and within families. The web

architecture and web-building behaviour of only a very small fraction of the 450 described species of symphytognathoids has been documented in some detail (Anapidae, Symphytognathidae, Mysmenidae, and Theridiosomatidae; Eberhard, 1981, 1982, 1987, 2000, 2001; Coddington, 1986b; Shinkai, 1997).

The “typical” anapid finished orb webs have additional elementary (structural) radii and sticky spirals above the plane of the horizontal orb (Fig. 18d). Such webs have been documented for most anapid genera, including *Acrobleps*, *Anapis*, *Anapisona*, *Chasmocephalon*, *Crassanapis*, and *Sheranapis* (Platnick and Shadab, 1978a; Eberhard, 1981, 1982, 1987; Coddington, 1986b, 2005a; Platnick and Forster, 1989; Griswold et al., 1998; Ramírez et al., 2004; Lopardo and Hormiga, 2008). This anapid web architecture resembles that of the mysmenid species of *Maymena*, not only in its general structure, but also in the behaviours used to construct the web (Fig. 5d,e; see below). However, not all anapids build this type of stereotyped orb web. The Chilean genus *Elanapis* (Ramírez et al., 2004) and the Tasmanian *Tasmanapis* (Fig. 18a) build a planar orb web of identical overall structure to those built by most members of Symphytognathidae (Ramírez et al., 2004; see below). Species of the Japanese anapid genus *Conculus* build a specialized aquatic orb web (Shinkai and Shinkai, 1988). Furthermore, there seems to be evidence of nonorbicular webs in anapids as well. The European *Comaroma simoni* builds a small, irregular web that resembles the cobweb of theridiids (Kropf, 1990); the aforementioned Chilean kleptoparasite *Sofanapis antillanca* does not make its own capture web (Ramírez and Platnick, 1999), but an irregular mesh superimposed on the host’s sheet web (Ramírez et al., 2004). In addition, micropholcommatines have been reported to spin irregular sheet webs (Hickman, 1944, 1945; Forster, 1959). At least one undescribed anapid species from Madagascar builds a horizontal sheet web, like those of cyatholipids, with the animals walking upside down, under the sheet (G.H., pers. obs.).

The typical orb webs of Symphytognathidae are horizontal and two-dimensional, with many anastomosing accessory radii and sticky spiral loops (Fig. 19a–d); most of the behaviours used to build these webs are similar to those observed in other symphytognathoids (see also Marples, 1951, 1955; Forster, 1959; Forster and Platnick, 1977; Eberhard, 1981, 1982, 1987; Coddington, 1986b, 2005b; Hiramatsu and Shinkai, 1993; Griswold et al., 1998; Griswold and Yan, 2003; Hormiga et al., 2007). However, most of these observations were based on the webs of several described and undescribed species of *Patu* or *Anapistula* from different continents, and of the South African *Symphytognatha imbulunga* (see Griswold and Yan, 2003 and references therein). As in Anapidae, there is evidence of atypical webs in symphytognathids. One species of *Anapistula*

was recently reported to build sheet webs (Cardoso and Scharff, 2009). In addition, the webs of the Tasmanian *Symphytognatha globosa* have been described as a “small irregular web like that of *Theridion*” (Hickman, 1931, p. 1326) consisting of a “few irregular threads in a more or less horizontal plane” (Hickman, in Forster and Platnick, 1977, p. 3). The remarkable and unique shape of the eggsac built by this species, with pointed protrusions over the surface, was observed on one occasion in Tasmania (Fig. 18e). The eggsac was located in the centre of a three-dimensional web, which lacked resemblance to an orb (Fig. 18e; this observation might correspond to a co-generic species, since no spider was collected, the identification of the webs was based on the shape of the eggsac). However, the “irregularity” of the web, as originally described by Hickman (1931), should be interpreted cautiously. The web of the Tasmanian mysmenid *Mysmena tasmaniae* (documented here for the first time) was also described as “few irregular threads, most of which were in an horizontal plane” (Hickman, 1979, p. 77) but this species builds a typical spherical mysmenid web (Fig. 5a). In addition, other *Symphytognatha* species have been collected from single threads (Martín J. Ramírez, pers. comm.; also L.L. and G.H., pers. obs.) and, as mentioned above, the kleptoparasitic *Curimagua bayano* does not seem to make its own capture web (Forster and Platnick, 1977; Vollrath, 1978).

In Mysmenidae, web architecture is also diverse, although some species do not build capture webs (see section *Evolution of kleptoparasitism in Mysmenidae* above for “*Isela*” and *Mysmenopsis* natural history). The webs of most mysmenid species have never been documented. Web architecture has been studied or documented in a few species of *Maymena*, “*Microdipoena*”, “*Mysmena*”, *Trogloneta*, *Simaoa*, and *Gaoligonga* (Marples, 1955; Forster, 1959; Shinkai, 1977; Hickman, 1979; Eberhard, 1981; Coddington, 1986b; Eberhard, 1987; Griswold et al., 1998; Hajer, 2000, 2002; Hajer and Reháková, 2003; Lopardo and Coddington, 2005; Hormiga et al., 2007; Miller et al., 2009; also pers. obs.). “*Mysmena*”, “*Microdipoena*”, *Simaoa*, and *Gaoligonga* species build unique, three-dimensional, spherical orb webs, with a proliferation of out-of-plane radii and sticky spirals resulting in a characteristic spherical shaped web (Fig. 5a–c). In contrast, the web of *Maymena* species is mainly planar but the hub is distorted upwards by one to several out-of-plane radial lines that attach to substrate above the web (Fig. 5d,e), which is identical to the typical anapid webs in structure and the stereotyped behaviours used to spin the webs (Coddington, 1986b; Eberhard, 1987; Griswold et al., 1998; Ramírez et al., 2004). The web of *Trogloneta granulum* was recently described in detail by Hajer (2000). The webs of other *Trogloneta* species remain unknown, although some undescribed species have been

collected from single threads in Australia (L.L., pers. obs.). *Trogloneta granulum* builds tiny three-dimensional webs. The shape, dimension, and arrangement of the individual components of the webs depend on the available space and the quality of the substrate (Hajer, 2000). The PLS araneoid triad, which produces the viscid silk, is retained in the adult males of *T. granulum*, suggesting the potential ability to spin webs and sticky silk. Surprisingly, only females and juveniles have been reported to spin webs, as males have been observed to stay on the previously built webs once they reach maturity and appear to be unable to spin webs on their own (Hajer, 2000). Even though the original description of the web of *T. granulum* considered it as an orb web, homology of its components with those of a typical orb web is dubious. The web was considered a “sheet web with regular elements” (not an orb web) by Schütt (2003), based on the literature. As originally described by Hajer (2000), no two identical hub patterns have been observed, suggesting that no stereotyped behaviour is involved in building these irregular meshes of silk. In addition, the so-called “radial threads”, regarded in the original description as homologous to the orb radii, are used for prey capture, that is, they are covered by sticky silk (as also are the “transverse threads”), and are attached to the substrate, conforming the frame of the web. Typical orb webs result from stereotyped behaviour in the construction of the hubs, and the radii are usually attached to the frame of the web, not to the substrate, and do not possess sticky silk (Eberhard, 1982; Coddington, 1986b). The web of *Trogloneta* might represent an intermediate stage between more typical orb webs and webs like those of theridiids or *Comaroma*. Until more data on the web-building behaviour of *Trogloneta* are available, we regard its web as a sheet.

In Theridiosomatidae, *Epeirotypus*, *Naatlo*, and *Theridiosoma* are known to build “typical” orb webs, with one radius outside of the orb plane functioning as a tension line (Fig. 18b,c), and temporary non-sticky “circles” instead of a non-sticky spiral. Several of their stereotypical web-building behaviours are similar to those reported for anapids and other symphytognathoids. The webs of *Wendilgarda*, *Ogulnius*, and *Epilineutes* are very different; some even spin webs attached to the water surface (Coddington and Valerio, 1980; Eberhard, 1981, 1982, 2000, 2001; Coddington, 1986a,b, 2005c; Griswold et al., 1998). Synaphrid web architecture remains largely unknown, and only *Synaphris lehtineni* has had its web described. This Ukrainian synaphrid is known to build a small, thin sheet web underneath stones in hollow depressions (Marusik et al., 2005, p. 129). Further details of its web architecture, and building behaviours of this and the remaining synaphrid species, are still unknown.

Based mainly on web architectural details and building behaviours, both Coddington (1986b) and Eberhard

(1987) proposed similar patterns of relationships for symphytognathoid families, although no formal phylogenetic analysis was performed. Theridiosomatidae was proposed as the most basal family of the group, followed by Symphytognathidae as sister to a clade comprising Anapidae plus Mysmenidae. The monophyly of symphytognathoids was later corroborated by means of a cladistic analysis of Araneoidea by Coddington (1990) and Griswold et al. (1998). Several web-related characters were included in their datasets, but the few symphytognathoid representatives included were known to spin the orb webs “typical” of each family. Nevertheless, Theridiosomatidae was again hypothesized to be the most basal lineage within symphytognathoids, sister to a clade comprising a monophyletic Mysmenidae and the clade Anapidae + Symphytognathidae.

Web architecture and the stereotypical behaviours involved in web building are phylogenetically informative. The webs of symphytognathoids suggest at least one striking case of convergently evolved shared web architectures (in both structure and the stereotyped behaviours used to spin the webs), which imply a conflict between morphological and behavioural information (Ramírez et al., 2004, p. 9). The first is provided by the three-dimensional webs of *Maymena* (Fig. 5d,e) and most anapids (Fig. 18d). The second comes from the planar webs of anapids such as *Elanapis aisen* and *Tasmanapis strahan* and the typical symphytognathid webs (Figs 18a and 19a–d; see also Ramírez et al., 2004; figs 9 and 10). This conflict may imply, for instance, an alternative placement of *Elanapis* and *Tasmanapis* within Symphytognathidae. Recently, Lopardo and Hormiga (2008) tested this hypothesis in part, by means of two modified phylogenetic analyses that included different symphytognathoid representatives with both types of web. They concluded that morphology placed *Elanapis* within Anapidae and *Maymena* within Mysmenidae, and suggested that the bidimensional webs of *Elanapis* and of symphytognathids have evolved independently (that is, the optimal tree allocated homoplasy to the behavioural characters).

Our total-evidence cladogram (Fig. 20; refer to Fig. 13 for character optimizations) also supports the latter evolutionary hypothesis, that is, the planar orb web within symphytognathoids has evolved twice independently (from a three-dimensional orb web, by the loss of the above-the-plane radii) in Symphytognathidae, and in a distal clade within Anapidae, comprising *Elanapis* and *Tasmanapis*, and excluding all three-dimensional orb-weaver anapids. Furthermore, this hypothesis implies that the orb web is the ancestral condition for symphytognathoids, and that it has been secondarily and independently modified into a sheet or a cobweb in Synsphyridae, *Trogloneta*, and *Comaroma*. In fact, the current phylogenetic pattern of relationships suggests that sheet webs of both Synsphyridae and

Trogloneta evolved independently from three-dimensional orb webs, while the cobweb of *Comaroma* evolved from the planar anapid orb web. The unique, spherical web of most “Mysmeninae” evolved once and was never lost, thus this remarkable architecture is a mysmenine synapomorphy.

Although valuable for phylogenetic reconstruction, information on web-building behaviour is extremely scarce. Web structure and related structural characters were scored for about 20 symphytognathoid species (out of more than 100 representatives), and behavioural characters corresponded to a mere five or six symphytognathoid taxa (see data matrix in Table S2). This is particularly unsatisfying, given that most of the behavioural characters in this dataset optimized as potential synapomorphies for symphytognathoids. Observation and documentation of web architectures in the field, and in particular, behavioural studies focused on the details of web-building behaviours, are critical to elucidate the web and to understand homologous structures and stereotypical behavioural units (Eberhard, 1981, 1982, 1987; Coddington, 1986b; Kuntner et al., 2008). While the opposite might be feasible in some groups (i.e. deducing web-building behaviours from finished webs; for example, in filistatids; Lopardo and Ramírez, 2007), homologizing and de-composing web structures to their basic behavioural units might shed some light on the problem of coding and understanding what arachnologists have lumped in the character-state category of “sheet web” (Hormiga et al., 1995; Scharff and Coddington, 1997; Griswold et al., 1998, 2005; Schütt, 2003; Lopardo and Hormiga, 2008; Blackledge et al., 2009).

Conclusions

We have assembled and analysed two large, separate datasets (morphology and multigene sequence data) of mysmenids and their close relatives, to provide the first cladistic hypothesis of relationships and the basis for a phylogenetic classification of Mysmenidae. Our working phylogenetic hypothesis provides an evolutionary and comparative framework for the study of character evolution. The results of the total-evidence analysis using parsimony under direct optimization support the monophyly of Mysmenidae and suggest a placement of the enigmatic genus *Iardinis* within Symphytognathidae. Mysmenidae is diagnosed by ca. 20 morphological synapomorphies, much in agreement with the results of the analysis of the morphological partition alone. Cladistic quantitative support for Mysmenidae is contradicting and not highly stable. The relationships of our taxonomic sample of Mysmenidae are fully resolved. Although most of the genes and gene combinations studied did not recover Mysmenidae monophyly, the nuclear partition (Table 5) and those combined data

partitions that included the morphological matrix, or under morphology alone, did recover monophyly of the family. A redefined Mysmenidae is also recovered by the combined parsimony analyses using static homology (strongly supported by morphology, and contradicted by the 28S fragment), and it is not recovered by individual genes or gene combinations, as observed above. Bayesian analyses based on morphology, DNA sequences, and both kinds of data also supported the monophyly of Mysmenidae, although the overall pattern of relationships among symphytognathoid families differed from the parsimony dynamic homology approach.

The results of the combined analysis support in part the monophyly and the relationships of “symphytognathoids” proposed by Griswold et al. (1998), as modified by Schütt (2003). The “symphytognathoid” clade is defined here to include Anapidae, Mysmenidae, Symphytognathidae, Theridiosomatidae, Synaphridae, and Micropholcommatinae *New Rank*. Theridiosomatidae is basal, sister to all remaining symphytognathoid families. The latter clade is here referred to as the “Anterior Tracheal System” (ANTS) clade. Mysmenidae is sister to a clade composed of Synaphridae plus Anapidae (circumscribed to include Micropholcommatinae) + Symphytognathidae (redefined to include *Iardinis*). Support and stability values for symphytognathoids are contradicting. Symphytognathoid monophyly is not recovered in any molecular partition analysed and seems to be supported only by morphology. Based on the preferred phylogenetic hypothesis from our total-evidence analysis, we have produced new diagnoses for all symphytognathoid families, and synonymized Micropholcommatidae with Anapidae, since the former is a distal clade within the latter.

Kleptoparasitism appears to have a single origin within mysmenids, at the base of “Mysmenopsinae”. The planar orb web evolved independently twice within symphytognathoids, from a three-dimensional web (in Symphytognathidae and distally within Anapidae). The orb web has been secondarily and independently modified into a sheet or cobweb at least three times in the “symphytognathoids”. The scarcity of behavioural data for symphytognathoids is problematic and demands caution when considering these evolutionary hypotheses. Clearly, much more behavioural data are needed for a better understanding of the diversification of web architectures in symphytognathoids.

Acknowledgements

This work is part of a PhD thesis at The George Washington University (GWU) by L.L., who wishes to thank her dissertation committee members (Charles E. Griswold, James M. Clark, Diana L. Lipscomb, and Marc W. Allard) for their support, critical reading,

comments, and suggestions that greatly improved her work. We deeply thank the people in the Giribet Lab (Harvard University, especially Akiko Okusu, Sarah L. Boyer, Stephanie W. Aktipis, and Diane Sheridan), and the Hormiga Lab (GWU, Fernando Álvarez-Padilla, Anahita Shaya, Claudio D. Gutman, Anastasia Kondakova, Dimitar S. Dimitrov, Ligia R. Benavides Silva, and Diana L. Lipscomb) for their contribution in the sequencing aspect of this research. Fernando Álvarez-Padilla and the NSF-AToL spiders project (see below) kindly provided unpublished sequences used in this work. We especially appreciate the help of the following AToL participants: Ward Wheeler, Lorenzo Prendini, Torsten Dikow, Dana Price, and Ellen Trimarco. Special thanks go to Dimitar S. Dimitrov and Peter Michalik for their assistance in the analyses of the data, to Pablo Goloboff for his help with TNT, and to Christian Kropf, Jaromir Hajer, Mark Harvey, and Charles E. Griswold for supplying inaccessible papers. No words would suffice to express our gratitude towards Andres Varón for his priceless time, advice, patience, and help with POY. Several friends and colleagues joined us in field trips around the world. We are grateful to Charles Griswold, Martín J. Ramírez, Nikolaj Scharff, Diana Silva-Dávila, Lisa Joy Boutin, and Tamás Szűts (Australia); Cristian J. Grismado, Ana Quaglino, Luis Piacentini, and Gonzalo Rubio (Argentina); Fernando Álvarez-Padilla and José Luis Castelo-Calvillo (Mexico); and Dimitar S. Dimitrov (USA). The field trip to Misiones (Argentina) was funded by the Cosmos Club Foundation Program of Grants-In-Aid to Young Scholars (to L.L.) and the NSF-AToL spider project. We further thank the authorities at the Administración de Parques Nacionales (APN, Argentina) and Ministerio de Ecología, R.N.R y Turismo de la Provincia de Misiones (Misiones, Argentina) for collecting permits in protected areas, the park rangers for assistance in the field, and Martín J. Ramírez for logistic help. The field trip to Mexico was funded by an NSF-PEET grant (see below). We also thank Tila Pérez, G. Montiel, and the IBUNAM staff (Mexico) for the logistic support and resources, and the Álvarez-Padilla family for their hospitality. The Australian field trip was funded by an NSF-AToL spider project and the NSF-PEET grant. We further thank Robert Raven (QM) for logistic help, and the Parks and Wildlife Service (Department of Primary Industries, Water and Environment, Tasmania, Australia) and the Department of Conservation and Land Management (Western Australia) for spider-collecting permits. Mark Harvey (Western Australian Museum, Perth) and Lisa Joy Boutin (Queen Victoria Museum and Art Gallery, Launceston, Australia) provided valuable help for our field work in Western Australia and Tasmania, respectively. We would also like to thank the Sheridan School and their staff at the Sheridan School Mountain Campus (Virginia, USA) for allowing us to collect in their property. For specimen

collection and donation, we are immensely grateful to Jaromir Hajer (Department of Biology, University J.E. Purkinje, Ustí nad Labem, Czech Republic), Richard Hoffman (Virginia Museum of Natural History, Martinsville, VA, USA), Cristian Kropf (Department of Invertebrates, Natural History Museum Bern, Bern, Switzerland), Antonio Melic (Spain), Martín J. Ramírez (Museo Argentino de Ciencias Naturales “Bernardino Rivadavia”, Buenos Aires, Argentina), and Robert Raven (Queensland Museum, South Brisbane, Australia). Our thanks extend to the following curators and assistants for kindly loaning precious type and non-type material: Abigail Blair (Otago Museum, Dunedin, New Zealand), Alistair Ramsdale (Bernice P. Bishop Museum, Hawaii, USA), Ansie Dippenaar-Schoeman (Plant Protection Research Institute, Queenswood, South Africa), Antonio D. Brescovit (Instituto Butantan, São Paulo, Brazil), Charles Griswold (California Academy of Sciences, San Francisco, USA), Christine Rollard and Elise-Anne Leguin (Muséum National d’Histoire Naturelle, Paris, France), Cristina Scioscia and Martín J. Ramírez (Museo Argentino de Ciencias Naturales “Bernardino Rivadavia”, Buenos Aires, Argentina), Debbie Jennings (Natal Museum, Pietermaritzburg, South Africa), Diana Silva-Dávila (Museo de Historia Natural, Universidad Nacional Mayor de San Marcos, Lima, Peru), Laura Leibesperger (Museum of Comparative Zoology, Harvard University, Cambridge, USA), Graham Milledge (Australian Museum, Sydney, Australia), Hieronymus Dastych (Zoologisches Institut und Museum, Universität Hamburg, Germany), Janet Beccaloni (Natural History Museum, London, United Kingdom), John Marris (Lincoln University, Canterbury, New Zealand), Jonathan Coddington (National Museum of Natural History, Smithsonian Institution, Washington, DC, USA), Jürgen Gruber (Naturhistorisches Museum, Vienna, Austria), Leon Baert (Institut Royal des Sciences Naturelles, Brussels, Belgium), Lisa Joy Boutin (Queen Victoria Museum and Art Gallery, Launceston, Australia), Nikolaj Scharff (Zoological Museum, University of Copenhagen, Denmark), Norman Platnick (American Museum of Natural History, New York, USA), Pablo Goloboff (Instituto Miguel Lillo, Tucumán, Argentina), Peter J. Schwendinger (Museum d’Histoire naturelle, Geneve, Switzerland), Peter Jäger and Julia Altmann (Natur-Museum und Forschung-Institut, Senckenberg, Germany), Phil Sirvid (Museum of New Zealand Te Papa Tongarewa, Wellington, New Zealand), Robert Raven (Queensland Museum, South Brisbane, Australia), Rowley Snazell (personal collection, United Kingdom), Rudy Jocque (Musée Royal Afrique Centrale, Tervuren, Belgium), Seppo Koponen (Zoological Museum, University of Turku, Finland), and Torbjorn Kronstedt (Naturhistoriska Riksmuseet, Stockholm, Sweden). Museum specimens for the molecular work were kindly provided by the California Academy of Sciences (Charles Griswold);

Museo Argentino de Ciencias Naturales “B. Rivadavia” (Cristina Scioscia and Martín J. Ramírez); and the National Museum of Natural History, Smithsonian Institution (Jonathan Coddington). L.L. thanks Martín J. Ramírez, Fernando Álvarez-Padilla, Dimitar S. Dimitrov, Ligia R. Benavides Silva, Matjaž Kuntner, Jeremy A. Miller, Ingi Agnarsson, Anahita Shaya, Anastasia Kondakova, Vanessa Degrassi, Joana Zanol P. Silva, Vinita Gowda, Maria del Rosario Castañeda, Alexandra Herrera Martínez, her family, friends, and Peter for their continuous support, encouragement, advice, and help. We are especially grateful to Gabriele Uhl for her support, and we deeply thank Miquel A. Arnedo and Martín J. Ramírez for their useful comments, suggestions, and critical reading of an earlier version of this manuscript. Funding for this research has been provided by a PEET grant (and an REU supplement) from the National Science Foundation (DEB-0328644) to G.H. and G.G., and in part by a Weintraub Fellowship and Research Enhancement Fund and Selective Excellence awards from The George Washington University (to G.H.), and by a National Science Foundation ATOL grant (EAR-0228699) to W. Wheeler, J. Coddington, G. Hormiga, L. Prendini and P. Sierwald.

References

- Agnarsson, I., 2002. Sharing a web—on the relation of sociality and kleptoparasitism in theridiid spiders (Theridiidae, Araneae). *J. Arachnol.* 30, 181–188.
- Altschul, S., Madden, T., Schäffer, A., Zhang, J., Zhang, Z., Miller, W., Lipman, D., 1997. Gapped BLAST and PSI-BLAST: a new generation of protein database search programs. *Nucleic Acids Res.* 25, 3389–3402.
- Álvarez-Padilla, F., Dimitrov, D., Giribet, G., Hormiga, G., 2009. Phylogenetic relationships of the spider family Tetragnathidae (Araneae, Araneoidea) based on morphological and DNA sequence data. *Cladistics* 25, 109–146.
- Arnedo, M., Oromí, P., Ribera, C., 2001. Radiation of the spider genus *Dysdera* (Araneae, Dysderidae) in the Canary Islands: cladistic assessment based on multiple data sets. *Cladistics* 17, 313–353.
- Arnedo, M., Coddington, J., Agnarsson, I., Gillespie, R., 2004. From a comb to a tree: phylogenetic relationships of the comb-footed spiders (Araneae, Theridiidae) inferred from nuclear and mitochondrial genes. *Mol. Phylogenet. Evol.* 31, 225–245.
- Arnedo, M., Hormiga, G., Scharff, N., 2009. Higher level phylogenetics of linyphiid spiders (Araneae, Linyphiidae) based on morphological and molecular evidence. *Cladistics* 25, 231–262.
- Asher, R.J., Horovitz, I., Sánchez-Villagra, M.R., 2004. First combined cladistic analysis of marsupial mammal interrelationships. *Mol. Phylogenet. Evol.* 33, 240–250.
- Assis, L.C.S., 2009. Coherence, correspondence, and the renaissance of morphology in phylogenetic systematics. *Cladistics* 25, 1–17.
- Baert, L., Jocqué, R., 1993. *Anapistula caecula* n.sp., the smallest known female spider (Araneae, Symphytognathidae). *J. Afr. Zool.* 107, 187–189.
- Baert, L., Murphy, J., 1987. *Kilifia inquilina*, a new mysmenid spider from Kenya (Araneae, Mysmenidae). *Bull. Br. Arachnol. Soc.* 7, 194–196.

- Baker, R.H., DeSalle, R., 1997. Multiple sources of character information and the phylogeny of Hawaiian *Drosophila*. Syst. Biol. 46, 654–673.
- Baker, R.H., Yu, X., DeSalle, R., 1998. Assessing the relative contribution of molecular and morphological characters in simultaneous analysis trees. Mol. Phylogenet. Evol. 9, 427–436.
- de Bivort, B.L., Clouse, R.M., Giribet, G. in press. A morphometrics-based phylogeny of the temperate Gondwanan mite harvestmen (Opiliones, Cyphophthalmi, Pettalidae). J. Zool. Syst. Evol. Res. doi:10.1111/j.1439-0469.2009.00562.x.
- Blackledge, T., Scharff, N., Coddington, J., Szűts, T., Wenzel, J., Hayashi, C., Agnarsson, I., 2009. Reconstructing web evolution and spider diversification in the molecular era. Proc. Natl Acad. Sci. USA 106, 5229–5234.
- Bleidorn, C., Hill, N., Erséus, C., Tiedemann, R., 2009. On the role of character loss in orbiiniid phylogeny (Annelida): molecules vs. morphology. Mol. Phylogenet. Evol. 52, 57–69.
- Bond, J., Hedin, M., 2006. A total evidence assessment of the phylogeny of the diverse North American trapdoor spider subfamily Euctenizinae (Araneae, Mygalomorphae, Cyrtaucheniidae). Mol. Phylogenet. Evol. 41, 70–85.
- Bremer, K., 1988. The limits of amino acid sequence data in angiosperm phylogenetic reconstruction. Evolution 42, 795–803.
- Bremer, K., 1994. Branch support and tree stability. Cladistics 10, 295–304.
- Brignoli, P., 1970. Contribution à la connaissance des Symphytognathidae paléarctiques (Arachnida, Araneae). Bull. Mus. Natn Hist. Nat. Paris 41, 1403–1420.
- Brignoli, P., 1980. On few Mysmenidae from the Oriental and Australian regions (Araneae). Rev. Suisse Zool. 87, 727–738.
- Brockmann, H.J., Barnard, C.J., 1979. Kleptoparasitism in birds. Anim. Behav. 27, 487–514.
- Bruvo-Madžarić, B., Huber, B., Steinacher, A., Pass, G., 2005. Phylogeny of pholcid spiders (Araneae: Pholcidae): combined analysis using morphology and molecules. Mol. Phylogenet. Evol. 37, 661–673.
- Carbone, C., Du Toit, J.T., Gordon, I.J., 1997. Feeding success in African wild dogs; does kleptoparasitism by spotted hyaenas influence hunting group size? J. Anim. Ecol. 66, 318–326.
- Cardoso, P., Scharff, N., 2009. First record of the spider family Symphytognathidae in Europe and description of *Anapistula ataecina* sp. n. (Araneae). Zootaxa 2246, 45–57.
- Clouse, R.M., De Bivort, B.L., Giribet, G., 2009. A phylogenetic analysis for the South-east Asian mite harvestman family Stylocellidae (Opiliones: Cyphophthalmi)—a combined analysis using morphometric and molecular data. Invertebr. Syst. 23, 515–529.
- Coddington, J., 1986a. The genera of the spider family Theridiosomatidae. Smithsonian Contrib. Zool. 422, 1–96.
- Coddington, J., 1986b. The Monophyletic Origin of the Orb Web. Stanford University Press, Palo Alto, CA, pp. 319–363.
- Coddington, J., 1990. Ontogeny and homology in the male palpus of orb-weaving spiders and their relatives, with comments on phylogeny (Araneocladata: Araneoidea, Deinopoidea). Smithsonian Contrib. Zool. 496, 1–52.
- Coddington, J., 2005a. Chapter 15: Anapidae. In: Ubick, D., Cushing, P., Paquin, P. (Eds.), Spiders of North America: an Identification Manual. American Arachnology Society, pp. 64–65.
- Coddington, J., 2005b. Chapter 58: Symphytognathidae. In: Ubick, D., Cushing, P., Paquin, P. (Eds.), Spiders of North America: an Identification Manual. American Arachnology Society, pp. 226–227.
- Coddington, J., 2005c. Chapter 63: Theridiosomatidae. In: Ubick, D., Cushing, P., Paquin, P. (Eds.), Spiders of North America: an Identification Manual. American Arachnology Society, pp. 244–245.
- Coddington, J., Scharff, N., 1994. Problems with zero-length branches. Cladistics 10, 415–423.
- Coddington, J., Valerio, C., 1980. Observations on the web and behavior of *Wendilgarda* spiders (Araneae: Theridiosomatidae). Psyche (Camb., Mass.) 87, 93–105.
- Colgan, D., McLauchlan, A., Wilson, G., Livingston, S., Edgecombe, G., Macaranas, J., Cassis, G., Gray, M., 1998. Histone H3 and U2 snRNA DNA sequences and arthropod molecular evolution. Austral. J. Zool. 46, 419–437.
- Cooper, W.E.-J., Pérez-Mellado, V., 2003. Kleptoparasitism in the Balearic lizard, *Podarcis lilfordi*. Amphib. Reptil. 24, 219–224.
- Coyle, F., Meigs, T., 1989. Two new species of kleptoparasitic *Mysmenopsis* (Araneae, Mysmenidae) from Jamaica. J. Arachnol. 17, 59–70.
- Crespi, B., Abbot, P., 1999. The behavioral ecology and evolution of kleptoparasitism in Australian gall thrips. Fla. Entomol. 82, 147–164.
- Curio, E. 1976. The Ethology of Predation. Springer, Berlin.
- Dimitrov, D., Arnedo, M., Ribera, C., 2008. Colonization and diversification of the spider genus *Pholcus* Walckenaer, 1805 (Araneae, Pholcidae) in the Macaronesian archipelagos: evidence for long-term occupancy yet rapid recent speciation. Mol. Phylogenet. Evol. 48, 596–614.
- Dominey, W.J., Snyder, A.M., 1988. Kleptoparasitism of freshwater crabs by cichlid fishes endemic to Lake Barombi Mbo, Cameroon, West Africa. Environ. Biol. Fishes 22, 155–160.
- Dunn, C., Hejnol, A., Matus, D., Pang, K., Browne, W., Smith, S., Seaver, E., Rouse, G., Obst, M., Edgecombe, G., Sørensen, M., Haddock, S., Schmidt-Rhaesa, A., Okusu, A., Kristensen, R., Wheeler, W., Martindale, M., Giribet, G., 2008. Broad phylogenomic sampling improves resolution of the animal tree of life. Nature 452, 745–749.
- Eberhard, W., 1981. Construction behaviour and the distribution of tensions in orb webs. Bull. Br. Arachnol. Soc. 5, 189–204.
- Eberhard, W., 1982. Behavioural characters for the higher classification of orb-weaving spiders. Evolution 36, 1067–1095.
- Eberhard, W., 1987. Orb webs and construction behavior in Anapidae, Symphytognathidae, and Mysmenidae. J. Arachnol. 14, 339–356.
- Eberhard, W., 2000. Breaking the mold: behavioral flexibility and evolutionary innovation in *Wendilgarda* spiders (Araneae, Theridiosomatidae). Ethol. Ecol. Evol. 12, 223–235.
- Eberhard, W., 2001. Trolling for water striders: active searching for prey and the evolution of reduced webs in the spider *Wendilgarda* sp. (Araneae, Theridiosomatidae). J. Nat. Hist. 35, 229–251.
- Eberhard, W., Platnick, N., Schuh, R., 1993. Natural history and systematics of arthropod symbionts (Araneae; Hemiptera; Diptera) inhabiting webs of the spider *Tengella radiata* (Araneae, Tengelidae). Am. Mus. Novit. 3065, 1–17.
- Edgecombe, G., Giribet, G., 2006. A century later—a total evidence re-evaluation of the phylogeny of scutigermorph centipedes (Myriapoda: Chilopoda). Invertebr. Syst. 20, 503–525.
- Elgar, M.A., 1988. Kleptoparasitism a cost of aggregating for an orb-weaving spider. Anim. Behav. 37, 1052–1055.
- Erlandsson, A., 1988. Food-sharing vs. monopolizing prey: a form of kleptoparasitism in *Velia caprai* (Heteroptera). Oikos 53, 203–206.
- Exline, H., Levi, H., 1962. American spiders of the genus *Argyrodes*. Bull. Mus. Comp. Zool. Harv. 127, 75–204.
- Fage, L. 1931. Araneae, 5e série, précédée d'un essai sur l'évolution souterraine et son déterminisme. Biospeologica (expér, LAZ) 71, 91–291.
- Farias, I.P., Ortí, G., Meyer, A., 2000. Total evidence: molecules, morphology, and the phylogenetics of cichlid fishes. J. Exp. Biol. (Mol. Dev. Evol.) 288, 76–92.
- Farris, J., 1990. Phenetics in camouflage. Cladistics 6, 91–100.
- Farris, J., 1997. The future of phylogeny reconstruction. Zool. Scr. 26, 303–311.
- Farris, J., Albert, V., Källersjö, M., Lipscomb, D., Kluge, A., 1996. Parsimony jackknifing outperforms neighbor-joining. Cladistics 12, 99–124.

- Felsenstein, J., 1985. Confidence limits on phylogenies: an approach using the bootstrap. *Evolution* 39, 783–791.
- Folmer, O., Black, M., Hoeh, W., Lutz, R., Vriejenhoek, R., 1994. DNA primers for amplification of mitochondrial cytochrome *c* oxidase subunit I from diverse metazoan invertebrates. *Mol. Mar. Biol. Biotechnol.* 3, 294–299.
- Forster, R., 1959. The spiders of the family Symphytognathidae. *Trans. R. Soc. N. Z.* 86, 269–329.
- Forster, R., Platnick, N., 1977. A review of the spider family Symphytognathidae (Arachnida, Araneae). *Am. Mus. Novit.* 2619, 1–29.
- Forster, R., Platnick, N., 1984. A review of the archaeid spiders and their relatives, with notes on the limits of the superfamily Palpimanoidea (Arachnida, Araneae). *Bull. Am. Mus. Nat. Hist.* 178, 1–106.
- Furness, R.W. 1987. Kleptoparasitism in Seabirds. Cambridge University Press, Cambridge, pp. 77–100.
- Gertsch, W., 1960. Descriptions of American spiders of the family Symphytognathidae. *Am. Mus. Novit.* 1981, 1–40.
- Giribet, G., 2001. Exploring the behavior of POY, a program for direct optimization of molecular data. *Cladistics* 17, S60–S70.
- Giribet, G., 2003. Stability in phylogenetic formulations and its relationship to nodal support. *Syst. Biol.* 42, 554–564.
- Giribet, G., 2010. A new dimension in combining data? The use of morphology and phylogenomic data in metazoan systematics. *Acta Zool. Stockholm* 91, 11–19.
- Giribet, G., Boyer, S.L., 2002. A cladistic analysis of the cyphophthalmid genera (Opiliones, Cyphophthalmi). *J. Arachnol.* 30, 110–128.
- Giribet, G., Wheeler, W., 1999. On gaps. *Mol. Phylogenet. Evol.* 13, 132–143.
- Giribet, G., Carranza, S., Bagnuà, J., Riutort, M., Ribera, C., 1996. First molecular evidence for the existence of a Tardigrada + Arthropoda clade. *Mol. Biol. Evol.* 13, 76–84.
- Giribet, G., Rambla, M., Carranza, S., Bagnuà, J., Riutort, M., Ribera, C., 1999. Phylogeny of the arachnid order Opiliones (Arthropoda) inferred from a combined approach of complete 18S and partial 28S ribosomal DNA sequences and morphology. *Mol. Phylogenet. Evol.* 11, 296–307.
- Giribet, G., Vogt, L., Pérez González, A., Sharma, P., Kury, A.B. 2010. A multilocus approach to harvestmen (Arachnida: Opiliones) phylogeny with emphasis on biogeography and the systematics of Laniatores. *Cladistics* 26, 408–437.
- Goloboff, P., 1993. Estimating character weights during tree search. *Cladistics* 9, 83–91.
- Goloboff, P., 1999. Analyzing large data sets in reasonable times: solutions for composite optima. *Cladistics* 15, 415–428.
- Goloboff, P. 2002. Techniques for Analyzing Large Data Sets. Vol. Brikhäuser Verlag, Basel, pp. 70–79.
- Goloboff, P., Farris, J., 2001. Methods for quick consensus estimation. *Cladistics* 17, S26–S34.
- Goloboff, P., Farris, J., Källersjö, M., Oxelman, B., Ramírez, M., Szumik, C., 2003a. Improvements to resampling measures of group support. *Cladistics* 19, 324–332.
- Goloboff, P., Farris, J., Nixon, K. 2003b. T.N.T.: Tree Analysis Using New Technology. Version 1.1 (August, 2008). Willi Hennig Society Edition. Program and documentation available from the authors, and at <http://www.zmuc.dk/public/phylogeny>.
- Goloboff, P., Mattoni, C., Quinteros, A., 2006. Continuous characters analyzed as such. *Cladistics* 22, 589–601.
- Goloboff, P., Farris, J., Nixon, K., 2008. TNT, a free program for phylogenetic analysis. *Cladistics* 24, 774–786.
- Golubchik, T., Wise, M.J., Easteal, S., Jermini, L.S., 2007. Mind the gaps: evidence of bias in estimates of multiple sequence alignments. *Mol. Biol. Evol.* 24, 2433–2442.
- González-José, R., Escapa, I., Neves, W., Cúneo, R., Pucciarelli, H., 2008. Cladistic analysis of continuous modularized traits provides phylogenetic signals in *Homo* evolution. *Nature* 453, 775–778.
- Griswold, C., 1985. *Isela okuncana*, a new genus and species of kleptoparasitic spider from southern Africa (Araneae: Mysmenidae). *Ann. Natal Mus.* 27, 207–217.
- Griswold, C., Meikle-Griswold, T., 1987. *Archaeodictyna ulova*, new species (Araneae: Dictynidae), a remarkable kleptoparasite of group-living eresid spiders (*Stegodyphus* spp., Araneae: Eresidae). *Am. Mus. Novit.* 2897, 1–11.
- Griswold, C., Yan, H.-M., 2003. On the egg-guarding behavior of a Chinese symphytognathid spider of the genus *Patu* Marples, 1951 (Araneae, Araneoidea, Symphytognathidae). *Proc. Calif. Acad. Sci.* 54, 356–360.
- Griswold, C., Coddington, J., Hormiga, G., Scharff, N., 1998. Phylogeny of the orb-web building spiders (Araneae, Orbiculariae: Deinopoidea, Araneoidea). *Zool. J. Linn. Soc. Lond.* 123, 1–99.
- Griswold, C., Ramírez, M., Coddington, J., Platnick, N. 2005. Atlas of phylogenetic data for entelegyne spiders (Araneae, Araneomorphae, Entelegynae), with comments on their phylogeny. *Proc. Calif. Acad. Sci.* 4th Ser. 56 (Suppl. II), 1–324.
- Hackett, S., Kimball, R., Reddy, S., Bowie, R., Braun, E., Braun, M., Chojnowski, J., Cox, W., Han, K.-L., Harshman, J., Huddleston, C., Marks, B., Miglia, K., Moore, W., Sheldon, F., Steadman, D., Witt, C., Yuri, T., 2008. A phylogenomic study of birds reveals their evolutionary history. *Science* 320, 1763–1768.
- Hajer, J., 2000. Web of *Trogloneta granulum* Simon (Araneae, Mysmenidae). *Bull. Br. Arachnol. Soc.* 11, 333–338.
- Hajer, J. 2002. The spinning activity of the spider *Trogloneta granulum* Simon, 1922 (Araneae, Mysmenidae). *Acta Univ. Purkynianae Stud. Biol.* VI, 21–38.
- Hajer, J., Reháková, D., 2003. Spinning activity of the spider *Trogloneta granulum* (Araneae, Mysmenidae): web, cocoon, cocoon handling behaviour, draglines and attachment discs. *Zoology* 106, 223–231.
- Hall, T., 1999. BioEdit: a user-friendly biological sequence alignment editor and analysis program for Windows 95/98/NT. *Nucleic Acids Symp. Ser.* 41, 95–98.
- Hammond, P.M., 1976. Kleptoparasitic behaviour of *Onthophagus suturalis* Peringuey and other dung beetles. *Coleop. Bull.* 30, 245–249.
- Hayashi, C. 1996. Molecular systematics of spiders: evidence from ribosomal DNA. PhD Thesis. Yale University, New Haven, CT, USA.
- Hedin, M., Maddison, W.P., 2001. Phylogenetic utility and evidence for multiple copies of elongation factor-1alpha in the spider genus *Habronattus* (Araneae: Salticidae). *Mol. Biol. Evol.* 18, 1512–1521.
- Hejnol, A., Obst, M., Stamatakis, A., Ott, M., Rouse, G.W., Edgecombe, G., Martinez, P., Bagnuà, J., Bailly, X., Jondelius, U., Wiens, M., Müller, W.E.G., Seaver, E., Wheeler, W., Martin-dale, M.Q., Giribet, G., Dunn, C. 2009. Assessing the root of bilaterian animals with scalable phylogenomic methods. *Proc. R. Soc. Lond. B Biol. Sci.* 276 (1677), 4261–4270.
- Hickman, V., 1931. A new family of spiders. *Proc. Zool. Soc. Lond. B.* 4, 1321–1328.
- Hickman, V., 1944. On some new Australian Apneumonomorphae with notes on their respiratory system. *Pap. Proc. R. Soc. Tasm.* 1943, 179–195.
- Hickman, V., 1945. A new group of apneumone spiders. *Trans. Conn. Acad. Arts Sci.* 36, 135–148.
- Hickman, V., 1979. Some Tasmanian spiders of the families Oonopidae, Anapidae and Mysmenidae. *Pap. Proc. R. Soc. Tasm.* 113, 53–79.
- Hiramatsu, T., Shinkai, A., 1993. Web structure and web-building behaviour of *Patu* sp. (Araneae: Symphytognathidae). *Acta Arach. Tokyo* 42, 181–185.
- Hormiga, G., Eberhard, W., Coddington, J., 1995. Web-construction behaviour in Australian *Phonognatha* and the phylogeny of nephiline and tetragnathid spiders (Araneae: Tetragnathidae). *Austral. J. Zool.* 43, 313–364.

- Hormiga, G., Scharff, N., Coddington, J., 2000. The phylogenetic basis of sexual size dimorphism in orb-weaving spiders (Araneae, Orbiculariae). *Syst. Biol.* 49, 435–462.
- Hormiga, G., Arnedo, M., Gillespie, R., 2003. Speciation on a conveyor belt: sequential colonization of the Hawaiian Islands by *Orsonwelles* spiders (Araneae, Linyphiidae). *Syst. Biol.* 52, 70–88.
- Hormiga, G., Álvarez-Padilla, F., Benjamin, S., 2007. First records of extant Hispaniolan spiders of the families Mysmenidae, Symphytognathidae and Ochyroceratidae (Araneae), including a new species of *Ochyrocera*. *Am. Mus. Novit.* 3577, 1–21.
- Huelsenbeck, J., Ronquist, F., 2001. MrBayes: Bayesian inference of phylogeny. *Bioinformatics* 17, 754–755.
- Humphries, C., 2002. Homology, Characters and Continuous Variables. Taylor & Francis, London, pp. 8–26.
- Iyengar, E.V., 2002. Sneaky snails and wasted worms: kleptoparasitism by *Trichotropis cancellata* (Mollusca, Gastropoda) on *Serpula columbiana* (Annelida, Polychaeta). *Mar. Ecol. Prog. Ser.* 244, 153–162.
- Jenner, R.A., 2004. Accepting partnership by submission? Morphological phylogenetics in a molecular millennium. *Syst. Biol.* 53, 333–342.
- Katoh, K., Toh, H., 2008. Recent developments in the MAFFT multiple sequence alignment program. *Brief. Bioinform.* 9, 286–298.
- Katoh, K., Misawa, K., Kuma, K.-i., Miyata, T., 2002. MAFFT: a novel method for rapid multiple sequence alignment based on fast Fourier transform. *Nucleic Acids Res.* 30, 3059–3066.
- Katoh, K., Kuma, K.-i., Toh, H., Miyata, T., 2005. MAFFT version 5: improvement in accuracy of multiple sequence alignment. *Nucleic Acids Res.* 33, 511–518.
- King, D.I., Rappole, J.H., 2001. Kleptoparasitism of laughingthrushes by Greater Racket-tailed Drongos in Burma (Myanmar). *Forktail* 17, 121–122.
- Kocher, T., Thomas, W., Meyer, A., Edwards, S., Paabo, S., Villablanca, F., Wilson, A., 1989. Dynamics of mitochondrial DNA evolution in animals: amplification and sequencing with conserved primers. *Proc. Natl Acad. Sci. USA* 86, 6196–6200.
- Kraus, O., 1955. Spinnen aus El Salvador (Arachnoidea, Araneae). *Abh. Senckenb. Naturforsch. Ges.* 493, 1–112.
- Kropf, C., 1990. Web construction and prey capture of *Comaroma simoni* Bertkau (Araneae). *Acta Zool. Fennica* 190, 229–233.
- Kruuk, H., 1972. The Spotted Hyena. University of Chicago Press, Chicago.
- Kuntner, M., Coddington, J., Hormiga, G., 2008. Phylogeny of extant nephilid orb-weaving spiders (Araneae, Nephilidae): testing morphological and ethological homologies. *Cladistics* 24, 147–217.
- Lee, M.S.Y., 2005. Squamate phylogeny, taxon sampling, and data congruence. *Org. Divers. Evol.* 5, 25–45.
- Lehtonen, S., 2008. Phylogeny estimation and alignment via POY versus Clustal + PAUP*: a response to Ogden and Rosenberg (2007). *Syst. Biol.* 57, 653–657.
- Lewis, P., 2001. A likelihood approach to estimating phylogeny from discrete morphological character data. *Syst. Biol.* 50, 913–925.
- Li, C., Ortí, G., Zhang, G., Lu, G., 2007. A practical approach to phylogenomics: the phylogeny of ray-finned fish (Actinopterygii) as a case study. *BMC Evol. Biol.* 7, 44.
- Lopardo, L., 2009. Systematics and evolution of the spider family Mysmenidae. PhD Thesis. The George Washington University. Available from <http://catalog.wrlc.org/cgi-bin/Pwebrecon.cgi?BBID=7840417>.
- Lopardo, L., Coddington, J., 2005. Chapter 40: Mysmenidae. In: Ubick, D., Cushing, P., Paquin, P. (Eds.), *Spiders of North America: An Identification Manual*. American Arachnology Society, pp. 175–177.
- Lopardo, L., Hormiga, G., 2007. On the Synaphrid Spider *Cepheia longiseta* (Simon 1881) (Araneae, Synaphridae). *Am. Mus. Novit.* 3575, 1–18.
- Lopardo, L., Hormiga, G., 2008. Phylogenetic placement of the Tasmanian spider *Acrobleps hygrophilus* (Araneae, Anapidae) with comments on the evolution of the capture web in Araneoidea. *Cladistics* 24, 1–33.
- Lopardo, L., Ramírez, M., 2007. The combing of cribellar silk by the prithine *Misionella mendensis*, with notes on other filistatid spiders (Araneae: Filistatidae). *Am. Mus. Novit.* 3563, 1–14.
- Lopardo, L., Ramírez, M., Grismado, C., Compagnucci, L., 2004. Web building behavior and the phylogeny of austrochiline spiders. *J. Arachnol.* 32, 42–54.
- Lopardo, L., Hormiga, G., Melic, A., 2007. Spinneret spigot morphology in synaphrid spiders (Araneae, Synaphridae), with comments on the systematics of the family and description of a new species of *Synaphris* Simon 1894 from Spain. *Am. Mus. Novit.* 3556, 1–26.
- López-Fernández, H., Honeycutt, R.L., Stiassny, M.L.J., Winemiller, K.O., 2005. Morphology, molecules, and character congruence in the phylogeny of South American geophagine cichlids (Perciformes, Labroidei). *Zool. Scr.* 34, 627–651.
- Lucas, J.R., 1986. Antlion pit construction and kleptoparasitic prey. *Fla. Entomol.* 69, 702–710.
- Marples, B., 1951. Pacific Symphytognathid spiders. *Pac. Sci.* 5, 47–51.
- Marples, B., 1955. Spiders from western Samoa. *J. Linn. Soc. Lond. (Zool.)* 42, 453–504.
- Marusik, Y., Lehtinen, P., 2003. Synaphridae Wunderlich, 1986 (Aranei: Araneoidea), a new family status, with a description of a new species from Turkmenistan. *Arthrop. Selecta* 11, 143–152.
- Marusik, Y., Gnelitsa, V., Kovblyuk, M., 2005. A new species of *Synaphris* (Araneae, Synaphridae) from Ukraine. *Bull. Br. Arachnol. Soc.* 13, 125–130.
- McCracken, K.G., Harshman, J., McClellan, D.A., Afton, A.D., 1999. Data set incongruence and correlated character evolution: an example of functional convergence in the hind-limbs of stiff tail diving ducks. *Syst. Biol.* 48, 683–714.
- Miller, J.A., 2007. Synaphridae of Madagascar (Araneae: Araneoidea): a new family record for the Afrotropical region. *Proc. Calif. Acad. Sci.* 58, 21–48.
- Miller, J.A., Griswold, C., Yin, C., 2009. The symphytognathoid spiders of the Gaoligongshan, Yunnan, China (Araneae: Araneoidea): systematics and diversity of micro-orbweavers. *ZooKeys* 11, 9–195.
- Moore, M., Bell, C., Soltis, P., Soltis, D., 2007. Using plastid genome-scale data to resolve enigmatic relationships among basal angiosperms. *Proc. Natl Acad. Sci. USA* 104, 19363–19368.
- Morissette, S., Himmelman, J.H., 2000. Subtidal food thieves: interactions of four invertebrate kleptoparasites with the sea star *Leptasterias polaris*. *Anim. Behav.* 60, 531–543.
- Müller, H.-G., 1987. Spiders from Colombia V. A new *Mysmenopsis* from the Ciénaga Grande de Santa Marta, northern Colombia (Araneida: Mysmenidae). *Bull. Br. Arachnol. Soc.* 7, 185.
- Nixon, K., 1999. The parsimony ratchet, a new method for rapid parsimony analysis. *Cladistics* 15, 407–414.
- Nixon, K., Carpenter, J., 1996. On simultaneous analysis. *Cladistics* 12, 221–241.
- Parker, C., Ruttan, L., 1988. The evolution of cooperative hunting. *Am. Nat.* 132, 159–198.
- Petrunkovitch, A., 1928. *Systema Araneorum*. *Trans. Conn. Acad. Arts Sci.* 29, 1–270.
- Pineau, P., Henry, M., Suspène, R., Marchio, A., Dettai, A., Debruyne, R., Petit, T., Lécru, A., Moisson, P., Dejean, A., Wain-Hobson, S., Vartanian, J., 2005. A universal primer set for PCR amplification of nuclear histone H4 genes from all animal species. *Mol. Biol. Evol.* 22, 1158.
- Pitcher, T.J., 1986. *Functions of Shoaling Behaviour in Teleosts*. Croom Helm, London, pp. 294–337.
- Platnick, N., 2010. The World Spider Catalog, Version 10.5. American Museum of Natural History. <http://research.amnh.org/entomology/spiders/catalog/index.html>.

- Platnick, N., Forster, R., 1986. On *Teutoniella*, an American genus of the spider family Micropholcommatidae (Araneae, Palpimanioidea). *Am. Mus. Novit.* 2854, 1–23.
- Platnick, N., Forster, R., 1989. A revision of the temperate South American and Australasian spiders of the family Anapidae (Araneae, Araneioidea). *Bull. Am. Mus. Nat. Hist.* 190, 1–139.
- Platnick, N., Shadab, M., 1978a. A review of the spider genus *Anapis* (Araneae, Anapidae), with a dual cladistic analysis. *Am. Mus. Novit.* 2663, 1–23.
- Platnick, N., Shadab, M., 1978b. A review of the spider genus *Mysmenopsis* (Araneae, Mysmenidae). *Am. Mus. Novit.* 2661, 1–22.
- Platnick, N., Coddington, J., Forster, R., Griswold, C., 1991. Spinneret morphology and the phylogeny of haplogyne spiders (Araneae, Araneomorphae). *Am. Mus. Novit.* 3016, 1–73.
- Posada, D., Buckley, T., 2004. Model selection and model averaging in phylogenetics: advantages of the AIC and Bayesian approaches over likelihood ratio tests. *Syst. Biol.* 50, 580–601.
- Posada, D., Crandall, K., 1998. MODELTEST: testing the model of DNA substitution. *Bioinformatics* 14, 817–818.
- Prendini, L., 2005. Comment on “Identifying spiders through DNA barcodes”. *Canad. J. Zool.* 83, 498–504.
- Prendini, L., Crowe, T., Wheeler, W., 2003. Systematics and biogeography of the family Scorpionidae (Chelicerata: Scorpiones), with a discussion on phylogenetic methods. *Invertebr. Syst.* 17, 185–259.
- Rae, T., 1998. The logical basis for the use of continuous characters in phylogenetic systematics. *Cladistics* 14, 221–228.
- Ramírez, M., Platnick, N., 1999. On *Sofanapis antillanca* (Araneae, Anapidae) as a kleptoparasite of austrochiline spiders (Araneae, Austrochilidae). *J. Arachnol.* 27, 547–549.
- Ramírez, M., Lopardo, L., Platnick, N., 2004. Notes on Chilean anapids and their webs (Araneae, Anapidae). *Am. Mus. Novit.* 3428, 1–13.
- Reader, T., 2003. Strong interactions between species of phytophagous fly: a case of intraguild kleptoparasitism. *Oikos* 103, 101–112.
- Regier, J., Shultz, J., Ganley, A., Hussey, A., Shi, D., Ball, B., Zwick, A., Stajich, J., Cummings, M., Martin, J., Cunningham, C., 2008. Resolving arthropod phylogeny: exploring phylogenetic signal within 41 kb of protein-coding nuclear gene sequence. *Syst. Biol.* 57, 920–938.
- Regier, J., Shultz, J., Zwick, A., Hussey, A., Ball, B., Wetzler, R., Martin, J., Cunningham, C., 2010. Arthropod relationships revealed by phylogenomic analysis of nuclear protein-coding sequences. *Nature* 463, 1079–1083.
- Rix, M., 2008. A new species of *Micropholcomma* (Araneae: Araneioidea: Micropholcommatidae) from Western Australia. *Rec. West. Aust. Mus.* 24, 343–348.
- Rix, M., Harvey, M., 2010. The spider family Micropholcommatidae (Arachnida, Araneae, Araneioidea): a relimitation and revision at the generic level. *ZooKeys* 36, 1–321.
- Rix, M., Harvey, M., Roberts, J., 2008. Molecular phylogenetics of the spider family Micropholcommatidae (Arachnida: Araneae) using nuclear rRNA genes (18S and 28S). *Mol. Phylogenet. Evol.* 46, 1031–1048.
- Ronquist, F., Huelsenbeck, J., 2003. MrBayes 3: Bayesian phylogenetic inference under mixed models. *Bioinformatics* 19, 1572–1574.
- Rosenthal, R.J., 1971. Trophic interaction between the sea star *Pisaster giganteus* and the gastropod *Kelletia kelletii*. *Fish. Bull.* 69, 669–679.
- Roth, V., Craig, P., 1970. Arachnida of the Galapagos Islands. *Mission zoologique Belge aux îles Galapagos et en Ecuador* (N et J Leleup 1964–1965). 2, 107–124.
- Scharff, N., Coddington, J., 1997. A phylogenetic analysis of the orb-weaving spider family Araneidae (Arachnida, Araneae). *Zool. J. Linn. Soc. Lond.* 120, 355–434.
- Schütt, K., 2000. The limits of the Araneioidea (Arachnida: Araneae). *Austral. J. Zool.* 48, 135–153.
- Schütt, K., 2002. The limits and phylogeny of the Araneioidea (Arachnida, Araneae). PhD Thesis. University of Berlin, Germany.
- Schütt, K., 2003. Phylogeny of Symphytognathidae s.l. (Araneae, Araneioidea). *Zool. Scr.* 32, 129–151.
- Schwendinger, P., Giribet, G., 2005. The systematics of the southeast Asian genus *Fangensis* Rambla (Opiliones: Cyphophthalmi: Stylocellidae). *Invertebr. Syst.* 19, 297–323.
- Scotland, R.W., Olmstead, R.G., Bennett, J.R., 2003. Phylogeny reconstruction: the role of morphology. *Syst. Biol.* 52, 539–548.
- Shinkai, E., 1977. Spiders of Tokyo III. *Acta Arach. Tokyo* 27, 321–336.
- Shinkai, E., 1997. The web structure and predatory behavior of *Wendilgarda* sp. (Araneae: Theridiosomatidae). *Acta Arach. Tokyo* 46, 53–60.
- Shinkai, A., Shinkai, E., 1988. Web structure of *Conoculus lyugadinus* Komatsu (Araneae: Anapidae). *Acta Arach. Tokyo* 37, 1–12.
- Simmons, M., Ochoterena, H., 2000. Gaps as characters in sequence-based phylogenetic analyses. *Syst. Biol.* 49, 369–381.
- Simon, C., Frati, F., Beckenbach, A., Crespi, B., Liu, H., Flook, P., 1994. Evolution, weighting, and phylogenetic utility of mitochondrial gene sequences and a compilation of conserved polymerase chain reaction primers. *Ann. Entomol. Soc. Am.* 87, 651–701.
- Sivinski, J., Stowe, M., 1980. A kleptoparasitic cecidomyiid and other flies associated with spiders. *Psyche* (Camb., Mass.) 87, 337–348.
- Sivinski, J., Marshall, S., Petersson, E., 1999. Kleptoparasitism and phoresy in the Diptera. *Fla. Entomol.* 82, 179–197.
- Sloan, N.A., 1979. Starfish encounters: an experimental study of its advantages. *Experientia* 35, 1314–1315.
- Sloan, N.A., 1984. Interference and aggregation: close encounters of the starfish kind. *Ophelia* 23, 23–31.
- Smith, N.D., Turner, A.H., 2005. Morphology's role in phylogeny reconstruction: perspectives from paleontology. *Syst. Biol.* 54, 166–173.
- Soltis, D., Gitzendanner, M., Soltis, P., 2007. A 567-taxon data set for angiosperms: the challenges posed by Bayesian analyses of large data sets. *Int. J. Plant Sci.* 168, 137–157.
- Spagna, J., Álvarez-Padilla, F., 2008. Finding an upper limit for gap costs in direct optimization parsimony. *Cladistics* 24, 787–801.
- Thaler, K., 1975. *Trogloneta granulum* Simon, eine weitere Reliktart der Nordostalpen (Arachnida, Aranei, “Symphytognathidae”). *Rev. Suisse Zool.* 82, 283–291.
- Thiele, K., 1993. The Holy Grail of the perfect character: the cladistic treatment of morphometric data. *Cladistics* 9, 275–304.
- Thornhill, R., 1979. Adaptive female-mimicking behavior in a scorpionfly. *Science* 205, 412–414.
- Townsend, T.M., Alegre, R.E., Kelley, S.T., Wiens, J., Reeder, T.W., 2008. Rapid development of multiple nuclear loci for phylogenetic analysis using genomic resources: an example from squamate reptiles. *Mol. Phylogenet. Evol.* 47, 129–142.
- Tso, I., Severinghaus, L., 1998. Silk-stealing by *Argyrodes lanyuensis* (Araneae: Theridiidae): a unique form of kleptoparasitism. *Anim. Behav.* 56, 219–225.
- Varón, A., Vinh, L., Bomash, I., Wheeler, W., 2008–2009. POY 4.0 and 4.1. American Museum of Natural History, New York. Available from <http://research.amnh.org/scicomp/projects/poy.php>.
- Vink, C., Hedin, M., Bodner, M., Maddison, W.P., Hayashi, C., Garb, J., 2008. Actin 5C, a promising nuclear gene for spider phylogenetics. *Mol. Phylogenet. Evol.* 48, 377–382.
- Vollrath, F., 1978. A close relationship between two spiders (Arachnida, Araneidae): *Curimagua bayano* synecious on a *Diplura* species. *Psyche* (Camb., Mass.) 85, 347–353.
- Vollrath, F., 1979a. Behaviour of the kleptoparasitic spider *Argyrodes elevatus* (Araneae, Theridiidae). *Anim. Behav.* 27, 515–521.
- Vollrath, F., 1979b. Vibrations: their signal function for a spider kleptoparasite. *Science* 205, 1149–1151.
- Vollrath, F., 1984. Kleptobiotic Interactions in Invertebrates. Chapman & Hall, New York, pp. 61–94.

- Wahlberg, N., Nylin, S., 2003. Morphology versus molecules: resolution of the positions of *Nymphalis*, *Polygonia*, and related genera (Lepidoptera: Nymphalidae). *Cladistics* 19, 213–223.
- Wheeler, W., 1995. Sequence alignment, parameter sensitivity, and the phylogenetic analysis of molecular data. *Syst. Biol.* 44, 321–331.
- Wheeler, W., 1996. Optimization alignment: the end of multiple sequence alignment in phylogenetics? *Cladistics* 12, 1–9.
- Wheeler, W., 2002. *Optimization Alignment: Down, Up, Error, and Improvements*. Birkhäuser, Basel, Boston, Berlin.
- Wheeler, W., Giribet, G., 2009. Chapter 6: Phylogenetic hypotheses and the utility of multiple sequence alignment. In: Rosenberg, M. (Ed.), *Perspectives on Biological Sequence Alignment*. University of California Press, Berkeley.
- Wheeler, W., Aagesen, L., Arango, C., Faivovich, J., Grant, T., D'Haese, C., Janies, D., Smith, W., Varón, A., Giribet, G., 2006. *Dynamic Homology and Phylogenetic Systematics: A Unified Approach Using POY*. American Museum of Natural History, New York.
- Whitehouse, M.E.A., 1986. The foraging behaviours of *Argyrodes antipodiana* (Theridiidae), a kleptoparasitic spider from New Zealand. *N. Z. J. Zool.* 13, 151–168.
- Whiting, M., Carpenter, J., Wheeler, Q., Wheeler, W., 1997. The Strepsiptera problem: phylogeny of the holometabolous insect orders inferred from 18S and 28S ribosomal DNA sequences and morphology. *Syst. Biol.* 46, 1–68.
- Wiens, J., 2001. Character analysis in morphological phylogenetics: problems and solutions. *Syst. Biol.* 50, 689–699.
- Wiens, J., 2004. The role of morphological data in phylogeny reconstruction. *Syst. Biol.* 53, 653–661.
- Wiens, J., Chippindale, P.T., Hillis, D.M., 2003. When are phylogenetic analyses misled by convergence? A case study in Texas cave salamanders. *Syst. Biol.* 52, 501–514.
- Wiens, J., Kuczynski, C., Smith, S., Mulcahy, D., Sites, J.J., Townsend, T.M., Reeder, T.W., 2008. Branch lengths, support, and congruence: testing the phylogenomic approach with 20 nuclear loci in snakes. *Syst. Biol.* 57, 420–431.
- Wilson, E.O., 1975. *Sociobiology*. Harvard University Press/Belknap Press, Cambridge, MA.
- Winchell, C., Sullivan, J., Cameron, C., Swalla, B., Mallatt, J., 2002. Evaluating hypotheses of deuterostome phylogeny and chordate evolution with new LSU and SSU ribosomal DNA data. *Mol. Biol. Evol.* 19, 762–776.
- Wittenberger, J.F., 1981. *Animal Social Behaviour*. Duxbury Press, Boston.
- Wobber, D.R., 1975. Agonism in asteroids. *Biol. Bull.* 148, 483–496.
- Wunderlich, J., 1980. Sternal-organe der Theridiosomatidae—eine bisher übersehene Autapomorphie (Arachnida: Araneae). *Verh. Nat. Wiss. Ver. Hamburg.* 23, 255–257.
- Wunderlich, J., 1995a. Die Beziehungen der Synaphrinae Wunderlich 1986 (Araneae: Anapidae). *Beitr. Araneol.* 4, 775–776.
- Wunderlich, J., 1995b. Drei bisher unbekannte Arten und Gattungen der Familie Anapidae (s.l.) aus Süd-Afrika, Brasilien und Malaysia (Arachnida: Araneae). *Beitr. Araneol.* 4, 543–551.
- Young, N., Healy, J., 2002. GapCoder automates the use of indel characters in phylogenetic analysis. *Bioinformatics* 4, 1–6.
- Zamora, R., 1990. Observational and experimental study of a carnivorous plant–ant kleptobiotic interaction. *Oikos* 59, 368–372.
- Zamora, R., Gómez, J.M., 1996. Carnivorous plant–slug interaction: a trip from herbivory to kleptoparasitism. *J. Anim. Ecol.* 65, 154–160.

Supporting Information

Additional Supporting Information may be found in the online version of this article:

Table S1. (a) Complete dataset, including all 109 taxa. Successful sequence fragments and other positive scor-

ings are depicted in green. The first column lists taxa, sorted by family. The second and third columns represent positive overall scoring of morphology and molecules, respectively. The remaining columns correspond to gene segments from 12S, 16S, and 18S. (b) Complete dataset, including all 109 taxa. Successful sequence fragments and other positive scorings are depicted in green. First column represents list of taxa, sorted by family. Second and third columns represent positive overall scoring of morphology and molecules, respectively. Remaining columns correspond to gene segments from 28S, CO1 and H3.

Table S2. Morphological data matrix. The first 350 characters correspond to discrete characters; the last seven characters are continuous. Polymorphic terminals are coded a = [01]; b = [02]; c = [03]; d = [04]; e = [12]; f = [13]; g = [14]; h = [23]; I = [34]. Inapplicable characters are scored as “–”; missing data as “?”.

Appendix S1. Morphological characters.

Appendix S2. List of specimens sequenced in this study. Generic assignment of unidentified mysmenid species (in parentheses after the identification code) is based on the phylogenetic hypothesis from the total-evidence analysis (see Figs 12 and 13).

Appendix S3. List of autapomorphic and unambiguous synapomorphic changes in the preferred hypothesis from the total-evidence dynamic analysis. Discrete morphological characters. Node numbers refer to nodes in consensus on Fig. 13. Only nodes/taxa with changes are listed.

Appendix S4. Cladograms resulting from the analyses performed in this study. See Tables 3 and 4 and text for details. Family codes used for unidentified species: ANAP, Anapidae; MYSM, Mysmenidae; SYMP, Symphytognathidae; TSMD, Theridiosomatidae.

Please note: Wiley-Blackwell is not responsible for the content or functionality of any supplementary materials supplied by the authors. Any queries (other than missing material) should be directed to the corresponding author for the article.

Appendix 1

Abbreviations

ALS, anterior lateral spinnerets; AME, anterior median eyes; AMNH, American Museum of Natural History, New York, USA; ANTS, Anterior Tracheal System clade; AtoL, Phylogeny of Spiders Project (NSF grant EAR-0228699); BMNH, Natural History Museum, London, United Kingdom; BS, Bremer support; C, tegular (bulbal) conductor; CAS, California Academy of Sciences, San Francisco, USA; CD, copulatory ducts; CI, consistency index; CO, copulatory openings; Cy, cymbium; CyC1, primary (internal) cymbial conductor; CyF, cymbial fold; CyFs, setae on cymbial fold; CyP, cymbial process; E, embolus; F, fundus; FD, fertilization ducts; gl, accessory gland; I, spermatic duct switchback I (drawing); II, spermatic duct switchback II (drawing); III, spermatic duct switch-

back III (drawing); IRSN, Institut Royal des Sciences Naturelles, Brussels, Belgium; IV, spermatic duct switchback IV (drawing); Jfq, jackknifing frequencies; MAP, major ampullate (gland spigot); MCZ, Museum of Comparative Zoology, Harvard University, Cambridge, USA; MHNG, Museum d'Histoire naturelle, Geneve, Switzerland; MNHN, Muséum National d'Histoire Naturelle, Paris, France; MPT, most parsimonious tree; MRAC, Musee Royal Afrique Centrale, Tervuren, Belgium; NMSA, Natal Museum, Pietermaritzburg, South

Africa; pa, patella; PBS, partitioned Bremer support; PC, paracymbium; PLS, posterior lateral spinnerets; PMS, posterior median spinnerets; RAS, random addition sequences; RFD, relative Bremer support or relative fit difference; RI, retention index; S, spermatheca/e; SB, spermatic duct switchback; SEM, scanning electron microscopy; T, tegulum; TBR, tree bisection–reconnection branch swapping; ti, tibia.